



**UNIVERSIDAD NACIONAL AUTÓNOMA DE MÉXICO**  
**PROGRAMA DE POSGRADO EN CIENCIAS DE LA TIERRA**  
**INSTITUTO DE GEOLOGÍA**

**EL HOLOCENO EN LAS MONTAÑAS DE CHIAPAS: DINÁMICAS AMBIENTALES  
Y DE LA VEGETACIÓN**

**TESIS**  
**QUE PARA OPTAR POR EL GRADO DE:**  
**DOCTOR EN CIENCIAS DE LA TIERRA**

**PRESENTA:**  
**JUAN FELIPE FRANCO GAVIRIA**

**TUTOR**  
**DR. ALEXANDER CORREA METRIO**  
**INSTITUTO DE GEOLOGÍA, UNAM**

**MIEMBROS DEL COMITÉ TUTOR**  
**MARGARITA CABALLERO MIRANDA, INSTITUTO DE GEOFÍSICA, UNAM**  
**CARLOS MARTORELL DELGADO, FACULTAD DE CIENCIAS, UNAM**

**CIUDAD UNIVERSITARIA, CD. MX., DICIEMBRE 2018**



Universidad Nacional  
Autónoma de México

Dirección General de Bibliotecas de la UNAM

**Biblioteca Central**



**UNAM – Dirección General de Bibliotecas**  
**Tesis Digitales**  
**Restricciones de uso**

**DERECHOS RESERVADOS ©**  
**PROHIBIDA SU REPRODUCCIÓN TOTAL O PARCIAL**

Todo el material contenido en esta tesis esta protegido por la Ley Federal del Derecho de Autor (LFDA) de los Estados Unidos Mexicanos (México).

El uso de imágenes, fragmentos de videos, y demás material que sea objeto de protección de los derechos de autor, será exclusivamente para fines educativos e informativos y deberá citar la fuente donde la obtuvo mencionando el autor o autores. Cualquier uso distinto como el lucro, reproducción, edición o modificación, será perseguido y sancionado por el respectivo titular de los Derechos de Autor.

## AGRADECIMIENTOS

Agradezco al Posgrado en Ciencias de la Tierra de la Universidad Nacional Autónoma de México por todo su apoyo durante mi formación académica.

La materialización de este proyecto fue gracias al apoyo financiero de las siguientes entidades: Consejo Nacional de Ciencia y Tecnología (CONACYT) por la beca de doctorado otorgada (CVU: 510171) y el financiamiento del proyecto CB-256406; Programa de Apoyo a Proyectos de Investigación e Innovación Tecnológica (PAPIIT) a través de los proyectos IN107716 e IA100714; Programa de Investigación en Cambio Climático (PINNC) y el apoyo económico de la beca National Geographic Society 9137-12.

Mi más sincero agradecimiento a mi director de tesis, Alexander Correa, por ayudarme a descubrir el fascinante mundo de la paleoecología. Gracias Alex por el apoyo incondicional, por inspirarme constantemente y por la libertad de desarrollar nuevas ideas y estrategias para mi trabajo científico.

A los miembros del comité tutorial, Dra. Margarita Caballero y Carlos Martorell, por todo el entusiasmo, comentarios y sugerencias a lo largo de la realización de la tesis.

A los miembros del jurado evaluador, Dra. Blanca Figueroa, Dra. Laura Beramendi y Dr. Jaime Escobar, por sus valiosas observaciones y comentarios al manuscrito.

A Liseth Pérez, Dr. Antje Schwalb, Sergio Cohuo y Laura Macario, quienes amablemente ofrecieron material sedimentario de algunas muestras modernas.

A la Dra. Socorro Lozano y Susana Nájera por las facilidades brindadas en la fase experimental de este proyecto.

A Edyta Sawisza, Dr. Krystina Szerocznska y Marta Wojewódka por su cálido recibimiento en el instituto de Geología de Varsovia, gracias por enseñarme el maravilloso mundo de los cladóceros.

Al Dr. Francisco Romero, y miembros del laboratorio de Geoquímica Ambiental de la UNAM (Laboratorio Nacional de Geoquímica y Mineralogía), en especial al Dr. Luis Gerardo Martínez y Astrid Vásquez por el apoyo en los análisis de fluorescencia de rayos X en los sedimentos.

A la Dra. Blanca Prado y su grupo de trabajo del Laboratorio de Edafología de la UNAM, por el apoyo en los análisis de carbono inorgánico y orgánico total, nitrógeno total, y fósforo total en sedimentos.

A la Comisión Nacional de Áreas Naturales Protegidas (CONANP), las comunidades lacandonas de Nahá y Metzabok, Miguel García y a todos los individuos que han estado involucrados en las campañas de campo.

A todos mis colegas del laboratorio de paleoecología, Day Caballero, Cecilia Cordero, Melbi Ramos, Emmanuel Jiménez, Minerva López, Emmanuel Gámez, Gustavo Olivares, Melisa Aranza, Esmeralda Cruz, Daniel Mendiola, Esteban Cruz, Yosahandy Vázquez, y Alejandra Díaz, por su buena energía y excelente compañía en escenarios académicos y no académicos.

A mi esposa, Ana Gallego, por su apoyo incondicional, cariño y paciencia. Infinitamente agradecido por darme una hija maravillosa y ser mi cómplice en esta linda aventura.

A mi familia, mi madre Isabel, mi hermana Mónica, mi abuelita Libia, Beatriz Sánchez, Sebastián, mis tíos y primos. Siempre les estaré agradecido por su apoyo y aliento, me hacen sentir amado y en casa, sin importar lo lejos que pueda estar.

Quiero dar un especial agradecimiento a mis amigos mexicanos, familia Mosqueda, Roberto, Aurora, Mari, Miguel, Chelo, Cristina, Fredy, Elsa y todos con los que compartí en este hermoso país. Nos abrieron sus corazones y acogieron de tal forma que nos hicieron sentir en casa.

*A Gabriela Franco Gallego,  
me has hecho más fuerte y feliz de lo que jamás hubiera podido imaginar. Te amo.*

*A la memoria de nuestro querido amigo Julián Hernández*

## CONTENIDO

|  |           |
|--|-----------|
| <b>RESUMEN.....</b>  | <b>3</b>  |
| <b>ABSTRACT.....</b>   | <b>5</b>  |
| <b>ACRÓNIMOS.....</b>  | <b>7</b>  |
| <b>PREFACIO.....</b>   | <b>9</b>  |
| <b>CAPÍTULO 1.....</b>   | <b>12</b> |
| <b>ALCANCES DE LA INVESTIGACIÓN.....</b>   | <b>12</b> |
| <b>INTRODUCCIÓN.....</b>   | <b>12</b> |
| <b>REVISIÓN DE LITERATURA.....</b>   | <b>15</b> |
| <b>HISTORIA CLIMÁTICA Y CULTURAL DE LAS TIERRAS MAYAS DURANTE EL HOLOCENO.....</b>   | <b>15</b> |
| 1.1. Introducción.....   | 15        |
| 1.2. Configuración ambiental de la Península de Yucatán.....   | 16        |
| 1.3. El marco cronológico de la evolución ambiental y cultural de las tierras mayas.....   | 18        |
| 1.4. Historia ambiental del Holoceno.....  | 20        |
| 1.5. Conclusiones.....   | 30        |
| <b>OBJETIVOS DE LA INVESTIGACION.....</b>  | <b>32</b> |
| <b>HIPÓTESIS.....</b>  | <b>33</b> |
| <b>CAPÍTULO 2.....</b>   | <b>34</b> |
| <b>MATERIALES Y MÉTODOS.....</b>   | <b>34</b> |
| 2.1. Área de estudio.....  | 34        |
| 2.2. Trabajo de campo.....   | 38        |
| 2.3. Trabajo de laboratorio.....   | 40        |
| 2.4. Análisis de datos.....  | 42        |
| <b>CAPÍTULO 3.....</b>   | <b>47</b> |
| <b>LA HUELLA DEL IMPACTO HUMANO EN EL ESPECTRO DE POLEN MODERNO DE LAS TIERRAS MAYAS.....</b>                                    | <b>47</b> |
| 3.1. Introduction.....   | 50        |
| 3.2. Material and Methods.....   | 52        |
| 3.3. Results.....  | 57        |
| 3.4. Discussion.....   | 64        |
| 3.5. Conclusions.....  | 69        |
| <b>CAPÍTULO 4.....</b>   | <b>72</b> |
| <b>EFFECTOS DE LA VARIABILIDAD CLIMÁTICA Y FACTORES DE ESTRÉS ANTROPOGÉNICOS EN LA VEGETACIÓN DE LAS TIERRAS ALTAS MAYA.....</b> | <b>72</b> |
| 4.1. Introduction.....   | 75        |
| 4.2. Regional background.....  | 78        |
| 4.3. Material and methods.....   | 82        |
| 4.4. Results.....  | 86        |
| 4.5. Discussion.....   | 95        |

|  |            |
|--|------------|
| 4.6. Conclusions.....  | 109        |
| <b>CAPÍTULO 5 .....</b>  | <b>112</b> |
| <b>DINÁMICA DE LA VEGETACIÓN DEL HOLOCENO, VARIABILIDAD CLIMÁTICA<br/>E IMPACTO HUMANO EN LA SELVA LACANDONA, ELEVACIONES MEDIAS DE<br/>MÉXICO TROPICAL.....</b> | <b>112</b> |
| 5.1. Introduction.....   | 115        |
| 5.2. Materials and methods.....  | 118        |
| 5.3. Results.....  | 124        |
| 5.4. Discussion.....   | 131        |
| 5.5. Conclusions.....  | 145        |
| <b>CAPÍTULO 6 .....</b>  | <b>147</b> |
| <b>SÍNTESIS: VARIABILIDAD AMBIENTAL EN LAS MONTAÑAS DE CHIAPAS<br/>DURANTE EL HOLOCENO: ESTIMACIÓN CUANTITATIVA BASADA EN EL<br/>POLEN.....</b>                  | <b>147</b> |
| 6.1. Introducción.....   | 147        |
| 6.2. Métodos.....  | 149        |
| ¿Cuáles son los principales gradientes ambientes expresados en los ensamblajes polen moderno y fósil? .....  | 151        |
| ¿Cuál fue la magnitud de los cambios en el clima y el impacto humano durante el Holoceno, en las montañas de Chiapas?.....                                       | 155        |
| <b>CONCLUSIONES Y PERSPECTIVAS .....</b>   | <b>160</b> |
| <b>REFERENCIAS.....</b>  | <b>163</b> |
| <b>APÉNDICES .....</b>   | <b>177</b> |
| Apéndice 3.1. Lista de lagos muestreados en la interface agua-sedimento.....   | 177        |
| Apéndice 3.2. Análisis de Taxa Indicadores de Umbrales.....  | 181        |
| Apéndice 4.1. Correlaciones de Pearson para datos de geoquímica.....   | 183        |
| Apéndice 4.2. Selección de variables ambientales por el método step-wise backward.. ...  | 184        |
| Apéndice 4.3. Información climática de la estación meteorológica La Soledad en el contexto de condiciones de El Niño y La Niña... ..                             | 185        |
| Apéndice 4.4. Análisis de material carbonizado de los núcleos sedimentarios de los lagos San Lorenzo y Esmeralda.. ..  | 186        |
| Apéndice 4.5. Registro multielemental de los lagos San Lorenzo y Esmeralda.....  | 187        |
| Apéndice 4.6. Análisis multidimensional no-métrico, ordenación de los taxa.....  | 188        |
| Apéndice 5.1. Funciones de densidad de probabilidad bivariadas para el espacio en la ordenación ocupado por las muestras modernas.....                           | 189        |
| Apéndice 5.2. Registro elemental de los núcleos sedimentarios OCO12-II y OCO16G-I.   | 190        |

## RESUMEN

La investigación realizada en esta tesis contribuye al conocimiento de las dinámicas de la vegetación, el clima y el impacto humano en las montañas de Chiapas durante el Holoceno. Para reconstruir los cambios ambientales ocurridos en el pasado se desarrolló una metodología basada en dos áreas de trabajo. La primera correspondió a la calibración entre ensambles de polen moderno y atributos medibles del ambiente como el clima y la influencia humana, en 130 muestras de sedimento superficial distribuidas en la zona maya. El segundo eje temático se refirió al análisis de secuencias sedimentarias de lagos localizados en el Parque Nacional Lagunas de Montebello y la Selva Lacandona, ambos sitios ubicados en las montañas de Chiapas. Las reconstrucciones de diferentes atributos del ambiente como el clima e impacto antrópico fueron cuantificados en el pasado mediante el proceso de calibración del polen moderno y las variables ambientales de interés. En términos generales, se resalta la habilidad del polen para reflejar diferentes gradientes ecológicos y ambientales, confirmando su uso potencial en las reconstrucciones paleoambientales. De acuerdo con los registros paleoecológicos y la calibración moderna, han prevalecido condiciones ambientales altamente variables en las montañas de Chiapas, durante los últimos 10,000 años. Dicha variabilidad se ha manifestado principalmente en cambios en patrones biogeográficos, climáticos y usos del suelo de la región. En el registro paleoecológico de la montañas de Chiapas se encontró una dominancia sistemática de taxa de origen Neártico durante periodos de alta inestabilidad climática (e.g. *Pinus*, *Quercus* y *Alnus*, Gentry, 1982). Sin embargo, bajo condiciones climáticas estables y de baja influencia humana, la vegetación fue dominada por taxa Neotropicales (e.g. *Hedyosmum*, *Alchornea*, *Moraceae* y *Melastomataceae*, Gentry, 1982). Taxa Neárticos respondieron de forma oportunista a perturbaciones naturales ocasionadas por las sequías y la alta estacionalidad, mientras los

elementos Neotropicales en mayor medida se asociaron con las sucesiones ecológicas, mediadas por la expresión de sus nichos ambientales en los climas regionales. Adicionalmente, del registro paleoecológico se logró inferir que, probablemente, la composición y estructura de los bosques de montaña en el presente, no tienen más de 800 años. Estos bosques han sido el resultado de condiciones climáticas relativamente estables, así como de una reducción sustancial del impacto humano que favoreció su establecimiento en la región. Por lo tanto, es muy probable que los diferentes tipos de vegetación que actualmente existen en las montañas de Chiapas fueron el producto de procesos ecológicos que actuaron bajo un legado de siglos de cambios naturales y antropogénicos.

## ABSTRACT

The research conducted in this thesis contributes to the knowledge of the vegetation, climate, and human impact dynamics in the mountains of Chiapas during the Holocene. To reconstruct environmental changes that occurred in the past was developed a methodology based on two components. The first corresponded to the calibration processes between modern pollen and environmental attributes such as climate and human influence, using 130 samples of surface sediments distributed in different lakes from the Maya region. The second was referred to the analysis of sedimentary sequences located in the Lagunas de Montebello National Park and the Lacandon forest, both sites located in the mountains of Chiapas. Different environmental attributes (e.g. climate and human impact) were quantified in the past through the calibration of modern pollen and environmental variables. The results show the pollen ability to reflect ecological and environmental gradients, confirming their potential use in paleoenvironmental reconstructions. According to paleoecological records and modern calibration, environmental conditions highly variable have prevailed in the mountains of Chiapas during the last 10,000 years. This variability has mostly expressed in biogeographic, climatic and land use patterns of the region. The paleoecological record shows a systematic dominance of Nearctic taxa (e.g. *Pinus*, *Quercus* and *Alnus*, Gentry, 1982) was found during periods of high climatic instability. However, Neotropical taxa (e.g. *Hedyosmum*, *Alchornea*, Moraceae and Melastomataceae, Gentry, 1982) dominated under stable climatic conditions and low human influence. Nearctic elements responded opportunistically to natural disturbances caused by droughts and high seasonality, whereas Neotropical taxa were associated with ecological successions, mediated the expression of their environmental niches in regional climates. The reconstructed vegetation changes indicate that the forests that today occupies the mountains of Chiapas date back to the

last 800 years. These forests have been the result of relatively stable climatic conditions, as well as a substantial reduction in the human impact, favoring their establishment in the region. Therefore, it is likely that vegetation types that today occupied the mountains of Chiapas resulted of ecological processes under a centuries-old legacy of natural and anthropogenic changes.

## ACRÓNIMOS

AP: Años calibrados antes del presente / Years cal before present

ANE/NE: Antes de la nuestra era / nuestra era

PCT: Periodo Clásico Terminal / Terminal Classic Period

BLT: Bosque Lluvioso Tropical / Tropical Rain Forest

BLMB: Bosque Lluvioso de Montaña Baja / Lower Montane Rain Forest

BLM: Bosque Lluvioso de Montaña / Montane Cloud Forest

BPE: Bosque de Pino-Encino / Pine-Oak Forest

BPEL: Bosque de Pino-Encino-*Liquidambar*

CP: Campos de cultivo / Croplands

BP: Años calibrados antes del presente / Calibrated years before present

ENSO: El Niño-Oscilación del Sur / El Niño-Southern Oscillation

ITCZ: Zona de Convergencia Intertropical / Intertropical Convergence Zone

MWP: Periodo Cálido Medieval / Medieval Warm Period

LIA: Pequeña edad de Hielo / Little Ice Age

AMT: Temperatura Media Anual / Annual Mean Temperature

MDR: Rango Medio Diurno / Mean Diurnal Range

IST: Isotermalidad / Isothermality

APP: Precipitación Anual / Annual Precipitation

PSE: Estacionalidad de la Precipitación / Precipitation Seasonality

HII: Índice de Influencia Humana / Human Influence Index

PCA: Análisis de Componentes Principales / Principal Components Analysis

DCA: Análisis de Correspondencia sin Tendencia / Detrended Correspondence Analysis

NMDS: Escalamiento Multidimensional no-métrico / Non-metric Multidimensional Scaling

TITAN: Análisis de Taxa Indicadores de Umbrales / Threshold Indicator Taxa Analysis

MANOVA: Análisis de Varianza Multivariada / Multivariate Analysis of Variance

IndVal: Valor Indicador / Individual Value

PDF: Función de densidad de probabilidad / Probability Density Function

AMS: Espectrometría de Masas con Acelerador / Accelerator Mass Spectrometry

XRF: Fluorescencia de Rayos X / X-Ray fluorescence

CM: Centro de México / Central Mexico

HL: Tierras altas de Centroamérica y Chiapas / Highlands of Central America and Chiapas

ME: Elevaciones medias de Centroamérica y Chiapas / Middle elevations of Central America and Chiapas

## PREFACIO

Más de 4,000 años de interacciones entre el hombre y su entorno han dejado una huella innegable en los recursos naturales del Norte de Centroamérica, un área de notable biodiversidad. Esta región ha sido hogar de las antiguas comunidades mayas, la cuales han estado íntimamente relacionadas con el manejo y gestión de los recursos naturales. En mi primera visita a Chiapas, al sureste de México, tuve la oportunidad de constatar la gran diversidad natural y cultural de una región con una larga historia de ocupación humana. De igual manera, fue una oportunidad excepcional de ver en persona cómo en las montañas de Chiapas coexistían especies templadas y tropicales, dando lugar a mosaicos de vegetación propios de bosques mesófilos de montaña. Bosques reconocidos por la gran biodiversidad que albergan, pero también por su alto grado de vulnerabilidad al cambio climático y las actividades humanas. Estos patrones fueron corroborados en campo al notar una alta fragmentación de los ecosistemas montañosos de Chiapas. Por ejemplo, en mi primera visita al lago Ocotulito, en la Selva Lacandona, pude notar cómo los esfuerzos de conservación de las comunidades de lacandones de Nahá eran insuficientes ante la creciente colonización del territorio por sus vecinos. Claramente se notó una conversión del bosque a la agricultura y ganadería en áreas no resguardadas por los lacandones. Procesos de conversión de selvas y bosques han escalado a niveles mayores, encontrando hoy en día un tercio de la vegetación que predominaba originalmente.

México es uno de los países megadiversos con mayor tasa de deforestación. El mismo desinterés de lo que ocurre con los ecosistemas naturales y malas políticas públicas han favorecido sustancialmente las pérdidas de los bosques en la región. Hay un dicho popular en el sentido de lo que no se conoce no se puede valorar. Proteger y manejar racionalmente los recursos biológicos requiere antes que nada conocerlos. Por ello resulta afortunado ofrecer

información sobre los cambios ambientales en el pasado del segundo estado más diverso de la República Mexicana, a través de un enfoque temporal más amplio. Los resultados aquí presentados corresponden a un ejemplo de una aportación producida por diferentes disciplinas como la paleoecología, paleoclimatología, ecología y geociencias, dedicadas al conocimiento de las dinámicas ambientales en Chiapas.

Este trabajo consta de seis capítulos que ofrecen un punto de partida para comprender los patrones de diversidad que hoy en día se reconocen en las montañas de Chiapas. Los primeros dos capítulos están dedicados a describir los alcances de la investigación y una visión general de los métodos aplicados. El Capítulo 1 presenta una introducción general, una revisión de literatura y los objetivos planteados en este trabajo. El Capítulo 2 presenta una descripción general del área de estudio y plantea los métodos de campo, laboratorio y análisis numéricos para alcanzar los objetivos planteados en el primer capítulo. Los capítulos siguientes (del 3 al 5) son los resultados de la investigación presentados como manuscritos en inglés que están actualmente publicados o en proceso de ser sometidos.

### **Capítulo 3.**

*La huella del impacto humano en el espectro de polen moderno de las tierras mayas.*

Para entender el registro paleoecológico en el contexto de la ocupación humana, es necesario estudiar la distribución del polen moderno a lo largo de gradientes de impacto humano. En este capítulo se estudian los patrones de distribución de ensambles de polen moderno a lo largo de gradientes ambientales que incluyen la influencia humana.

### **Capítulo 4.**

*Efectos de la variabilidad climática y factores de estrés antropogénicos en la vegetación de las tierras altas mayas durante el Holoceno tardío.*

Este capítulo corresponde a la reconstrucción de las dinámicas ambientales y de la vegetación de las Lagunas de Montebello, durante el Holoceno tardío. El registro paleoambiental se basó en el análisis de polen y geoquímico de dos secuencias sedimentarias lacustres de cuerpos de agua ubicados a elevaciones de entre 1450 y 1500 m s.n.m.

### **Capítulo 5.**

*Dinámica de la vegetación y disturbios del Holoceno en la Selva Lacandona, elevaciones medias de México tropical.*

Este capítulo constituye el registro paleoambiental los últimos 10,000 años en la Selva Lacandona. Al ser el registro más largo facilita la comprensión de las condiciones ambientales antes y después de la predominancia de actividades humanas. Esto permitió establecer una línea base para los procesos naturales y antropogénicos que operaron durante los últimos milenios en las montañas de Chiapas.

### **Capítulo 6.**

Los resultados principales de esta investigación fueron resumidos y sintetizados en este capítulo para luego obtener las conclusiones. Además, se plantearon recomendaciones para el futuro e incertidumbres.

# CAPÍTULO 1

## ALCANCES DE LA INVESTIGACIÓN

### INTRODUCCIÓN

La flora del sureste de México y Guatemala está entre la más diversa de los trópicos (Rzedowski 2006). Mientras las tierras bajas poseen un alto grado de endemismo (Ibarra-Manríquez et al. 2002), las tierras altas y montañosas contienen el mayor número de especies de *Pinus* y *Quercus* en el mundo (Farjon & Styles 1997; Nixon 2006). Estos patrones de diversidad son promovidos principalmente por una alta heterogeneidad de hábitats resultantes de pronunciados gradientes ecológicos y por la mezcla de vegetación proveniente de altas latitudes en Norte América y bajas en Centro y Sur América. En tal sentido, los gradientes climáticos abruptos y la presencia de una amplia variedad de ecosistemas hacen que las zonas montañosas sean convenientes para investigar los efectos del pasado, presente y futuro cambio ambiental.

Los ecosistemas de montaña han sido particularmente vulnerables a los cambios ambientales en el pasado (van't Veer & Hooghiemstra 2000). Por ejemplo, durante el Último Máximo Glacial (aproximadamente 23,000 a 18,000 años antes del presente) la temperatura media anual en la Península de Yucatán estaba 5 °C por debajo de su valor actual, lo que causó migración de especies desde tierras altas hacia elevaciones bajas (Correa-Metrio et al. 2012a). En contraste, las temperaturas altas generaron desplazamientos ascendentes de las especies vegetales y una reducción sustancial de los rangos de distribución de las especies o incluso extinción regional debido a restricciones topográficas o edáficas (Islebe & Hooghiemstra 1997; Correa-Metrio et al. 2012a). Las antiguas actividades humanas también han llevado a cambios rápidos en los ecosistemas. Durante el Holoceno tardío (los últimos 4,000 años), los cambios en los

ecosistemas de la Península de Yucatán y montañas adyacentes se han atribuido principalmente a las actividades humanas relacionadas con la antigua civilización Maya (Islebe et al. 1996; Leyden 2002; Dull 2004a; Palka 2009). Así, aparentemente el Holoceno tardío estuvo caracterizado por una disminución sustancial de la cobertura forestal regional y un aumento de la erosión como consecuencia de las actividades humanas (Leyden et al. 1993; Wahl et al. 2006; Anselmetti et al. 2007; McNeil 2012). Sin embargo, la interpretación de los paleo-registros es relativamente ambigua en lo relacionado a las interacciones hombre-clima, debido a la ausencia de métodos cuantitativos que permitan conocer la magnitud de los cambios.

Los efectos de la variabilidad climática sobre el desarrollo de las comunidades humanas han sido ampliamente documentados, en especial los efectos de El Niño/Oscilación del Sur (ENSO por sus siglas en inglés) y de sequías recurrentes (Brenner et al. 2002; Moy et al. 2002; Medina-Elizalde et al. 2010). Sin embargo, poco se conoce sobre las interacciones y mecanismos de retroalimentación existentes entre la dinámica climática y la alteración antrópica del paisaje. En este proyecto se plantea ofrecer elementos referentes a los mecanismos intermediarios dentro de la variabilidad ambiental que podrían considerarse naturales y/o antropogénicos en las elevaciones medias y altas de las tierras mayas.

La paleoclimatología y paleoecología ofrecen un enfoque holístico para cuantificar los efectos del clima y/o actividades humanas sobre la dinámica de la vegetación en el pasado (Delcourt & Delcourt 1991). Para estudiar las dinámicas temporales de un ecosistema, ambas disciplinas ofrecen información del pasado a través de indicadores sensibles a las condiciones ambientales. Una manera de evaluar las interacciones entre el hombre, clima y vegetación es a través del análisis de indicadores paleoclimáticos (e.g. geoquímica, susceptibilidad magnética y sedimentología) y paleoecológicos (e.g. polen, diatomeas y material carbonizado) de núcleos

sedimentarios lacustres. Por ejemplo, el análisis de polen, el material carbonizado y la geoquímica de los sedimentos, permiten reconstruir en conjunto la vegetación (polen), los regímenes de incendios (material carbonizado) y diferentes condiciones climáticas e hidrológicas (geoquímica y susceptibilidad magnética) de un área en particular (Delcourt & Delcourt 1991; Bradley 2015). Las secuencias sedimentarias preservan un archivo de cambios climáticos y ecológicos del pasado, convirtiéndose en una herramienta ideal para investigar las interacciones complejas entre el clima, el hombre y la vegetación. De igual manera, con este tipo de aproximaciones se podrían cuantificar los cambios ambientales a partir de relaciones funcionales construidas mediante el estudio de las relaciones modernas entre los diferentes indicadores y el ambiente (e.g. Birks 2003).

El objetivo principal de este capítulo es presentar una síntesis de los estudios paleoecológicos y paleoclimáticos que se han llevado a cabo en las tierras bajas mayas donde el acervo de información es mayor que en las tierras altas. La vegetación de las tierras bajas ha sido especialmente sensible a cambios en el clima y patrones de ocupación humana durante los últimos 10,000 años. En tal sentido, surge la incertidumbre sobre los cambios ambientales que tomaron lugar en las zonas más elevadas, como las montañas de Chiapas, durante periodos de condiciones ambientales estresantes para la vegetación. Así, se abre un camino para el establecimiento de los objetivos de investigación de este estudio.

## REVISIÓN DE LITERATURA

### HISTORIA CLIMÁTICA Y CULTURAL DE LAS TIERRAS MAYAS DURANTE EL HOLOCENO

#### 1.1. Introducción

El paisaje que se conoce hoy en las tierras mayas es el resultado de una larga y compleja historia de variabilidad ambiental a través de los últimos miles de años. La variabilidad climática y las transformaciones de la cobertura terrestre por los seres humanos han sido los principales factores que han controlado los cambios ambientales de las tierras mayas durante los últimos milenios (Beach et al. 2006; Wahl et al. 2016). Las tierras mayas se han convertido en una región de gran interés científico dada la aparente asociación entre cambios climáticos y la antigua cultura Maya como un escenario análogo a lo moderno.

La historia ambiental de los últimos cuatro milenios en las tierras mayas ha sido ampliamente estudiada a través de registros paleoambientales (e.g. Leyden 2002; Metcalfe et al. 2009) y arqueológicos (e.g. Beach et al. 2006; Palka 2014). Los registros paleoambientales se han basado en diferentes indicadores (e.g. polen, isótopos estables, material carbonizado, etc.) para documentar cambios en el clima y las coberturas terrestres del pasado. Estos elementos analíticos han aportado información del componente físico, relacionado con los diferentes eventos climáticos ocurridos durante el Holoceno (Hodell et al. 2005a; Mueller et al. 2009). Muchos de estos eventos han tenido una influencia importante en el desarrollo de las comunidades humanas y naturales (Brenner et al. 2002). En términos de los registros arqueológicos e históricos, el principal elemento de cambio en las coberturas forestales ha sido la agricultura, misma que incluye la deforestación, el cultivo, el terracedo (establecimiento de terrazas en laderas), entre otras actividades (Beach et al. 2006; McNeil 2012). Esta revisión busca sintetizar la información

paleoambiental de los registros lacustres en las tierras bajas del área Maya, donde hay un mayor acervo de información.

## **1.2. Configuración ambiental de la Península de Yucatán**

Las tierras bajas mayas incluyen la Península de Yucatán y tierras bajas adyacentes de México, Belice y Guatemala (Fig. 1.1). En términos generales, esta región se encuentra sobre un terreno kárstico compuesto por carbonatos de origen Cretácico y Cenozoico (Weidie 1985). La topografía kárstica ha favorecido la formación de un gran número de lagos y pequeñas depresiones esparcidas a lo largo de todo el territorio, mismas que han permitido la acumulación de un amplio acervo de historia ambiental del Cuaternario.

El principal enfoque de esta revisión son las tierras bajas mayas del centro y sur, de 15 a 18° latitud Norte y de 88 a 92° longitud Oeste. En esta región, el clima es influenciado por la migración estacional de la Zona de Convergencia Intertropical (ITCZ siglas en inglés) y las variaciones en la masa de agua cálida del Atlántico (Wang et al. 2006). De tal forma, se presentan una temporada húmeda de mayo a noviembre y una seca de diciembre a mayo. La precipitación por su parte incrementa de norte a sur (500 a 4000 mm/año) (Deevey et al. 1980).

La región también se encuentra influenciada por la actividad de El Niño-Oscilación del Sur (ENSO siglas en inglés) que causa variabilidad interanual en la precipitación (Magaña et al. 2003). La fase cálida de ENSO es conocida como El Niño, y demarca un debilitamiento de los vientos alisios, permitiendo que las aguas tropicales se acumulen hacia el Pacífico este (Trenberth 1997). Esta acumulación de agua cálida afecta el gradiente de temperatura, dificultando el desplazamiento hacia el norte de la ITCZ. En términos

generales, los eventos de El Niño provocan una disminución de la precipitación de verano durante la mitad de la estación lluviosa. En contraste, la fase fría del ENSO (La Niña) provoca que las lluvias invernales aumenten, asociadas al desplazamiento hacia el sur de la corriente del jet subtropical y aumentando el número de “Nortes” sobre el Golfo de México e incluso sobre la Península de Yucatán (Magaña et al. 2003). Los Nortes son masas de vapor de agua polares que al pasar por el Golfo de México se cargan de humedad, y que resulta en un aumento de la precipitación invernal y descensos en la temperatura (Romero-Centeno et al. 2003).

La Península de Yucatán se destaca por su alto número de especies arbóreas endémicas (72 especies), junto a sus particulares tipos de suelo, clima, fisiografía, orografía, hidrogeología y fauna (Islebe et al. 2015). Diferentes estudios han demostrado la alta afinidad en la flora de la Península con las tierras bajas de Centroamérica (Estrada-Loera 1991; Ibarra-Manríquez et al. 2002). Esta región presenta una clara división geográfica entre las zonas del norte y sur, resultando en heterogéneas distribuciones de especies (Espadas-Manrique et al. 2003). En general, la vegetación varía según la precipitación recibida. El patrón biogeográfico general de la Península muestra un gradiente sur-norte desde el bosque tropical lluvioso al bosque de matorrales con estadios intermedios de bosques estacionales, semidecíduos y deciduos (Ibarra-Manriquez & Oyama 1992; Rzedowski 2006). En las montañas adyacentes, se encuentran tres tipos de vegetación de menor a mayor elevación: bosque mesófilo de montaña, bosque de *Quercus* y bosques de coníferas (Rzedowski 2006).



**Figura 1.1.** Mapa de las tierras bajas mayas de Mesoamérica y localización de sitios discutidos en el documento. Los puntos corresponden a lagos con registros sedimentarios bien definidos: 1) Lago Petén Itzá, 2) Laguna Quexil, 3) Laguna Salpetén, 4) Lago Puerto, 5) Lago Paixban, 6) Laguna del Río Nuevo, 7) Laguna Chichancanab, y 8) Punta Laguna.

### 1.3. El marco cronológico de la evolución ambiental y cultural de las tierras mayas

Los estudios paleoambientales han logrado asignar un contexto cronológico a las reconstrucciones basado en dataciones radiométricas de archivos naturales (e.g. sedimentos lacustres, espeleotemas, anillos de crecimiento en árboles, etc), principalmente de radiocarbono ( $^{14}\text{C}$ ). Así, las edades de radiocarbono son reportadas como edades calibradas antes del presente (AP, siendo 1,950 el presente). Para efectos comparativos y coherencia

con fuentes paleoambientales, las fechas presentadas en esta revisión son convertidas a edades AP o ka para miles de años. En la escala de tiempo geológica, el Holoceno, dentro del cual se enmarca este trabajo, corresponde al periodo de la historia de la Tierra que cubre aproximadamente los últimos 11,700 años (Roberts 1998). Se ha considerado la siguiente subdivisión geológica del Holoceno, basada en los mayores eventos de cambio ambiental: Grinlandiense (Holoceno temprano, 11,700 – 8,200 AP), Nordgripiense (Holoceno medio, 8,200 – 4,200 AP) y Megalayense (Holoceno tardío, 4,200 AP al presente).

En estudios arqueológicos, las unidades temporales son seleccionadas del registro cultural prehistórico ancladas a las dataciones de radiocarbono. Así, la cronología de la prehistoria de Mesoamérica comienza con el periodo Paleoindio desde el arribo del hombre a las Américas, el cual se extiende hasta el Arcaico que va de 10,200 a 4,500 AP. En la cronoestratigrafía cultural Maya, el tiempo asociado al Arcaico se conoce como el “Precerámico”, el cual se refiere a una etapa de desarrollo antes del uso de las cerámicas y el establecimiento de villas. Posteriormente, conforme se fueron organizando las comunidades mayas y cambiaron sus actividades y costumbres, se establecieron los siguientes periodos estandarizados: 1) Preclásico (ca. 4,500 – 1,750 AP, 2,000 ANE – 250 NE), 2) Clásico (1,750 – 1,050 AP, 250 – 900 NE), y 3) Posclásico (1,050 - 450 AP, 900 – 1,500 NE). Estos periodos fueron delimitados basados en cambios en el desarrollo de las civilizaciones mesoamericanas. La expansión de la agricultura y el surgimiento de las primeras ciudades fueron los sucesos más destacados del Preclásico (Sharer & Traxler 2006). El desarrollo de la agricultura fue un elemento clave para que en el Periodo Clásico prosperaran y se expandieran los principales centros cívicos mayas. Sin embargo, para la transición Clásico Terminal-Posclásico (1,100-900 AP, 850 – 1,050 NE) la mayoría de centros cívicos se desplomaron como estructura social, constituyendo el evento

comúnmente conocido como el “Colapso Maya” (Adams 1973). Posteriormente, para finales del Posclásico (600 – 450 AP, 1,350 – 1,500 NE) se ha documentado la reestructuración de algunos asentamientos distribuidos principalmente hacia las tierras bajas del norte. A pesar de la aparente recuperación en el Posclásico Tardío, el desarrollo de los asentamientos mayas fue interrumpido nuevamente durante el Periodo Colonial y La Conquista, caracterizados por una pérdida importante de la población nativa (Demarest 2004; Sharer & Traxler 2006).

#### **1.4. Historia ambiental del Holoceno**

El Holoceno es considerado un interglacial que inicia alrededor de 11,700, aunque el aspecto fundamental que contrasta con otros interglaciales del Pleistoceno es la marca del hombre que se impone en la época actual. El inicio del Holoceno se caracterizó por una transición rápida de un periodo frío a un periodo cálido (Fig. 1.2). Los registros tropicales de las tierras bajas del Petén, en el norte de Guatemala (Fig. 1.1) ofrecen información sobre el cambio climático y sus efectos sobre los ecosistemas terrestres durante la transición Pleistoceno/Holoceno. Estos registros incluyen el análisis sedimentario de los lagos Petén Itzá (Hillesheim et al. 2005; Correa-Metrio & Bush 2012), Quexil (Deevey et al. 1979; Leyden 1984) y Salpetén (Leyden 1984, 2002). En términos generales, los espectros de polen y las propiedades sedimentarias de los diferentes lagos, indican la dominancia de bosques templados, niveles bajos en los lagos y condiciones secas antes de ca. 11,100 AP. El bosque tropical se estableció en ca. 11,100 AP (Leyden 1984; Hillesheim et al. 2005; Correa-Metrio et al. 2012a), aunque las propiedades sedimentarias indicaban varios ciclos de humedad-sequía, sugiriendo distintos cambios en la humedad efectiva. La transición

hacia condiciones húmedas se completó en ca. 10300 AP, cuando las condiciones húmedas del Holoceno temprano fueron más persistentes (Hillesheim et al. 2005; Metcalfe et al. 2009).

Durante el Holoceno el ser humano se ha adaptado en una variedad de formas a los cambios ambientales. Desde su probable arribo a las Américas ca. 25,000 – 15,000 AP, se han registrado diferentes adaptaciones desde el hemisferio Norte hasta el Sur (Meltzer 1997; Braje et al. 2017; Moreno-Mayar et al. 2018). Después de pasar el último periodo glacial en zonas templadas y secas, donde la cobertura forestal era mucho menor que ahora, los humanos se encontraron en circunstancias ecológicas nuevas. Los bosques tropicales se fueron expandiendo para el final de esta transición, y surgieron nuevas estrategias para vivir en estos hábitats en un plazo bastante corto (Roberts 1998).

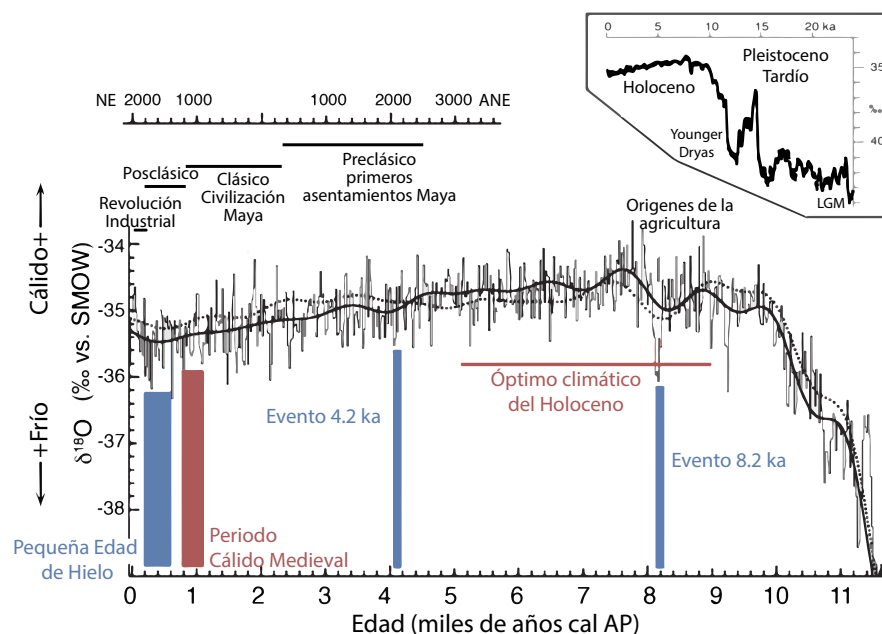


**Figura 1.2.** Registros isotópicos de núcleos de hielo de Groenlandia (Johnsen et al. 2001), eventos climáticos, y cronología Maya, para el Holoceno.

#### *1.4.2. Holoceno temprano (11,700 – 8,200 AP)*

Aunque durante el Pleistoceno se presentaron fluctuaciones climáticas de gran magnitud, el Holoceno también se ha caracterizado por presentar eventos climáticos importantes asociados a cambios en la temperatura polar, en la disponibilidad de humedad en los trópicos y cambios en la circulación atmosférica (Mayewski et al. 2004). El principal mecanismo de cambio en los sistemas tropicales corresponde al sistema climático regional afectado por posición media de la ITCZ la cual, durante el Holoceno temprano, se localizaba más al norte (Haug et al. 2001). El inicio del Holoceno fue testigo del comienzo de procesos ambientales que han continuado hasta el presente (e.g formación de suelos, sucesión de plantas, ontogenia de lagos y migración de fauna) (Roberts 1998). También, durante este periodo se establecieron condiciones más húmedas en el norte del Neotrópico y los bosques tropicales de las tierras mayas (Curtis et al. 1998; Leyden 2002; Hillesheim et al. 2005; Correa-Metrio et al. 2012a).

La presencia de capas de carbonatos en secuencias sedimentarias del Lago Petén Itzá (Hillesheim et al. 2005) e incrementos del  $\delta^{18}\text{O}$  de estalagmitas del sureste de México (Bernal et al. 2011), mostraron la incidencia de sequías en Centroamérica en 9,400 y 8,200 AP. Tales eventos coincidieron con una disminución en la temperatura inferida a partir de bajos valores del  $\delta^{18}\text{O}$  en el núcleo de hielo GISP2 (Johnsen et al. 2001) y variaciones en la abundancia de granos de hematita teñidos (HSG, por sus siglas en inglés) encontrados en núcleos del Atlántico Norte (Bond et al. 2001). El porcentaje de HSG es considerado un indicador de los cambios en la cantidad y trayectoria de grandes masas de hielo que circulan en la superficie del Atlántico Norte (Bond et al. 2001), sugiriendo enfriamientos del Atlántico Norte. Los eventos secos anteriormente mencionados pudieron tener una

relación con enfriamientos del Atlántico Norte, asociados a un desplazamiento hacia el sur de la ITCZ. Por ejemplo, el evento seco en ca. 8,200 AP coincide con el enfriamiento más prolongado en el Hemisferio Norte desde el Younger Dryas (Fig. 1.2). De hecho, capas de carbonatos encontradas en sedimentos de los Lagos Paixban y Petén Itzá ofrecen evidencia que Yucatán fue más seco en 8200 AP (Hillesheim et al. 2005; Wahl et al. 2016). También, el registro de polen muestra que durante este evento, los porcentajes de taxa forestales disminuyeron y las concentraciones de polen fueron menores que el resto del periodo (Wahl et al. 2016). A pesar de que no se conocen con exactitud los mecanismos que activaron este cambio de carácter aparentemente global, se conjetura una disminución sustancial de la luminosidad solar y la descarga de agua del deshielo de los glaciales al Atlántico Norte (Bond et al. 2001; Cheng et al. 2009).

De acuerdo con los registros de polen fósil, el Holoceno temprano se caracterizó en esta región por la sustitución de *Pinus*, *Quercus*, y otros taxa de bosques templados por elementos de bosques tropicales como Moraceae, *Brosimum* y *Alchornea* (Islebe et al. 1996; Leyden 2002; Correa-Metrio et al. 2012a). Las asociaciones tropicales no se desarrollaron por completo hasta más tarde, por lo que quizás los bosques del Holoceno temprano carecen de análogos modernos (Leyden 2002). Una mayor disponibilidad de humedad unida a eventos fríos registrados en Centroamérica durante el Holoceno temprano, pudieron haber favorecido la dominancia de especies de Moraceae. Algunas especies de la familia Moraceae como *Brosimum aliscatrum* pueden soportar temperaturas más bajas que otros taxa tropicales (Miranda & Hernández 1963).

La historia de incendios inferida a partir del registro de material carbonizado del Lago Petén Itzá sugiere un periodo de alta frecuencia de incendios en Mesoamérica entre 10,500 y 5,000 AP (Correa-Metrio et al. 2012a). El incremento de los incendios se atribuye

a incrementos en la temperatura y la estacionalidad relacionada con la máxima insolación durante el Holoceno temprano y medio, así como por la mayor disponibilidad de biomasa como combustible (Hillesheim et al. 2005; Correa-Metrio & Bush 2012). Los diferentes registros sugieren que los cambios en la vegetación y en el patrón de incendios durante este periodo son principalmente una consecuencia del clima, dada la ausencia de indicadores de ocupación humana en la región.

#### *1.4.3. Holoceno medio (8,200 – 4,200 AP)*

Las condiciones húmedas persistieron durante gran parte del Holoceno medio, aunque se han identificado algunos eventos de sequía entre 6,900 y 5,800 AP, principalmente en San José Chulchacá, al norte de la Península de Yucatán (Leyden 2002). Probablemente, en los alrededores de Petén Itzá también se experimentaron estas sequías, aunque los cambios hacia vegetación seca son interpretados como un efecto del impacto antrópico (Islebe et al. 1996). A lo largo del Holoceno, los registros de polen del norte de Petén muestran la dominancia de bosques tropicales y riparios como una respuesta a una mayor disponibilidad de humedad (e.g. Islebe et al. 1996; Leyden 2002; Wahl et al. 2006; Wahl et al. 2016).

Evidencias paleoecológicas y arqueológicas sugieren que en las tierras bajas mayas la forma de vida de los pobladores humanos cambió alrededor de 7,000 AP, pasando de cazadores y recolectores a una dependencia de alimentos derivados de plantas domésticas (Piperno 2006; Palka 2014). Esto marcó el periodo en el cual los humanos asumieron el papel de agricultores. La evidencia palinológica indica que el Holoceno medio estuvo fuertemente influenciado por la agricultura temprana en diferentes regiones de las tierras bajas mayas entre 4,600 y 5,300 AP (Pohl et al. 1996; Wahl et al. 2006) y en las costas de

Veracruz alrededor de 7,600 AP (Pope et al. 2001). De hecho, la domesticación y propagación de cultivos nativos importantes como maíz (*Zea spp*) y calabaza (e.g. *Cucurbita moschata* Duchesne) en Centroamérica ocurrió entre 10,000 y 5,000 AP (Piperno 2006). Sin embargo, el incremento de los incendios aparentemente relacionados con la actividad humana, también podrían ser el resultado de una tendencia hacia condiciones más secas (Mueller et al. 2009; Schüpbach et al. 2015). Así, la extensión y magnitud de las actividades humanas durante el Holoceno medio aún son inciertas.

Durante el Holoceno medio (ca. 5800 AP) se reactivaron e intensificaron los eventos El Niño (Moy et al. 2002; Conroy et al. 2008). Debido a las limitaciones de los registros lacustres para diferenciar variabilidad climática anual o interanual, los eventos relacionados con ENSO pueden pasar desapercibidos, aunque periodos marcados por alta frecuencia de esta anomalía tienden a promediar en condiciones secas (Magaña et al. 2003). Por ello, el registro de ENSO durante el Holoceno depende de registros anualmente laminados como espeleotemas o sedimentos de alta resolución. En la actualidad, los registros paleoclimáticos de alta resolución temporal provienen principalmente de espeleotemas en el sureste de México y norte de Yucatán (e.g. Medina-Elizalde et al. 2010; Bernal et al. 2011). El ENSO ha sido un importante mecanismo causante de la variabilidad en la precipitación durante el Holoceno medio y temprano, así como del establecimiento de las condiciones climáticas modernas en México.

#### *1.4.4. Holoceno tardío (de 4,200 AP al presente)*

La transición Holoceno medio - Holoceno tardío estuvo caracterizada por un evento de aridez ca. 4,200 AP (Fig. 1.2) en latitudes medias y bajas (Walker et al. 2012). Este fue un fenómeno climático generalizado que se reflejó en diferentes registros del Norte América y varias partes de Asia, África y América del Sur (Mayewski et al. 2004). Es posible que el mecanismo causante de este evento fuera la migración hacia el sur de la ITCZ, pudiendo explicar la aridez de las latitudes bajas y siendo consistente con el incremento de la fuerza de los vientos alisios sobre el Atlántico Norte. Este evento también coincide con enfriamientos del agua superficial del Atlántico Norte (Bond et al. 1997) aunque no se ha registrado como tal en Centroamérica. Diversos registros paleoambientales de las tierras bajas señalan un cambio rápido de la vegetación caracterizado por pérdidas importantes de la cobertura forestal e incrementos en las tasas de erosión de los suelos, entre 4,500 y 3,500 AP (Anselmetti et al. 2006; Mueller et al. 2009). Es probable que los cambios abruptos en la vegetación en esta región fueran el resultado del estrés climático ocurrido ca. 4,200 AP, sumado al incremento de asentamientos y la gran demanda de recursos de las comunidades mayas antiguas (Beach et al. 2006; Sharer & Traxler 2006). En cualquier caso, las causas de la pérdida de vegetación y demás impactos ambientales en la región son actualmente temas de debate (e.g. Battistel et al. 2018).

Las pérdidas de cobertura forestal y la expansión de asentamientos mayas empezaron a lo largo del Preclásico (de 4,200 a 1,750 AP; de 2,250 a 200 ANE). Posteriormente, para el Clásico, los mayas necesitaron de gran cantidad de recursos naturales para construir prominentes centros cívicos como el Mirador y Tikal, en el Petén guatemalteco, y Cerros en el Norte de Belice (Palka 2009; Nations 2010). De hecho, los

centros y asentamientos humanos crecieron y se expandieron abruptamente, especialmente en las tierras bajas entre 1,750 y 1,000 AP (200 y 950 NE). Para este periodo los registros paleoecológicos sugieren una alta transformación de la vegetación sintetizada a través de procesos de deforestación y quemas agrícolas (Islebe et al. 1996; Wahl et al. 2006). Los registros arqueológicos en Tikal, uno de los mayores centros ceremoniales de las tierras bajas, también sugieren una deforestación generalizada durante el Clásico (e.g. Lentz & Hockaday 2009). Después del apogeo Maya (con una duración de alrededor 600 años), éstos colapsaron como civilización al final del periodo Clásico (Sharer & Traxler 2006). Las grandes ciudades fueron abandonadas y la estructura estatal se desplomó entre 1,150 y 950 AP (800 y 1,000 NE), constituyendo el Periodo Clásico Terminal (PCT), asociado al evento histórico conocido como el “Colapso Maya” (Adams 1973).

Las causas del colapso aún se debaten, y van desde alteraciones naturales como la ocurrencia de sequías severas y alta actividad volcánica, hasta sociales como la mala gestión ambiental por parte de las comunidades. Desde los 90s, la investigación paleoambiental ha ofrecido una fuerte evidencia que relacionan el Colapso Maya en el Petén con las sequías de las tierras bajas durante el PCT (Fig. 1.3, Hodell et al. 1995; Medina-Elizalde et al. 2010; Bhattacharya et al. 2015). De hecho, registros paleoambientales del norte de la Península sugieren que la sequía del PCT no consistía en una mega sequía de casi 200 años como se pensaba, sino que consistió en una serie de eventos secos separados por condiciones relativamente húmedas (Hodell et al. 2005a). De igual manera, las sequías recurrentes durante el PCT fueron encontradas en registros paleoclimáticos de la Punta Laguna (Hodell et al. 2007) y la cuenca de Cariaco al norte de Venezuela (Haug et al. 2003), sugiriendo un alcance regional del fenómeno. Estos eventos secos ocurrieron durante la transición climática hacia condiciones cálidas enmarcadas en el

Periodo Cálido Medieval (MWP, por sus siglas en inglés) entre 900 y 600 AP (1,050 y 1350 NE) (Fig. 1.2). De acuerdo con la documentación histórica, el MWP fue un ciclo de calentamiento en Europa y oriente de Norte América, pero con enfriamientos en el norte del Pacífico (Gornitz 2009). En Centroamérica el MWP estuvo caracterizado por anomalías climáticas (Correa - Metrio et al. 2016), que pudieron amplificar las sequías asociadas con el PCT, llevando a la fase terminal del evento (deMenocal 2001). Diferentes investigaciones han refutado tal hipótesis, tomando en cuenta que los mayas crecieron como civilización cuando afrontaban un periodo de incremento de aridez durante el Holoceno medio, al cual estas comunidades mostraron adaptación (Sharer & Traxler 2006).

Luego de los efectos del calentamiento en el MWP ocurrió un cambio hacia condiciones frías enmarcadas en un periodo conocido como la Pequeña edad de Hielo (LIA, por sus siglas en inglés), caracterizado por una disminución de la temperatura entre 500 y 275 AP (1,450 y 1,675 NE) (Fig. 1.2), y conectado con los mínimos de actividad solar Maunder y Spörer (Bradley 2015). En la Península de Yucatán y gran parte del Caribe, cerca del inicio de la LIA se presentaron condiciones de aridez (Hodell et al. 2005b). Los espectros de polen del Cenote San José Chulchacá mostraron una disminución de los bosques tropicales dominados por *Brosimum*, indicando una disminución sustancial de la humedad (Leyden 2002). También la señal de isótopos de oxígeno de los Lagos Chichancanab y Salpetén mostró cambios durante la LIA, sugiriendo dominancia de condiciones secas (Hodell et al. 2005a). En contraste, el registro de múltiples indicadores del Lago Verde en los Tuxtlas-México, indica condiciones húmedas alrededor de este periodo (e.g. incrementos del nivel del lago y expansión de la vegetación tropical) (Lozano-García et al. 2007). Tal discrepancia es explicada por la amplia heterogeneidad topográfica

de los Tuxtlas que sirvió como zona de amortiguamiento para reducir la intensidad y duración de la larga estación seca que caracterizó a LIA.

Durante los últimos 800 años, que representan el Periodo Posclásico y el Periodo Colonial, los bosques de las tierras bajas presentaron una recuperación, mientras los incendios disminuyeron en ausencia de grandes poblaciones humanas y actividades agrícolas. Algunos investigadores sugieren que la recuperación del bosque ocurrió durante el Posclásico dado que las representantes de vegetación cerrada dominaron los espectros de polen para este periodo (e.g. *Brosimum*, Moraceae, *Ficus* y Sapotaceae) (e.g. Curtis et al. 1998; Wahl et al. 2006; Mueller et al. 2010). Así mismo, datos geoquímicos y sedimentológicos del Lago Petén Itzá mostraron una reducción sustancial de la erosión seguido por la estabilización de los suelos debido a una mayor cobertura forestal (Mueller et al. 2010). Los registros históricos dan cuenta de la presencia de selvas exuberantes durante el periodo de colonización entre 420 y 200 AP (1,520 y 1,750 NE) (Palka 2009). Durante la colonización, la recuperación de la vegetación fue interrumpida por la extracción de madera y tala de los bosques para sostener el desarrollo de las colonias europeas. Finalmente, a través del siglo XX se presentó una recuperación transitoria de los bosques en algunas regiones de la Península de Yucatán, más como un resultado de las políticas de conservación modernas (Bray & Klepeis 2005).

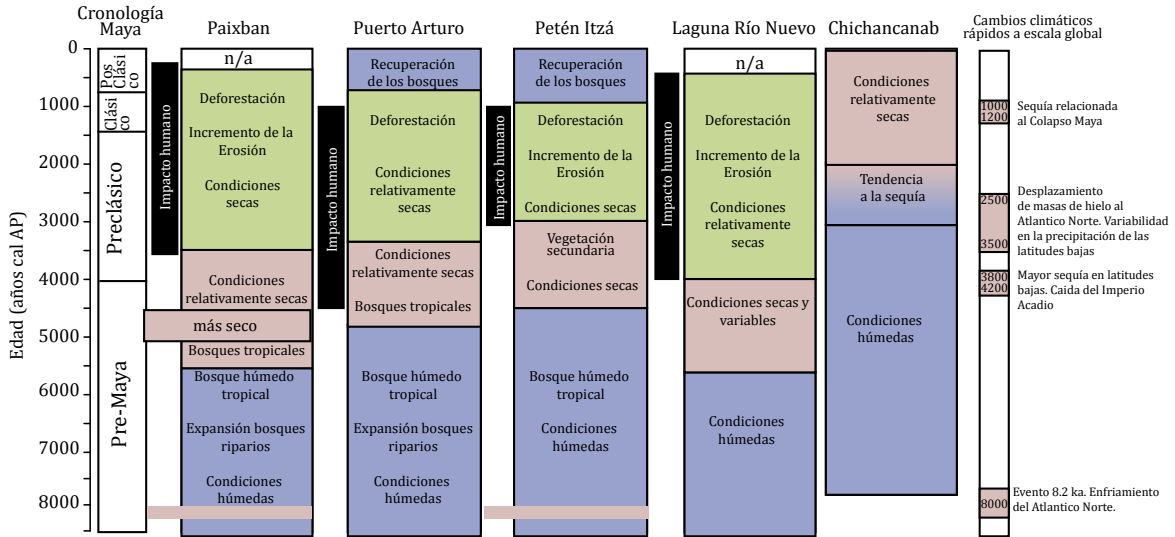


**Figura 1.3.** Resumen de la interpretación de los principales registros paleoambientales de las tierras bajas mayas. Reconstrucciones del Lago Paixban (Wahl et al. 2016), Lago Puerto Arturo (Wahl et al. 2006), Lago Petén Itzá (Curtis et al. 1998; Mueller et al. 2009), Laguna Río Nuevo (Metcalf et al. 2009), y el Lago Chichancanab (Hodell et al. 2005a). En el extremo derecho se presentan los principales eventos de cambio climático rápido a escala global (Mayewski et al. 2004).

## 1.5. Conclusiones

Estudios paleoambientales de las tierras bajas mayas revelan un registro continuo de cambios culturales, en el clima y en la vegetación durante el Holoceno. Sin embargo, existen otros enfoques para la reconstrucción del pasado que deben ser tomados en cuenta en cualquier reconstrucción paleoambiental. La correlación temporal de los registros paleoecológicos y arqueológicos/históricos para reconstruir con mayor precisión los efectos de las actividades humanas sobre el paisaje representan un desafío mayor para la comunidad científica (Gaillard et al. 2015). La dificultad de unir estos registros subyace en que las resoluciones temporales y espaciales entre diferentes tipos de líneas de evidencia varían fuertemente. Así mismo, surge la necesidad de obtener reconstrucciones

cuantitativas de los cambios ambientales en el pasado, tomando en cuenta que las tierras mayas se caracterizaron por ser escenario de cambios fuertes en la vegetación, clima e impacto humano.

La reconstrucción paleoambiental basada en registros localizados en las tierras bajas (Fig. 1.3) sugiere la dominancia de condiciones secas durante la transición Pleistoceno-Holoceno. Posteriormente, se presentó un cambio abrupto hacia condiciones húmedas durante el Holoceno temprano, las cuales redundaron en el llenado de diferentes lagos, así como la dominancia de bosques tropicales en la región. Estos cambios han sido atribuidos en gran medida al desplazamiento de la ITCZ hacia el norte y un clima menos estacional que el presente (Haug et al. 2001). Las condiciones húmedas persistieron hasta el Holoceno medio, periodo durante el cual aumentó de la variabilidad climática y se presentaron condiciones secas. Para el Holoceno tardío, se evidenciaron diferentes eventos secos en la región, aunque no fue un proceso generalizado. Los periodos de máxima ocupación humana durante el Holoceno tardío, se caracterizaron por una deforestación extensiva en la región. Durante los últimos 800 años, algunas regiones de las tierras mayas han experimentado una recuperación sustancial de los bosques. Sin embargo, en áreas como el norte de Yucatán, persistió la alteración de los ecosistemas forestales por actividades humanas sin permitir su recuperación.

Finalmente, la historia ambiental de la región sugiere que es muy probable que el origen de los bosques mayas esté conectado a variaciones de condiciones secas y húmedas que limitaron las dinámicas de la antigua civilización Maya. En tal sentido, se destaca la íntima relación entre el clima y el hombre, la cual fue reflejada en cambios de estructura y composición del bosque durante los últimos milenios.

## OBJETIVOS DE LA INVESTIGACION

Este trabajo busca ofrecer información sobre la respuesta de las comunidades de plantas a los cambios en el clima y uso del suelo, usando información paleoambiental de varios sitios e indicadores. De esta forma el presente estudio comprende la evolución de la vegetación en las montañas de Chiapas durante los últimos 10,000 años, enfatizando los efectos potenciales de cambios en el clima y patrones de ocupación humana. Para lograr esta meta se plantearon tres diferentes etapas que obedecieron a los siguientes objetivos particulares.

i) Evaluar las relaciones entre ensambles de polen moderno y atributos ambientales (e.g. clima e impacto humano) con el fin de evaluar la habilidad del polen en reflejar diferentes gradientes ecológicos y ambientales.

ii) Analizar dos secuencias sedimentarias provenientes de sitios contrastantes dentro de las montañas de Chiapas, para reconstruir las dinámicas ambientales y de la vegetación durante el Holoceno.

iii) Usar las relaciones entre el polen moderno y los atributos del ambiente como complemento de los registros fósiles para obtener una reconstrucción objetiva de las dinámicas ambientales regionales que incluyen el clima y el impacto humano.

## HIPÓTESIS

Las hipótesis que sirven como línea base para la investigación se presentan a continuación, estas están divididas en una hipótesis de trabajo y otra conceptual y metodológica.

### i) Hipótesis de trabajo

Dados los cambios en el régimen climático que sucedieron durante el Holoceno temprano y medio en la región Maya (Hodell et al. 2007), las montañas de Chiapas experimentaron un cambio de bosques húmedos tropicales a bosques estacionales. Estos últimos facilitaron el establecimiento de comunidades humanas, mismas que ejercieron su influencia sobre su composición y estructura.

### ii) Hipótesis conceptual y metodológica

El razonamiento clásico en estudios paleoecológicos entiende los cambios en la vegetación a través del tiempo como una suma de factores endógenos y exógenos (e.g. el clima, las actividades humanas y la misma dinámica de los ecosistemas) (Delcourt & Delcourt 1991). Dicha generalización se puede resolver con el uso de diferentes líneas de evidencia fósil asociadas a diferentes condiciones ambientales como el polen, la geoquímica y el material carbonizado en los sedimentos. Así, es posible, en escalas de tiempo prehistóricas, diferenciar individualmente los efectos de los diferentes factores que estructuran la vegetación.

## CAPÍTULO 2

### MATERIALES Y MÉTODOS

#### **2.1. Área de estudio**

Este estudio se desarrolló en las montañas de Chiapas en el Sureste de México, pertenecientes a la provincia fisiográfica denominada Sierras de Chiapas y Guatemala, aproximadamente entre las coordenadas 17.5° a 16.0° latitud Norte y 91.0° a 93.0° longitud Oeste (Fig. 2.1A). En esta región se reconocen tres subregiones fisiográficas (Müllerried 1957): (1) Los Altos de Chiapas con alturas desde ~1500 hasta 2800 m s.n.m.; (2) La Sierra Lacandona, que consta de serranías paralelas de altitud variada que fluctúa entre 500 y 1500 m s.n.m.; (3) el abrupto sistema de montañas del Norte (con cimas hasta los 2200 m s.n.m.). En el contexto geológico, las montañas de Chiapas se localizan en la provincia tectónica de Fallas de Transcurrencia de Cinturón Chiapaneco de Pliegues y Fallas (Ortega-Gutiérrez et al. 1992). Esta región hace parte de la cuenca hidrográfica Grijalva-Usumacinta, en donde abundan cuerpos lacustres permanentes producto del pasaje kárstico que caracteriza la región. La mayoría de los cuerpos lacustres se encuentra en la Selva Lacandona (Sierra Lacandona) y el Parque Nacional Lagunas de Montebello (Altos de Chiapas), ofreciendo una oportunidad excepcional para el estudio de la dinámica ambiental del pasado a través del estudio de secuencias sedimentarias lacustres.

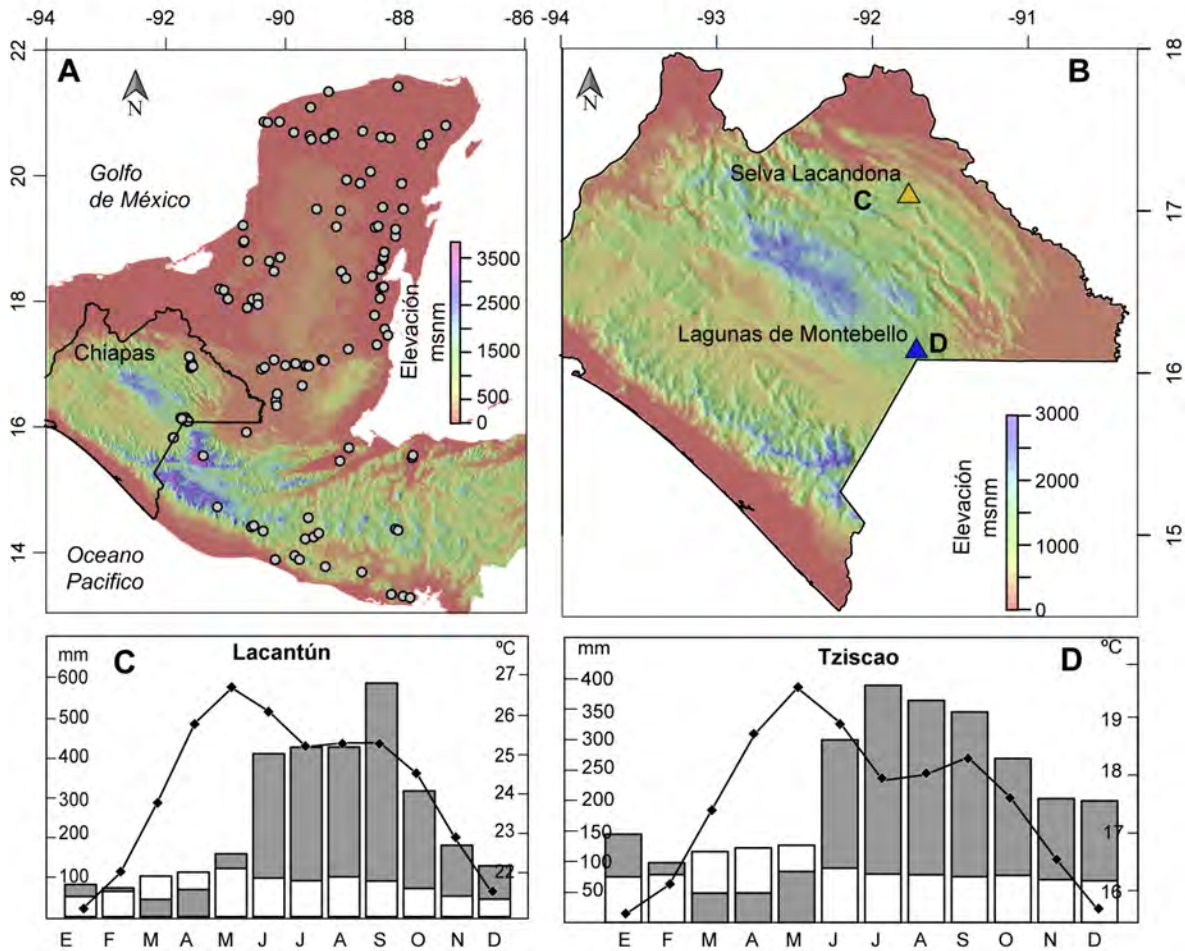


**Figura 2.1.** **A.** Mapa de localización de las montañas de Chiapas y distribución de muestras superficiales. **B.** Localización de los núcleos sedimentarios de la Selva Lacandona (triángulo amarillo) y el Parque Nacional Lagunas de Montebello (triángulo azul). Información climática; precipitación mensual (barra gris), evapotranspiración potencial (barra blanca) y temperatura media mensual (línea negra) extraída de las estaciones meteorológicas **C.** Lacantún en la Selva Lacandona y **D.** Tzisco en el Parque Nacional Lagunas de Montebello (Servicio Meteorológico Nacional, 2017).

### 2.1.1. Selva Lacandona

Las Selva Lacandona se localiza al sureste de Chiapas y representa la subprovincia fisiográfica conocida como la Sierra Lacandona ( $16.95^{\circ}$  N,  $91.60^{\circ}$  O, Fig. 2.1B). Esta zona está conformada por varias serranías paralelas con elevaciones que fluctúan entre los 300 y 1500 m s.n.m., constituidas principalmente por rocas calizas y areniscas de origen

Cretácico y Terciario respectivamente (Tejada-Cruz et al. 2009). El clima dominante en la Selva Lacandona es cálido sub-húmedo con lluvias en verano según la clasificación de Köppen modificado por García (1998). De acuerdo con los datos de la estación meteorológica Lacantún (Servicio Meteorológico Nacional, 2017a), la temperatura media anual es de 21.8 °C, con un mínimo medio mensual de 19.4 °C en enero y máximo de 23.7 °C durante mayo y junio (Fig. 2.1C). La precipitación media anual es de 1932 mm, de los cuales 1716 mm se distribuyen entre mayo y diciembre, y los 146 mm restantes en la temporada seca entre enero y abril.

La conjunción del clima regional y una alta heterogeneidad del paisaje produce un mosaico de vegetación compuesto por vegetación tropical y templada. Los principales tipos de vegetación son el bosque lluvioso tropical (BLT), bosque lluvioso de montaña baja (BLMB), bosque lluvioso de montaña (BLM), y bosque de Pino-Encino (BPE) (Breedlove 1981). Estos tipos de vegetación han sido influenciados por una larga historia de disturbios naturales y antropogénicos que han promovido la expansión de vegetación secundaria en la región (Hernández-Nava 2003). El BLT y BLMB corresponden al tipo de vegetación dominante en la Selva Lacandona, los cuales se extienden a lo largo de gradientes de elevación que van de 300 a 800 m s.n.m. Ambos tipos de bosque presentan una composición florística similar, aunque el BLMB presenta un dosel de menor altura. Los árboles dominantes para estas asociaciones son principalmente: *Alchornea latifolia*, *Brosimum alicastrum* Sw., *Calophyllum brasiliense*, *Pseudomedea oxiphyllaria*, *Swietenia macrophylla* y *Terminalia amazonia* (Pennington & Sarukhán 2005; CONABIO 2013). El BLM también llamado bosque mesófilo de montaña ó bosque montano de niebla (Hamilton et al. 1995; Rzedowski 2006) se caracteriza por la coexistencia de especies de latifoliadas y coníferas. Estos bosques se establecen principalmente en las laderas y crestas

de las montañas, en altitudes por encima de 900 m s.n.m. Algunas especies típicas del BLM son *Clethra* spp., *Clusia* spp., *Hedyosmum mexicanum*, *Myrica cerifera*, *Podocarpus matudai*, *Ulmus mexicana* y varias especies de *Pinus* y *Quercus* (Hernández-Nava 2003). Cabe mencionar que estas asociaciones incluyen árboles deciduos y semideciduos como *Liquidambar styraciflua* L., *Nissa sylvatica*, *Sapium* sp. y *Styrax* spp. (CONABIO 2013). El BPE ocupa sitios por encima de los 1000 m s.n.m, principalmente en las cumbres de las montañas y áreas con baja disponibilidad de humedad. Este tipo de vegetación es dominada por pocas especies de pinos (e.g. *Pinus maximinoi* y *P. oocarpa*), acompañados en una menor representación por encinos (e.g. *Quercus benthamii* y *Q. crassifolia*). Al BPE también se encuentran asociados *Ardisia* sp., *Eugenia* sp., e *Ilex brandegeana*. Bajo condiciones de alto disturbio es común encontrar en la Selva Lacandona grandes manchones de vegetación secundaria dominados por *Acacia pennatula*, *Bursera simaruba*, *Ceiba pentandra* y *Cecropia* spp., así como varias especies de las familias Asteraceae y Poaceae (Hernández-Nava 2003; Pennington & Sarukhán 2005).

### 2.1.2. Parque Nacional Lagunas de Montebello

El Parque Nacional Lagunas de Montebello corresponde a un área natural protegida de ~ 6200 ha localizada en los Altos de Chiapas, con elevaciones de entre 1400 y 1700 m s.n.m. (16.12° N, 91.73° O, Fig. 2.1B). El clima regional dominante es semicálido con presencia de abundantes lluvias en verano (García 1998). De acuerdo con los datos de la estación meteorológica Tzisco (Servicio Meteorológico Nacional, 2017b), la temperatura media anual es de 17.5°C, con una mínima de 15.6°C en enero y máxima de 19.5 en mayo. La

precipitación anual alcanza un promedio de 2500 mm, con la estación seca ocurriendo entre marzo y mayo (Fig. 2.1D).

El parque Nacional Lagunas de Montebello se caracteriza por albergar un mosaico de vegetación regional altamente diverso que se podría generalizar en tres tipos de vegetación: Bosque de pino (BP), bosque de pino-encino-*Liquidambar* (BPEL) y bosque lluvioso de montaña (BLM) (Breedlove 1981; Rzedowski 2006). El BP es común en áreas perturbadas o sujetas a temperaturas extremas, alta radiación solar, y/o baja humedad en los suelos (Ramirez-Marcial et al. 2010). El BPEL se localiza al Este del Parque, y se caracteriza por una mezcla de elementos de coníferas con especies de latifoliadas, que incluyen *Pinus oocarpa*, *P. maximinoi*, *Liquidambar styracifula*, en co-dominancia con *Quercus sapotifoli* (Ramirez-Marcial et al. 2010; CONABIO 2013). Los remanentes del BLM se encuentran en la parte norte del Parque, dominados por especies de latifoliadas y su distribución depende de la disponibilidad de humedad de los suelos y las actividades antropogénicas. Estos factores restringen el BLM a sitios con relieve accidentados en laderas pronunciadas que reciben poca luz del sol directa y sujetos a un mínimo disturbio humano (Ramirez-Marcial et al. 2001). El dosel y sotobosque de estos bosques incluyen *Clethra* spp., *Clusia guatemalensis*, *Miconia* spp., *Podocarpus matudi*, *Turpina tricomuta*, *Pronus brachybotria* y *Ulmus mexicana* (CONABIO 2013).

## **2.2. Trabajo de campo**

En 2012, 2013 y 2016 fueron recolectados núcleos de sedimentos de dos lagos localizados en las montañas de Chiapas. Los lagos muestreados fueron el Lago Ocotitalito (núcleos OCO12-II y OCO16G-I) y el Lago San Lorenzo (LIQ13-I) pertenecientes a la Selva

Lacandona y el Parque Nacional Lagunas de Montebello respectivamente (Fig. 2.1B). En el Lago Ocotitalito fueron recolectados dos núcleos dado que los sedimentos superficiales de la primera secuencia (OCO12-I) no fueron recuperados en el proceso de extracción. El segundo núcleo sedimentario recuperado (OCO16G-I) representó el paquete sedimentario faltante. Los lagos fueron seleccionados entre una gran variedad de cuerpos lacustres, dada las características geomorfológicas del área circundante, tipos de sedimentos, el tamaño del cuerpo de agua y la facilidad de acceso para alcanzar. También, características morfométricas del lago como pendientes suaves, fondos relativamente planos y una profundidad no mayor de 30 metros (alcance del equipo de perforación), facilitaron la extracción de núcleos completos y sin perturbaciones. Las secuencias sedimentarias largas (OCO12-II y LIQ13I) fueron extraídas mediante el uso de un nucleador Livingstone modificado (Colinvaux et al. 1999b), equipo que garantiza una recuperación de aproximadamente el 95% del sedimento en incrementos de un metro. La secuencia corta en lago Ocotitalito (OCO16G-I) fue recuperada mediante el uso de un nucleador de gravedad UWITEC. Con el propósito de generar un contexto moderno para la interpretación de los resultados de análisis sedimentarios fósiles, se recolectaron y analizaron muestras de sedimentos superficiales. Parte del conjunto de datos de polen moderno derivaron de trabajos previamente publicados (77 muestras de la Península de Yucatán y montañas adyacentes, Correa-Metrio et al. 2011) y de la recolección y análisis de 48 muestras nuevas, extendiendo el muestreo hacia Guatemala, Honduras y El Salvador (Fig. 2.1A y Apéndice 3.1).

### 2.3. Trabajo de laboratorio

Los núcleos sedimentarios y las muestras modernas fueron trasladados al Instituto de Geología de la UNAM donde han sido almacenados en condiciones óptimas para garantizar la preservación de indicadores biológicos. Los núcleos fueron seccionados longitudinalmente en dos partes iguales con el objeto de obtener una sección de trabajo y otra de archivo. Posteriormente, cada secuencia fue descrita en términos de color, textura y reacción al HCl para evaluar cualitativamente contenido de carbonatos. Se tomaron muestras de sedimento cada centímetro en las secuencias de trabajo para el análisis geoquímico y cada ~4 cm para el análisis de polen y material carbonizado. El marco cronológico de cada secuencia sedimentaria se estableció mediante la datación por radiocarbono de 16 muestras (8, 4 y 4 muestras para OCO12-II, OCO16-I y LIQ13-I respectivamente). Las edades fueron obtenidas mediante la técnica de espectrometría de masas por aceleración (AMS, por sus siglas en inglés) por el laboratorio comercial de servicios Beta Analytic Inc. (Miami, EEUU).

Los análisis de geoquímica elemental se llevaron a cabo sobre muestras secas y molidas, usando un analizador de Fluorescencia de Rayos X (FRX) NITON XL3t – Thermo Scientific. Se determinaron las concentraciones de As, Ca, Cu, Fe, K, Mn, Pb, Ti, Rb, Sr, Zn y Zr, todas ellas medidas en partes por millón (ppm) y eventualmente transformadas a porcentajes. Las muestras de los núcleos también fueron sometidas al análisis de material carbonizado para reconstruir la frecuencia de incendios a través del tiempo. Para tal efecto, muestras de 1 cm<sup>3</sup> fueron defloculadas mediante el uso de pirofosfato de sodio (Na<sub>4</sub>P<sub>2</sub>O<sub>7</sub>) para luego separar los fragmentos de material carbonizado manualmente usando un estereoscopio (Clark 1988). Una vez separados los fragmentos de cada muestra, se tomaron

fotografías digitales para calcular su número y sus tamaños mediante el uso del software especializado ImageJ (Rasband 2005). La concentración de material carbonizado fue expresada como área ocupada por los fragmentos carbonizados en milímetros cuadrados por cada centímetro cúbico de sedimento ( $\text{mm}^2/\text{cm}^3$ ).

Las muestras de polen moderno y fósil fueron sometidas a análisis palinológicos, para lo cual cada centímetro cúbico muestreado fue tratado mediante técnicas estándar para la recuperación del contenido polínico (Faegri & Iversen 1989). Adicionalmente, las muestras fueron sometidas a una separación gravimétrica con el objeto de obtener un material concentrado de polen más limpio (Krukowski 1988). Posteriormente, el material polínico recuperado fue analizado en un microscopio de luz transmitida bajo magnificaciones de 400 y 1000x. Los palinomorfos fueron identificados a nivel de familia o género mediante el uso de colecciones de referencia disponibles (Palacios-Chávez et al. 1991; Roubik & Moreno 1991; Colinvaux et al. 1999b; Bush & Weng 2007). Los conteos de polen se llevaron a cabo hasta alcanzar una suma de 200 granos por muestra. Dada su alta representación en los espectros de polen de la región, elementos de vegetación acuática y los taxa *Moraceae*, *Quercus* y *Pinus* fueron contados, pero excluidos de la suma de polen (Correa-Metrio et al. 2011). Posteriormente, las cuentas de polen de cada taxón encontrado fueron transformadas a porcentajes de la suma de polen, de manera que los elementos excluidos eventualmente alcanzaron porcentajes por encima de 100%. Para interpretar los cambios en la vegetación, se graficaron diagramas de polen moderno y fósil en el programa C2 (Juggins 2007).

Se generó una clasificación *a priori* de las muestras modernas según su proveniencia en: Altos de Chiapas, tierras bajas de la Península de Yucatán, y elevaciones medias de Chiapas y de Centroamérica. Cada sitio representado en los datos de polen

moderno se describió en términos del clima y el impacto humano moderno. Las variables climáticas usadas fueron la Temperatura Media Anual (AMT, por sus siglas en inglés), Rango Medio Diurno (MDR), Isotermalidad (IST), Precipitación anual (APP) y estacionalidad de la precipitación (PSE), las cuales fueron obtenidas de la base de datos climáticos WorldClim que tiene una resolución espacial 30-arcsegundos (Hijmans et al. 2005). El impacto humano fue evaluado usando el Índice de Influencia Humana (HII), el cual corresponde a una base de datos global de 30-segundos-arco de resolución, creada de la superposición de nueve capas datos que incluyen la densidad poblacional, usos del suelo, infraestructura y el acceso como elementos principales (Sanderson et al. 2002). Los límites de este índice oscilan de 0 a 64, otorgando el valor mínimo a regiones altamente conservadas o prístinas y el valor máximo a lugares totalmente urbanizados.

## **2.4. Análisis de datos**

### *2.4.1. Modelos de edad*

Las edades de radiocarbono obtenidas en cada núcleo fueron calibradas en años antes del presente (AP de aquí en adelante) mediante la curva IntCal13 (Reimer et al. 2013), y se construyeron modelos Bayesianos profundidad-edad mediante el software Bacon (Blaauw & Christen 2011). Bacon divide una secuencia en varias secciones verticales (por defecto *ancho*= 5 cm de espesor), y a partir de millones de iteraciones estima la tasa de acumulación (en años/cm) para cada una de estas secciones. En combinación con la fechas de inicio estimadas para la primera sección, estas tasas de acumulación forman el modelo de edad-profundidad (Blaauw & Christen 2011).

#### 2.4.2. Ordenación multivariada

Cuando se dispone de un conjunto de datos de polen fósil y moderno, las técnicas multivariadas ofrecen la posibilidad de interpretar de forma resumida los datos para reconstruir las diferentes etapas ambientales reflejadas por los indicadores fósiles (Birks & Gordon 1985). Generalmente el análisis multivariado de datos paleoecológicos conduce a la calibración de las señales de ensambles de polen en términos de las variables ecológicas o ambientales de interés, permitiendo interpretaciones *a priori* de los resultados derivados de secuencias fósiles (Correa-Metrio et al. 2012a).

En estudios paleoecológicos se han aplicado de forma rutinaria técnicas de re-escalamiento multidimensional como el Análisis de Componentes Principales (PCA, por sus siglas en inglés) y el análisis de correspondencia (Birks & Gordon 1985). Sin embargo, estos métodos violan diferentes supuestos implícitos en datos ecológicos (como la respuesta no lineal de las especies a los gradientes ambientales) llevando a ordenaciones desequilibradas y sesgadas (Hill & Gauch 1980). De forma alternativa, el Análisis de Correspondencia sin Tendencia (DCA, por sus siglas en inglés) y el Escalamiento Multidimensional No-métrico (NMDS, por sus siglas en inglés) son técnicas que no suponen una respuesta lineal de las especies a los gradientes ambientales. Además, estas técnicas son relativamente fáciles de interpretar. Por lo tanto, en este trabajo se emplearon técnicas de ordenación como DCA y NMDS para inferir la señal de los ensambles de polen modernos y fósiles con respecto a diferentes variables ambientales. En ambos análisis, la interpretación de la estructura ambiental que subyace la ordenación se basó en regresiones de los puntajes de las muestras modernas contra atributos del ambiente de los sitios modernos.

El DCA fue empleado en la ordenación de muestras fósiles y modernas cuando el conjunto de datos representaba gradientes ambientales amplios. EL DCA reduce el efecto arco producido por otras técnicas de ordenación (Hill & Gauch 1980). Una vez producida la ordenación, los ejes se vuelven a escalar para descomprimir los extremos del gradiente que resultaron comprimidos por el efecto arco previamente mencionado. Como la ordenación se divide en segmentos, la varianza se distorsiona, lo cual impide la interpretación de *valores propios* como fracciones de varianza (Gauch 1982). En este caso, los *valores propios* deben interpretarse como un reflejo de la importancia relativa de los ejes por la corrupción de la varianza y no como un valor porcentual de varianza explicada como en el PCA (Legendre & Legendre 1998). Una característica del DCA es que las unidades de los ejes son desviaciones estándar (SD) las cuales pueden ser utilizadas para inferir cuantitativamente cambios ecológicos de la comunidad (Hill & Gauch 1980). EL DCA produce puntajes para las especies y muestras (Hill & Gauch 1980). Las puntuaciones de las especies indican la posición relativa de los taxa en el espacio reducido con respecto a la forma en que varían a lo largo del tiempo. Posteriormente, el espacio definido por la especies se utiliza para ordenar la muestras (Correa-Metrio et al. 2014).

El NMDS proyecta datos multivariados a lo largo de ejes latentes basado en la distancia entre objetos, mientras conserva la topología del conjunto de datos original (McCune et al. 2002). Por lo tanto, las muestras con puntajes parecidos se esperaría que presentaran similitudes en términos de la composición y estructura de los ensambles de polen. El NMDS difiere de varios métodos de ordenación debido a que una pequeña cantidad de ejes se eligen explícitamente antes del análisis y los datos se ajustan a esas dimensiones, de manera que no hay ejes ocultos de variación (Legendre & Legendre 1998). En segundo lugar, no es una técnica que se base en *valores propios* como el PCA. Por lo

tanto, una ordenación por NMDS puede rotarse, invertirse o centrarse en cualquier configuración deseada (McCune et al. 2002). Para este trabajo el NMDS fue basado en el índice de disimilitud de Bray-Curtis y construido en tres dimensiones. Se utilizó el índice de Bray-Curtis porque se ha demostrado su relación sistemática con la distancia ecológica (Faith et al. 1987) y usaron tres dimensiones porque se disminuye sustancialmente el estrés de la ordenación, permitiendo una ordenación más natural de las muestras. Diferente al DCA, los puntajes de las muestras se obtuvieron directamente de la ordenación, mientras los puntajes por taxón se calcularon usando el promedio ponderado de los puntajes del sitio. Las ordenaciones multivariados se realizaron en R (R Core Team 2017), usando el paquete *vegan* (Oksanen et al. 2017) .

#### *2.4.3. Análisis de taxa indicadores de umbrales ecológicos*

Se realizó un Análisis de Taxa Indicadores de Umbrales Ecológicos (TITAN, por sus siglas en inglés) a los datos de polen moderno para obtener una comprensión de los cambios en la distribución de cada taxón a lo largo de gradientes ambientales (en este caso la influencia humana) (Baker & King 2010). También, con este análisis se estudió la influencia del ambiente en la estructura de las comunidades. Esta técnica corresponde a una mezcla entre el análisis de puntos de cambio y el análisis de especies indicadoras (Dufrêne & Legendre 1997). Cada taxón se organiza a lo largo del gradiente ambiental de interés y con el análisis de especies indicadoras se le otorga un valor indicador (IndVal), puntajes que expresan la fuerza de asociación de un taxón en cada lado de un punto de cambio potencial (Dufrêne & Legendre 1997). Los puntajes de Indval permutados se estandarizan como puntajes (z) y sumados para valores positivos o negativos para cada punto de cambio. Adicionalmente, los

picos de la suma ( $z$ ) resaltan el umbral de la comunidad alrededor del cual varios taxa muestran cambios críticos en la abundancia alrededor de un punto en el gradiente. En este trabajo, la calidad y estimación de los puntos de cambio críticos fue evaluada usando 1000 permutaciones y 500 réplicas por *bootstrapping* (remuestreo con reemplazamiento) usando el paquete personalizado TITAN2 en R (Baker et al. 2015). Información más detallada del método se puede encontrar en Baker and King (2010).

## CAPÍTULO 3

### LA HUELLA DEL IMPACTO HUMANO EN EL ESPECTRO DE POLEN MODERNO DE LAS TIERRAS MAYAS

### THE HUMAN IMPACT IMPRINT ON THE MODERN POLLEN SPECTRA FO THE MAYA LANDS

**Felipe Franco-Gaviria<sup>1</sup>, Dayenari Caballero-Rodríguez<sup>1</sup>, Alexander Correa-Metrio<sup>2</sup>,  
Liseth Pérez<sup>2</sup>, Antje Schwalb<sup>3</sup>, Sergio Cohuo<sup>3</sup>, Laura Macario-Gonzalez<sup>3</sup>**

<sup>1</sup> Posgrado en Ciencias de la Tierra, Universidad Nacional Autónoma de México,  
Coyoacán, Ciudad de México, México 04510.

<sup>2</sup> Instituto de Geología, Universidad Nacional Autónoma de México, Coyoacán, Ciudad de  
México, México 04510.

<sup>3</sup> Institut für Geosysteme und Bioindikation, Technische Universität Braunschweig, Langer  
Kamp 19c, Germany 38106.

*Boletín de la Sociedad Geológica Mexicana*

<http://dx.doi.org/10.18268/BSGM2018v70n1a4>

## **Resumen**

Para entender el registro paleoecológico en el contexto de la ocupación humana, es necesario examinar la distribución del polen moderno a lo largo de gradientes climáticos y de impacto humano. Este estudio analiza las respuestas del polen moderno de 125 muestras superficiales a la influencia humana de la región Maya, usando tres aproximaciones básicas: i) la evaluación de la habilidad de espectros de polen moderno para distinguir los principales tipos de vegetación antropogénica y natural, ii) el uso del análisis de correspondencia sin tendencia (DCA, por sus siglas en inglés) para evaluar los patrones de distribución del polen a lo largo de gradientes ambientales que incluyen la influencia humana, y iii) la evaluación de las respuestas de taxa individuales a un gradiente de influencia humana a través del análisis de taxa indicadores de umbral. Las 125 muestras de la interfaz agua-sedimento se dividieron en cuatro grupos que corresponden a los principales tipos de vegetación de la región Maya (bosque de pino-encino, cultivos y pastizales, bosque estacional tropical, y bosque tropical siempre verde). En términos de las respuestas a nivel de taxón, nosotros detectamos 20 elementos asociados significativamente con el gradiente de influencia humana. Estos elementos fueron asignados a grupos de respuesta negativos (disminuciones) o positivos (incrementos) dependiendo de la dirección de respuesta. La mayoría de los elementos arbóreos de bosques estacionales tropicales disminuyeron, mientras elementos no-arbóreos típicamente de vegetación antrópica aumentaron en respuesta a diferentes niveles de influencia humana. Adicionalmente, fue detectado un cambio abrupto a nivel de comunidad para un índice de influencia humana de 15. Cuando la influencia humana supera este umbral, elementos importantes de la vegetación natural son afectados negativamente, mientras elementos oportunistas son favorecidos. En general, el estudio de la distribución del polen a lo largo

de gradientes ambientales así como la identificación de taxa indicadores de impacto humano ofrecen herramientas valiosas para interpretar los registros de polen fósil de la región Maya.

**Palabras clave:** Vegetación antropogénica y natural, Índice de Influencia Humana (HII), polen moderno, análisis de taxa indicadores de umbrales, tierras mayas.

**Abstract:**

To understand human occupation in the context of paleoecological records from the Maya region, there is need to explore the distribution of modern pollen along climate and human impact gradients. In this study, we analyze the responses of pollen assemblages from 125 surface samples to human influence in the Maya region, using three basic approaches: i) the evaluation of using modern pollen spectra to distinguish the main anthropogenic and natural vegetation types, ii) the usage of detrended correspondence analysis (DCA) to evaluate the distribution patterns of pollen along environmental gradients including human influence, and iii) the evaluation of the responses of taxon-specific elements to the human influence gradient that expresses on the modern landscape, using threshold indicator taxa analysis. The 125 locations where mud-water interface samples were retrieved from were divided into four groups that correspond to the major vegetation types of the Maya region (coniferous and *Quercus* forest, croplands and pastures, tropical seasonal forest, and tropical evergreen forest). In terms of individual taxa responses, we detected 20 elements significantly related to human influence gradient. These were assigned to negative (decreasing) or positive (increasing) response groups depending on the response direction. Mostly arboreal elements from tropical seasonal forests decreased, while elements non-

arboreal typically from anthropogenic vegetation increased in response to different levels of human influence. Also, a community-level abrupt point change was detected at a human influence index of 15. When human influence exceeds this threshold, important elements of the natural vegetation are negatively affected while opportunistic elements become favored. Overall, the study of pollen distribution along environmental gradients and the identification of taxa indicators of human impact provide valuable tools for the interpretation of fossil pollen records from the Maya region.

**Keywords:** Anthropogenic and natural vegetation, Human Influence Index (HII), modern pollen, threshold indicator taxa analysis, Maya lands.

### **3.1. Introduction**

Over millennia, humans have adapted to environmental changes in a variety of ways, causing substantial transformation of the lands they occupy (Dearing 2006). In Mesoamerica, transformations of natural environments have been a common feature at least since the mid Holocene, and have manifested mostly through the exploitation of wild plants and the establishment of crops (Palka 2009). It is expected that human activities and occupation of the landscape would follow the complexities of the environmental mosaic with differential focus on regions where environmental conditions are more suitable for human settlement and occupation. However, paleoecological and archaeological evidence suggest human occupation has not only been the result of physical geography, but there have also been historic and societal components (Leyden 1987; Sharer & Traxler 2006). Mesoamerica has been home to the Maya civilization for more than 4,000 years (Sharer &

Traxler 2006). The most readily recognized aspects of this culture are its large urban centers and the seemingly extensive agricultural systems, two features that strongly impacted their territory and the surrounding resources (Beach et al. 2006; Piperno 2006). This intense human-environment interaction has taken place through most of the Holocene. Understanding how human activities have modified the environment at different spatial and temporal scales provides important insights to the understanding of the environmental system and how it evolves under the influence of human populations.

Pollen analysis has been widely used for reconstructing past changes in vegetation and their associated drivers (Delcourt & Delcourt 1991). In the Maya region, modern pollen assemblages represent current parental vegetation and the underlying environmental gradients (Correa-Metrio et al. 2011). However, our ability to understand the nature and extent of past human impacts on vegetation based on pollen strongly relies on identifying key indicator taxa from modern pollen associations. In pollen assemblages from the Maya lands, the clearest signal for human influence or impact would be the presence of cereals (e.g. *Zea mays*, primary indicators *sensu* Piperno 1998), manioc (*Manihot esculenta*), and squash (*Cucurbita* sp.). However, synanthropic plants growing on farming contexts and disturbed sites are also detected in the pollen spectrum, although the scope of their environmental indication remains unclear. Maya communities have been characterized by adopting agroforestry systems (the Maya Milpa) involving the management of some trees and non-arboreal elements (Nigh & Diemont 2013). Thus, taxa favored by the spread of human activities would be particularly useful to reconstruct vegetation changes associated with forest management, agricultural activity, and their effects on natural ecosystems (Brun 2011). By analyzing modern pollen assemblages in terms of human influence, we aim to establish a basis to better assess human-induced landscapes using fossil pollen records. The

pollen signal of human activities would benefit from selecting those groups with a distinctive response to the human impact.

In this study, we examine pollen assemblages' responses to a human influence gradient, aiming to evaluate the sensitivity of pollen to human impact at community and taxon levels. To assess human impact, we used the modern global data set of Human Influence Index (HII, Sanderson et al. 2002), a spatial product that provides an assessment of the level of anthropogenic influence on the landscape. The index integrates human population density, degree of land transformation, accessibility, and power infrastructure into an index that can be estimated for any given region. Characterizing the relationship between pollen assemblages and HII allows the identification of potential pollen indicators for human impact. We hypothesize that individual taxa and assemblages would show strong relationships with the HII and would exhibit sharp, nonlinear responses as thresholds at certain levels of landscape alteration. Thus, the main objectives of this study are: first, to assess whether pollen assemblages respond to human influence determined by the HII; second, to identify potential indicator pollen taxa of human influence; and third, to analyze patterns of changes at community level and the possible existence of critical thresholds in the vegetation along the human influence gradient.

## **3.2. Material and Methods**

### *3.2.1 Study area*

The study area is located in the zone culturally delimited as Maya region, roughly between 13.30° to 21.40°N and from 87.30° to 95.30° W (Fig. 3.1), spanning from the lower Lempa River in El Salvador to the Isthmus of Tehuantepec in Mexico, and covering about 324,000

km<sup>2</sup> of tropical lands. The region could be roughly divided into three main geographical zones: *i*) the southern highlands that include the mountains of Honduras, Guatemala and Chiapas, *ii*) the southern lowlands that cover Petén in northern Guatemala, northern Honduras, Belize, and the southern portions of Yucatan Peninsula; and *iii*) the northern lowlands on the central and northern portion of Yucatan Peninsula.

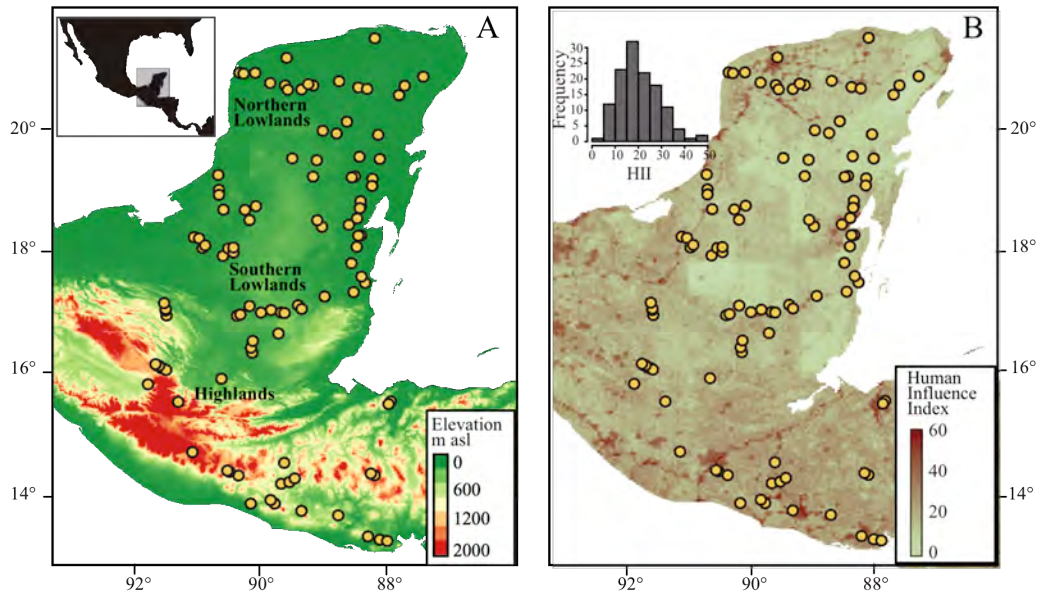


**Figure 3.1.** Study area. **A.** Digital elevation model of the terrain indicating the main geographical zones in the Maya region, and **B.** Human Influence Index (HII) along the region with their respective frequencies. Yellow dots show the location of the sampled lakes (see Apéndice 3.1, for the list of samples and their geographic coordinates).

The Climate is warm in the lowlands and becomes cooler towards the highlands, with differences among regions mostly produced by rainfall patterns. High topographic diversity expressed through large elevations gradients and rain shadows lead to significant precipitation variability across the region. In the highlands and the mountains annual precipitation can reach up to 5000 mm, while in northwestern Yucatan it barely reaches 500 mm (Méndez & Magaña 2010). The climate is primarily controlled by the atmospheric

patterns influenced by the Intertropical Convergence Zone and the Bermuda High, which together cause a markedly wet season from May to November, and a dry season from December to May (Wilson 1980; Magaña et al. 2003).

Temperature and precipitation are the main drivers of natural vegetation patterns across the Maya lands, whereas precipitation seasonality and edaphic features exert a more local control on vegetation associations. Scrubs and tropical deciduous forests naturally cover the northernmost and driest portion of the Yucatan Peninsula, whereas tropical semi-deciduous forests dominate the central and northeast areas, where conditions are still dry but less seasonal. As precipitation rises southward, tropical evergreen forest emerge, with intermissions of woody savannas around Belize and northern Guatemala, commonly associated with local edaphic conditions (Rzedowski 2006). The highland mountains are characterized by three basic types of vegetation, namely mountain mesophyllous forest, *Quercus* forest, and coniferous forest (Nixon 2006; Rzedowski 2006).

Human impact has caused important changes in the natural vegetation mostly through deforestation. These changes have favored a widespread distribution of human-induced vegetation characterized mainly by croplands and pastures in the entire region (Loveland et al. 2000; Rzedowski 2006). Anthropogenic vegetation in Mesoamerica is the result of both modern land uses and least five millennia of extensive human occupation (Pohl et al. 1996). The earliest cultivation of maize and the associated impact on vegetation have been reported between 5,000 and 4,500 years in Belize and Guatemala (Pohl et al. 1996; Piperno 2006; Wahl et al. 2006). Crops of diverse sizes included maize (*Zea mays*), beans (*Phaseolus* spp.), squash (*Cucurbita* sp.), and papaya (*Carica papaya*). Also, the ancient legacy of Mayan agroforestry has been in use in the region and it is widespread among present-day farmers. These activities include the *Maya milpa* that consists of annual

rotation of crops with a series of managed arboreal species (e.g. *Brosimum alicastrum*, *Bursera simaruba*, *Cecropia peltata*, and *Zwietenia macrophylla*), which under abandonment lead to their dominance in the reestablished forest (Quintana-Ascencio et al. 1996; Ford & Nigh 2009; Nigh & Diemont 2013). Besides the previously mentioned species, in the *Maya milpa*, species such as *Acacia cornigera*, *Brosimum alicastrum*, *Bursera simaruba*, *Cecropia peltata*, *Zwietenia macrophylla*, and *Vitex gaumeri* are also commonly found (Ford & Nigh 2009). Currently, new production systems such as cattle raising and other crops (e.g. sugarcane and coffee) are also widespread along the region (Sharer & Traxler 2006).

### 3.2.2. Pollen and human influence data sets

The pollen data set was composed of modern sediment samples collected along the Maya region. Whereas part of the dataset came from previously published work (77 samples from the Yucatan Peninsula and adjacent mountains, Correa-Metrio et al. 2011), 48 new samples were collected, extending the sampling towards Guatemala, Honduras and Salvador (Apéndice 3.1). The preparation and analysis of the new samples followed the protocols described by Correa-Metrio et al. (2011) to ensure homogeneity of the entire dataset. All pollen counts were transformed to percentages of the pollen sum to offset differences in sample size (Birks & Gordon 1985).

Human influence at the sampled sites was assessed using the global Human Influence Index (HII) dataset, which has a spatial resolution of 1 km<sup>2</sup> (Sanderson et al. 2002). HII values range from zero for fully pristine areas, to 64 for totally urbanized

regions (for details see Sanderson et al., 2002 and <http://sedac.ciesin.columbia.edu/data/set/wildareas-v2-human-footprint-geographic>).

### 3.2.3. Data analysis

A Detrended Correspondence Analysis (DCA, Hill & Gauch 1980) on the pollen dataset was used to explore the ability of pollen assemblages to reflect human impact patterns at community level. The DCA was meant to identify the ecological space represented by the pollen samples through the *a priori* interpretation of taxa ordination (Correa-Metrio et al. 2014). HII values per taxon were calculated through averages of HII of the sites weighted by taxon relative abundance. Subsequently, HII per species and sites were compared with DCA taxa and sites scores respectively, and their relationship was generalized through non-parametric locally weighted regression (Cleveland & Devlin 1988).

Given oversampling of some localities within the studied region, the original dataset was geographically resampled, using a grid 2x2-km grid, where only one sample was selected from each cell. The resampling was replicated 500 times. Additionally, the resampled dataset was submitted to a filter to avoid undesirable effects of rare species (only taxa with a minimum abundance of 1% in 5% of the samples were selected, after Correa-Metrio et al. 2010).

The magnitude, direction and uncertainty of responses of individual taxa and community to the studied human influence gradient were estimated through a Threshold Indicator Taxa Analysis (Baker & King 2010). The method finds values along the studied environmental gradient (HII in this case) where the largest community change occurs. An indicator value is calculated for each taxon at each candidate change-point along human

impact gradient and change-points with maximum indicator values are retained (for details see Dufrene & Legendre 1997). Scores of indicator values are subsequently standardized to obtain a Z-scores for each taxon, such that positive and negative responses can be distinguished (Baker & King 2010). Community level thresholds can be estimated as the summation of individual taxon responses represented by Z-scores. A bootstrap resampling is performed to evaluate statistical significance of Z-scores, which can be summarized as follows: *i) high purity* when the Z-scores associated with the taxon is found within the same segment and shows the same direction in at least 90% of the bootstrapping runs (1000 in total); and *ii) high reliability* when at least 95% of bootstrapping were significantly different from a random distribution ( $p < 0.05$ ). All analyses were performed using R (R Core Team 2017), especially packages TITAN 2.0 (Baker & King 2013) and Vegan 2.4 (Oksanen et al. 2017).

### **3.3. Results**

#### *3.3.1. Pollen assemblages and human influence index at the Maya lands*

With an average pollen count of 427 grains per sample, the 125 samples totaled 192 pollen taxa. The different kind of highlands formations (mountain mesophyllous forest, *Quercus* forest, and coniferous forest) did not display a particular pollen signature. Therefore the samples of these locations were grouped together as coniferous-*Quercus* forest (CQF). These samples were localized at elevations above 1400 m a.s.l. (e.g. Atilán, Chilangatorio, Esmeralda, and 5-Lakes) and showed high percentages of *Pinus*, *Quercus*, *Liquidambar* and *Myrica* (Fig. 3.2). Croplands and pastures (CP) were characterized by a dominance of non-arboreal pollen (e.g. Amaranthaceae, *Byrsonima*, Poaceae and Solanaceae) and high

percentages of Cucurbitaceae and *Zea*, both taxa characteristic of croplands (Fig. 3.2). These samples covered a broad altitudinal gradient (from 0 to 1200 m a.s.l.) and sites near to urban centers, roads, and farming areas (e.g. Amatitlán, El Espino and Jucutuma) (Fig. 3.2). Samples from seasonal vegetation (scrubs, deciduous and semi-deciduous forests) did not differ in their pollen spectra, so were grouped as tropical seasonal forest (TSF). This group had the largest sample size with 51 locations from lowlands and mountain depressions, and its pollen spectra were dominated by *Acacia*, *Bursera*, *Vitex* and *Mimosa*. Pollen assemblages from locations classified as tropical evergreen forest (TEF), under 800 m a.s.l. (e.g. Yaxhá, Macanché and Sacpuy) were dominated by *Brosimum*, *Ficus*, *Trema*, Moraceae, and Melastomataceae (Fig. 3.2).

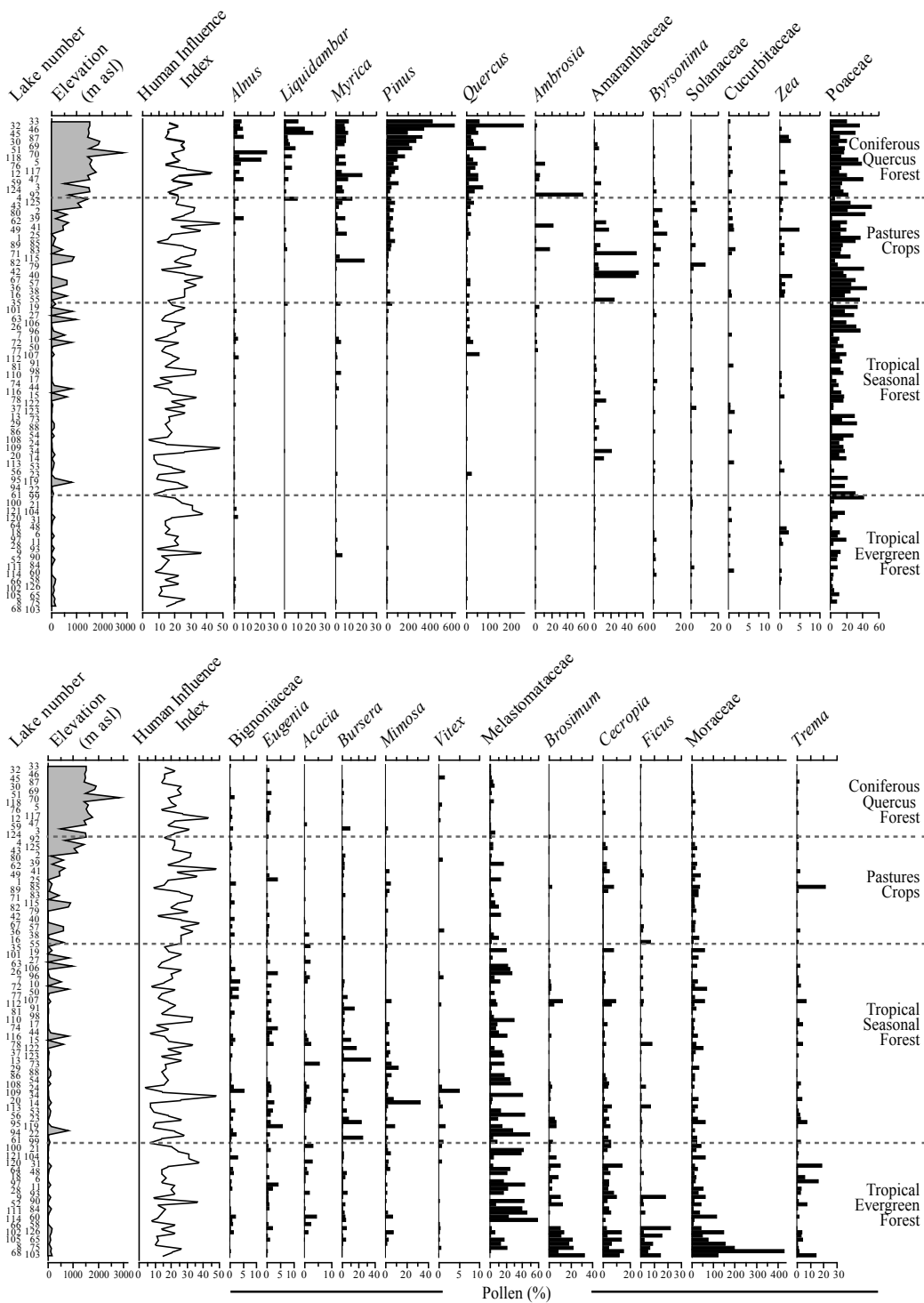


**Figure 3.2.** Pollen percentage diagram of mud-water interface samples from 125 lakes. Selected pollen taxa with at minimum presence of 1% in at least five samples are shown. Taxa were arranged according to their scores of Detrended Correspondence Analysis, while samples were organized according to the vegetation type of the area where the sample was recovered.

Values of HII for the studied locations varied from 4 and 7 at the most preserved locations (Cobá and Chacan-Bata), to 43 and 48 at the most impacted localities (Calderas and El Espino). The higher values of HII were found at CP locations (26.3 in average), followed by CQF (21.8 in average), and lastly, TEF and TSF obtained similar HII (18 in average; Fig. 3.2).

DCA scores produced a split of vegetation types along Axis 1 (eigenvalue 0.51, axis length 2.92) and Axis 2 (eigenvalue 0.24, axis length 3.1) (Figure 3.3C). *Liquidambar*, *Myrica*, *Pinus*, and *Quercus* showed positive scores, while *Brosimum*, *Ficus*, Melastomataceae, and Moraceae displayed negative scores. Elements that usually characterize disturbance, such as Amaranthaceae, *Ambrosia*, Poaceae, Solanaceae, and *Zea* were associated with scores near zero. Results from DCA ordination for the sites showed a clear separation of vegetation types along the first two axes (Fig. 3.3D). Samples from CQF were ordinated in the positive end (quadrants I and IV), while CP locations showed a wide distribution along the central of Axis 2. Samples from TSF and TEF were separate in the negative side (quadrants II and III respectively).

A positive non-linear relationship between DCA Axis 1 taxa scores and their weighted HII was evident according to loess regression with low residual error standard (RSE, 2.3) (Fig. 4.3A). The loess analysis also suggested a breakpoint along the HII gradient between 20 and 22. The comparison between HII values and DCA Axis 1 scores per sites did not show a relationship with a loess-regression adjusted very poor (RSE=8.3) (Fig. 3.3B).

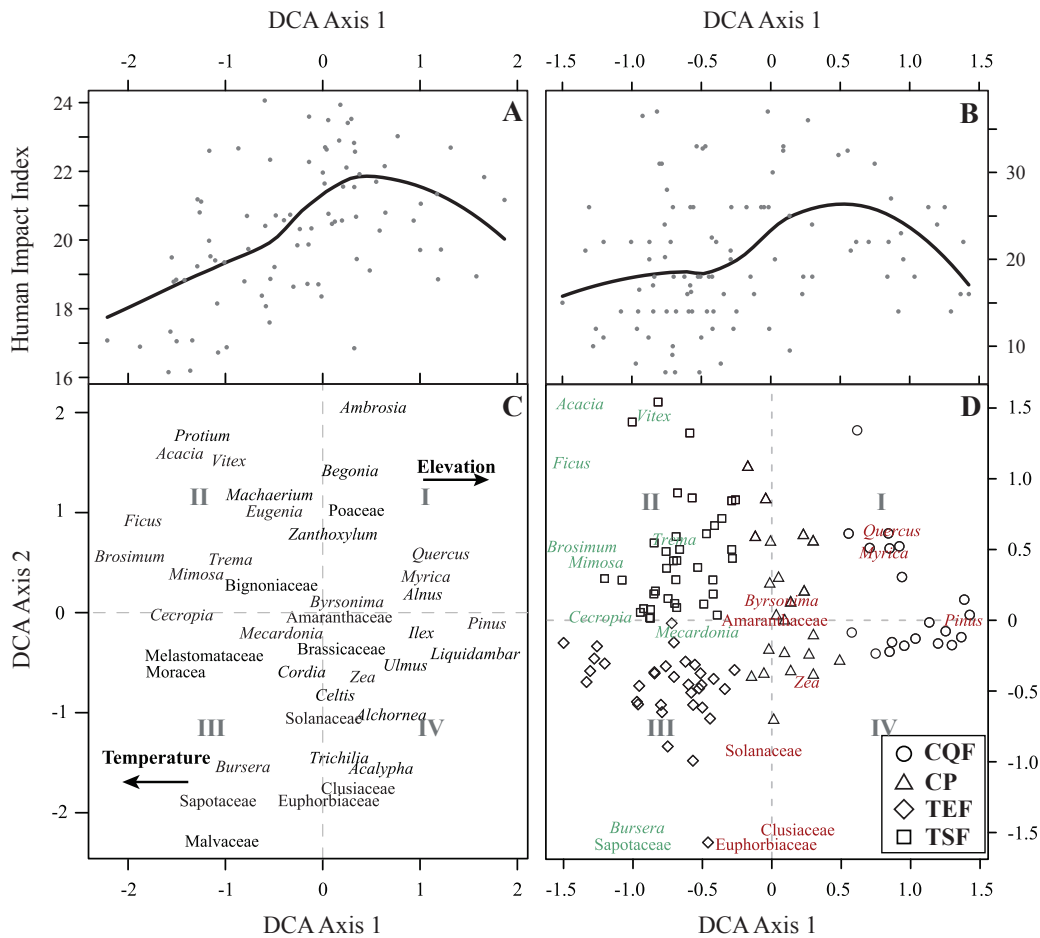


**Figure 3.3.** Detrended correspondence analysis (DCA) of modern pollen from Maya lands. **A.** Locally weighted non-parametric regression (loess) for human influence index as a function of DCA Axis 1 taxon scores. **B.** Loess regression for human influence index as a function of DCA Axis 1 sample scores. **C.** Ordination of taxa. **D.** Samples ordination with taxa selected from the Threshold Indicator Taxa analysis, negative (green) and positive (red) responses to the human influence CQF: Coniferous and *Quercus* forest; CP: croplands and pastures; TSF: tropical seasonal forest; TEF: tropical evergreen forest.

### 3.3.2. Threshold indicator taxa analysis

The spatial resampling and the presence/persistence filter generated a reduced dataset composed of 112 samples and 76 pollen taxa. Through taxa indicators analysis, 20 of the 76 taxa were identified as pure or reliable indicators of human impact (Fig. 3.4A). Negative responses (Z-) to HII were found for *Mimosa*, *Vitex*, *Bursera*, *Ficus*, Sapotaceae, *Brosimum*, *Trema* and *Cecropia*, which displayed lower occurrence and abundance along a short length of human impact gradient (11 in average). *Eugenia*, *Mecardonia* and *Acacia* also decreased as HII increased but along a wider length of gradient (29 in average). Nine taxa showed positive responses to HII. Among them, *Zea*, *Byrsonima*, *Pinus*, and *Myrica* responded along short sections of the human impact gradient (13 in average), while Solonaceae, Euphorbiaceae, Clusiaceae, Amaranthaceae, and *Quercus* did so along a wider gradient (25 in average).

About the community responses along human influence gradient, the summation of Z-scores (sum(Z)) indicated a change point at 15 of HII (5<sup>th</sup>, 95<sup>th</sup> quantiles of HII = 12, 20 respectively), having sharp, well-defined peak in sum(Z-) scores (Fig. 3.4B). Except for *Mimosa*, *Vitex*, *Eugenia*, and *Cecropia*, significant Z- taxa had points changes narrow the threshold and 95% quantiles. The sum(Z+) scores showed a change-point in 24 of HII (5<sup>th</sup>, 95<sup>th</sup> quantiles of HII = 14, 30), but it was not considered as a threshold response because wide quantiles and poorly defined peak in sum(Z+) (Fig. 3.4B). Few taxa had well defined synchronous change points along human influence gradient (Fig. 3.4A), indicating gradual changes in sum(Z+) scores between 14 and 30 values of HII.

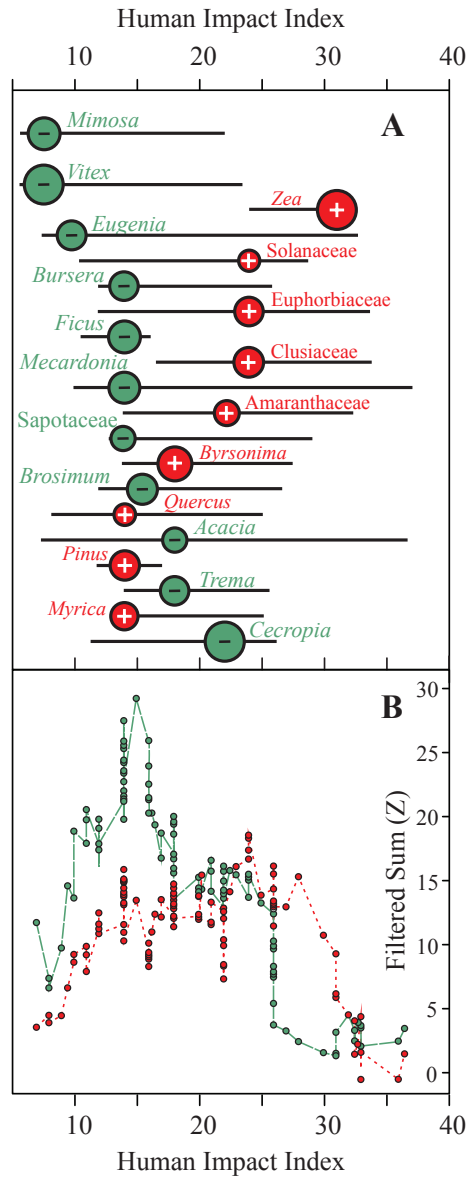


**Figure 3.4.** Threshold Indicator Taxa Analysis. **A.** Inflection points (5<sup>th</sup>, 95<sup>th</sup> bootstrap quantile intervals) for significant pollen taxa along human influence gradient. Significant indicator pollen are taxa with, IndVal  $p < 0.05$ , purity  $> 0.90$  and reliability  $> 0.95$  for 1000 bootstrap and 250 permutation replicates. Green and red circles represent change points associated with negative and positive responses respectively. Note that Z scores are sized proportion to the magnitude of the response. **B.** Community changes for pollen taxa. Summation of individual taxon responses represented by Z- and Z+ scores.

### 3.4. Discussion

#### 3.4.1. Modern pollen signal

Modern pollen assemblages clearly reflect the local vegetation types, as previously reported for the Maya lands (e.g. Islebe et al. 2001; Domínguez-Vásquez et al. 2004; Bhattacharya et al. 2011; Correa-Metrio et al. 2011). However, although vegetation of the studied region is represented by at least 10 different vegetation types, our pollen spectra distinguished four main associations: CQF, TSF, TEF, and CP (Fig. 3.2). The lack of distinction into more specific vegetation types is likely a result of including samples from areas highly impacted by human activities. Human-induced vegetation such as croplands and pastures are widely distributed in the region, simplifying vegetation and diversity, and therefore blurring the ability of pollen to distinguish specific vegetation associations. Nevertheless, the low taxonomic resolution of pollen analysis is likely a structural problem to distinguish among vegetation types (Correa-Metrio et al. 2011). In the lowlands, the pollen signal might be masked by genera shared by different forest types that are not distinguishable at the species level. In the mid elevation and highlands, anemophilous taxa that have been widely recognized as problematic (e.g. Lozano-Garcia & Xelhuanzi-López 1997; Correa-Metrio et al. 2011; Correa-Metrio et al. 2012c) causing further masking of the pollen signal. Although a pollen-based, clear-cut distinction of forest types according to modern vegetation is not possible, the pollen signal reflects the continuous nature of the realized biological and environmental gradients.

Our results also produced a clear distinction of CP assemblages dominated by non-arboreal taxa such as *Ambrosia*, *Amaranthaceae*, *Solanaceae*, *Zea*, and *Poaceae*, a finding previously reported for the region (Bhattacharya et al. 2011; Correa-Metrio et al. 2011).

These taxa were also commonly found in large numbers within the CQF locations, which would suggest an important component of human-impacted vegetation within these areas. Nevertheless, CQF enrichment of these elements is probably also the result of the environmental hardship that vegetation experiences at high elevations through the entire year.

#### *3.4.2. Pollen assemblages of the Maya lands: ecological and human signals at assemblage level.*

The DCA Axis 1 showed a clear separation of TEF and TSF on its negative side, while CQF was ordinated towards the positive end (Fig. 3.3D). Thus, DCA Axis 1 is clearly reflecting a temperature gradient, a finding previously reported for Central America and the Maya lowlands (e.g. Bush & Colinvaux 1990; Correa-Metrio et al. 2011; Correa-Metrio et al. 2012a). CP samples obtained scores near zero in the DCA Axis 1 (Fig. 3.3D), although they were not necessarily coming from intermediate temperatures. According to the loess regressions, HII manifests in the ordination through a non-linear pattern (Figs. 3.3A and 3.3B). This pattern is probably the result of cosmopolitan taxa commonly associated with human impacts (e.g. Amaranthaceae, *Ambrosia*, Asteraceae, and Poaceae) acting as a gravity center of the ordination and therefore representing the transition between contrasting environments, in this case from lowlands to highlands (Fig. 3.3C). Indeed, this transition zone likely reflects a simplifying effect of people on the landscape (Caballero-Rodríguez et al. 2017), explaining the changes from complex tropical ecosystems to most simple temperate ecosystems in terms of its structure.

On quadrants II and III of the DCA, Axis 2 produced a clear separation of lowland systems into TEF (negative scores) and TSF (positive scores) (Fig. 3.3D), implying a seasonality gradient previously reported for the region (Correa-Metrio et al. 2011; Correa-Metrio et al. 2012a). At the center and the positive end of Axis 1, however, CP and CQF samples were widely distributed along Axis 2. This finding reflects two independent factors on these pollen spectra groups: i) the widespread distribution of CP samples along the region in terms of the seasonality gradient, and therefore the lack of association of HII with DCA Axis 2, and ii) the lack of a clear precipitation seasonality gradient along the CQF sampled sites (Fig. 3.3D).

Although the temperature/elevation gradient led the DCA ordination, there was a signal of human influence in the vegetation suggested by the significant correlation between Axis1 taxa scores and their weighted HII (Fig. 3.3A). However, loess regression on HII data as a function of Axis 1 site scores produced by the DCA did not show a pattern as clear as that of the taxa scores (Fig. 3.3B). Thus, pollen spectra reflect human influence on vegetation through a taxon approach, and the assemblage signal is rather weak.

#### *3.4.3. Human influence indication at taxon level.*

The threshold indicator taxa analysis allowed the identification of 20 pollen taxa whose presence and abundance were significantly associated with human influence (Fig. 3.4A). Most of the elements that showed a decreasing response to HII were arboreal and their distribution was confined to the lower end of the impact gradient (Fig. 3.4A). The inflection point in the response of these elements was found below a HII of 20, except for *Cecropia* (Fig. 3.4A). According to the DCA, *Mimosa*, *Vitex*, *Eugenia*, *Ficus*, *Brosimum*, *Acacia*, and

*Trema*, all of them negative responders to HII, were associated with TSF (Fig. 3.3D). Alternatively, only *Bursera* and Sapotaceae resulted associated with TEF, pointing to the dominance of negative responders in the TSF and suggesting a high sensibility of these ecosystems to human impact. These forests are established mostly in the lowlands from the Yucatan Peninsula, where high seasonality probably potentiates the effects of human activities. Differently, more stable climates through the year at the TEF locations might buffer human impact. *Cecropia* and *Mecardonia* did not show a clear grouping with a single vegetation type, but they were rather ordinated at the TSF-TEF transition. Particularly, *Cecropia*, a taxa widely recognized as a component of secondary forest (Rzedowski 2006; Bhattacharya et al. 2011), showed a negative response along HII gradient. This apparent discrepancy might indicate that, albeit tolerant to certain disturbance levels, this taxon also results affected when the human impact gets intensified. Indeed, the inflection point of its response to HII was found at a rather high value (22, Fig. 3.4A).

Taxa with positive responses to human influence were characterized by both, non-arboreal and arboreal elements, spread along a substantial portion of the studied HII gradient (Fig. 3.4A). *Zea*, Solanaceae, Euphorbiaceae, Clusiaceae, Amaranthaceae, and *Byrsonima* were distributed along mid to high HII indexes, and according to the DCA were mostly associated with CP locations (Fig. 3.3D). However, their central location on DCA axis 1 suggests that they can be found in any vegetation association. These elements have been reported as disturbance indicators in modern and fossil pollen studies from Central America (Wahl et al. 2006; Bhattacharya et al. 2011; Correa-Metrio et al. 2011). *Myrica*, *Pinus*, *Quercus* and *Byrsonima*, all of them arboreal to shrub elements from CQF (Fig. 3.3D), showed increases at low to moderate levels of human influence. Low intensity

anthropogenic activities such as agroforestry systems, particularly in montane areas can generate patchy open habitats, which can be rapidly colonized by opportunistic taxa (Cayuela et al. 2006). However, *Pinus* and *Quercus* should be interpreted with caution because they are high pollen producers and long-distance dispersers (Mazier et al. 2006; Correa-Metrio et al. 2011), implying a significant regional input that may not necessarily reflect local conditions.

Other taxa commonly identified as indicators of disturbance as *Ambrosia*, Asteraceae, *Celtis*, and Poaceae (Pohl et al. 1996; Bush 2002b; Correa-Metrio et al. 2011) were not identified as significantly responding to human impact. However, they resulted ordinated near the origin of DCA axis 1 (Fig. 3.3C), a region that our loess regressions identified with maximum HII values for both taxa and sites. The lack of significant response to the HII gradient through the threshold taxa analysis might be a result of their cosmopolitan distribution (Marchant et al. 2002). Their association with human impact might be better reflected by their abundances than by their occurrence along the studied sites, and both attributes are taken into account by the used method.

#### *3.4.4. Threshold identification*

The summation of Z values to evaluate community level responses showed a substantial decline around a HII of 15 (Fig. 3.4B), suggesting almost synchronous response of all taxa that decline with human impact. Responses to human disturbance of forests, insects and lake biological communities showed similar thresholds for low and intermediate perturbation levels (Cardoso et al. 2013; Kovalenko et al. 2014; Rodrigues et al. 2016). Likely, once the level of human pressure exceeds a given threshold, important elements of

forest cover are affected simultaneously, benefiting opportunistic species. Although we detected 7 of 11 taxa with thresholds near a HII of 15, the uncertainty at community level is rather high, pointing at the individualistic response of biological populations to disturbance. Thus, there is not a single threshold that explains the response the entire community, but instead there might be a common level where the risk of taxa loss is high. On the other hand, asynchrony among positive responders (Fig. 3.4A) was evident in the several change points (at 14, 18, 24, and 26 HII values) and broad confidence limits produced a relatively weak aggregate signal of community response (Fig. 3.4B). Thus, it is possible that the occupation of these taxa in human disturbed areas depends on more complex factors, for example the temporal structure of the disturbance.

### **3.5. Conclusions**

The main vegetation associations of the Maya lands (CQF, CP, TSF, and TEF) were identifiable through the study of their associated pollen spectra. They showed a clear separation in the DCA ordination, and their distribution along the two first axes showed climatic and anthropogenic influence gradients. TEF and CP were clearly distinguishable by their respective pollen assemblages, while vegetation associations within TSF and CQF were rather difficult to identify. The lack of distinction into more vegetation units is likely the result of three factors: i) the generalized impact of human impact along the study area and subsequent simplification of the natural vegetation, ii) the low taxonomic resolution in the pollen analysis, and iii) the continuous nature of the realized biological and environmental gradients.

Responses of modern pollen to human influence gradient at taxon-specific levels were most significant than at community level. Twenty pollen taxa were significantly related to human influence, although they were representative of different vegetation associations. Arboreal elements from tropical seasonal forests showed a decreasing response to HII, indicating the high sensitivity of these areas to human influence. Differently, only two taxa from tropical evergreen forests were negative responders to HII, suggesting these forests are more resilient to human impact. Most taxa that showed a positive response to HII were non-arboreal, and they dominated in samples from croplands and pastures. Overall, our findings provide useful tools for interpreting the paleoecological record based on the study of taxon responses to human impact.

The threshold analysis allowed the identification of a community level threshold of human impact. When human impact exceeds a threshold of 15, important elements of the vegetation are negatively affected simultaneously, allowing the dominance of taxa with affinity with and/or tolerance to human disturbances. This finding highlights the importance of continuing to protect natural areas from human activities, because according to our results, incipient human impact levels lead to important losses of forest structure. Indeed, forests that continuously experience environmental hardship are the most sensitive to human activities. Particularly in areas such as the Maya region, where for thousands of years a large number of sites have been subject to different levels of anthropogenic stress.

### **Acknowledgments**

This research was funded by grants Conacyt 252148, PAPIIT-UNAM IA100317 and IN107716, and Deutsche Forschungsgemeinschaft (DFG, SCHW 671/16-1). We appreciate the help of all colleagues and institutions involved in this work. Special thanks to the

students team from the Instituto Tecnológico de Chetumal, Centro Interdisciplinario de Ciencias Marinas, and Universidad Autónoma de San Luis Potosí for their help in the field. We would like to thank the following colleagues and institutions: Manuel Elías (El Colegio de la Frontera sur, Chetumal Unit, Mexico); Alexis Oliva; and the team from the Asociación de Municipios del Lago de Yojoa y su Área de Influencia (AMUPROLAGO, Honduras); María Renée Álvarez, Margarita Palmieri, Eleonor de Tott, Roberto Moreno (Universidad del Valle de Guatemala, Guatemala); Consejo Nacional de Áreas Protegidas (CONAP, Guatemala); Néstor Herrera; and Ministerio de Medio Ambiente (San Salvador, El Salvador).

## CAPÍTULO 4

### EFFECTOS DE LA VARIABILIDAD CLIMÁTICA Y FACTORES DE ESTRÉS ANTHROPOGÉNICOS EN LA VEGETACIÓN DE LAS TIERRAS ALTAS MAYA

### EFFECTS OF LATE HOLOCENE CLIMATE VARIABILITY AND ANTHROPOGENIC STRESSORS ON THE VEGETATION OF THE MAYA HIGHLANDS

**Franco-Gaviria, F.<sup>1\*</sup>, A. Correa-Metrio<sup>2</sup>, C. Cordero-Oviedo<sup>1,4</sup>, M. López-Pérez<sup>3</sup>, G.M. Cárdenes-Sandí<sup>4</sup>, and F.M. Romero<sup>2</sup>.**

**1.** Posgrado en Ciencias de la Tierra, Universidad Nacional Autónoma de México,

Coyoacán, Ciudad de México, México 04510.

**2.** Instituto de Geología, Universidad Nacional Autónoma de México, Coyoacán, Ciudad de

México, México 04510.

**3.** Posgrado en Ciencias Biológicas, Universidad Nacional Autónoma de México,

Coyoacán, Ciudad de México, México 04510.

**4.** Escuela Centroamericana de Geología, Universidad de Costa Rica, San José, Costa Rica.

*Quaternary Science Reviews*

<https://doi.org/10.1016/j.quascirev.2018.04.004>

## **Resumen**

La variabilidad climática y las actividades humanas han moldeado a las comunidades de vegetación de la región Maya del sur de México y Centroamérica en escalas de tiempo de cientos a miles de años. Gran parte de los esfuerzos de investigación en la región se han centrado en las tierras bajas, con relativamente poco conocimiento sobre la historia ambiental de las tierras altas. En este trabajo se presentan datos de dos secuencias sedimentarias recuperadas en los Altos de Chiapas, México. El objetivo fue discernir la contribución relativa del clima y el impacto humano en el desarrollo de la vegetación regional durante el Holoceno tardío. Los registros paleoecológicos revelan una tendencia a largo plazo hacia condiciones secas con sequías superpuestas a escala de cientos de años. Una tendencia hacia la disminución de humedad de 3,400 a 1,500 AP fue consistente con el desplazamiento hacia el sur de la Zona de Convergencia Intertropical, mientras que las sequías periódicas fueron probablemente una consecuencia de forzamientos como El Niño. Estas condiciones unidas a la densa ocupación humana, convirtieron la vegetación de bosque a sistemas más abiertos. De acuerdo con los registros paleoecológicos, el abandono cultural de la zona ocurrió ca. 1,500 AP, favoreciendo la recuperación del bosque que fue algo limitada por la baja disponibilidad de humedad. Alrededor de 600 AP, las condiciones más húmedas promovieron el establecimiento de los bosques montanos modernos, que consisten en una mezcla diversa de elementos templados y tropicales. Los tipos de vegetación que ocuparon el área de estudio durante los últimos milenios han permanecido dentro del envoltorio definido por el mosaico de vegetación moderna. Este hallazgo resalta la importancia de los micro hábitats para mantener la biodiversidad a través del tiempo, incluso bajo escenarios de alta variabilidad climática y presión antropogénica.

**Palabras clave:** Centroamérica; impacto humano; Holoceno; Maya; bosque montano de niebla; paleoecología; dinámica de la vegetación

### **Abstract**

Climate variability and human activities have shaped the vegetation communities of the Maya region of southern Mexico and Central America on centennial to millennial timescales. Most research efforts in the region have focused on the lowlands, with relatively little known about the environmental history of the regional highlands. Here we present data from two sediment sequences collected from lakes in the highlands of Chiapas, Mexico. Our aim was to disentangle the relative contributions of climate and human activities in the development of regional vegetation during the late Holocene. The records reveal a long-term trend towards drier conditions with superimposed centennial-scale droughts. A declining moisture trend from 3,400 to 1,500 cal yr BP is consistent with previously reported southward displacement of the Intertropical Convergence Zone, whereas periodic droughts were probably a consequence of drivers such as El Niño. These conditions, together with dense human occupation, converted the vegetation from forest to more open systems. According to the paleoecological records, cultural abandonment of the area occurred ca. 1,500 cal yr BP, favoring forest recovery that was somewhat limited by low moisture availability. About 600 cal yr BP, wetter conditions promoted the establishment of modern montane cloud forests, which consist of a diverse mixture of temperate and tropical elements. The vegetation types that occupied the study area during the last few millennia have remained within the envelope defined by the modern vegetation mosaic. This finding highlights the importance of microhabitats in the maintenance

biodiversity through time, even under scenarios of high climate variability and anthropogenic pressure.

**Keywords:** Central America; human impact; Holocene; Maya; montane cloud forest; paleoecology; vegetation dynamics.

#### **4.1. Introduction**

Given the confluence of diverse climates with a rich topography, southeastern Mexico harbors some of the greatest vegetation diversity found throughout Mexico and Central America (Ramirez-Marcial et al. 2001; Rzedowski 2006). Thus, the region has been studied intensively with respect to patterns of modern vegetation diversity, and how its long history of climate variability and human occupation gave rise to the modern regional ecosystems (Curtis et al. 1998; Leyden 2002; Domínguez-Vásquez et al. 2004; Bryant et al. 2005; Hodell et al. 2005b; Correa-Metrio et al. 2012a; Correa-Metrio et al. 2013). The intersection of the Neotropical and Nearctic biogeographic realms (Udvardy 1975) produced a gradient characterized by tropical vegetation in the lowlands and temperate elements in the highlands. Effects of dense human occupation are evident through at least the last 4,000 years in the lowlands (Leyden, 2002), and have certainly exerted an important influence on the evolution of vegetation composition and structure. Nevertheless, little is known about how natural and anthropogenic factors affected the vegetation of the highlands. Of special interest is the period of post-abandonment (ca. 1,500 cal yr BP), when the montane cloud forests that occupy the area today developed.

The highlands of Chiapas are composed of valleys and ridges at elevations between 1500 and 2500 meters above sea level (m asl) in the central part of the state of Chiapas,

southeastern Mexico. Its geographic location and physiography give rise to conditions that promote high biodiversity given the intersection of two biogeographic realms across steep environmental gradients. Neotropical taxa from Central America and the Yucatan Peninsula intermingle with Nearctic elements from Central Mexico (Rzedowski, 2006). Tropical montane cloud forests (MCF) represent a prime example of how the mixture of floras can yield diverse vegetation (Hamilton et al. 1995). Study of the temporal dynamics of these vegetation types provides an opportunity to understand the effect of environmental stressors of different magnitude and intensity on biodiversity patterns, and shed light on the environmental dynamics of the Maya highlands.

Natural environmental variability over time caused rapid shifts in regional plant diversity. For example, following the Last Glacial Maximum, the average annual temperature in the Yucatan Peninsula was between 5 and 10°C lower than present (Correa-Metrio et al. 2012a; Hodell et al. 2012), causing downslope migration of species. Additionally, there have been multiple episodes of late Holocene extreme droughts, associated with substantial changes in the composition and structure of vegetation and the patterns of human occupation (Curtis et al., 1998; Leyden, 2002; Correa-Metrio et al., 2012a). Much of this environmental variability was caused by abrupt climatic changes that, in turn, caused vegetation changes. Such rapid vegetation responses imply the persistence of small plant populations in areas with localized, favorable conditions, which facilitate the process of recolonization (Bush 2002a; Correa - Metrio et al. 2016).

On the windward side and under the cloud line of mountainous regions, orographic precipitation and topography interact to create a broad range of microclimates. These microhabitats offset some of the effects of extreme regional climates and climatic

variability on vegetation (Bush, 2002a). In these areas, moisture-laden air rises along the slopes, becoming cloudiness and rain. Thus, local humidity probably serves as a buffer to extreme droughts, preventing the loss of diversity throughout the late Quaternary. Extremely steep slopes are less likely to be occupied by people and therefore could have acted as biodiversity “reservoirs” that facilitated post-abandonment plant recolonization. Thus, vegetation responses to exogenic disturbances in these areas were likely buffered by higher moisture availability.

Here we present a paleoecological reconstruction based on two sedimentary records collected from two lakes in the highlands of Chiapas, southeastern Mexico. The two neighboring sites, about 6 km from one another, represent contrasting topographic and physiographic environments that enabled us to evaluate the spatial and temporal consistency of the environmental history of the area. Our study provides insights into the response of plant communities to changes in climate and land use through a multi-site, multi-proxy approach. Our aim was to investigate the impacts of environmental stressors (e.g. droughts, fires, land-use changes, etc.) on tropical mountain vegetation during the late Holocene. We used pollen, charcoal, and geochemical analyses to address three basic questions: (1) what is the relationship between modern and fossil vegetation diversity, as revealed by the comparison of modern and fossil pollen spectra?, (2) do late Holocene climate patterns in the area reflect trends reported elsewhere in the northern Neotropics?, and (3) Was the 9<sup>th</sup>-century cultural collapse in the lowlands evident in the highlands?

## 4.2. Regional background

Lagunas de Montebello National Park is a ~6,022-ha protected area in the central highlands of Chiapas, southern Mexico (Fig. 4.1). The area lies on Lower Cretaceous karstic limestones, which favored the development of a lake district that includes more than 50 water bodies, including dolines, uvalas, and poljes (Padilla-Sánchez 2007).

The region is characterized by a mean annual temperature of 18 °C and mean annual precipitation of ~2500 mm. Temperature shows an annual range of ~4 °C, with the coldest and warmest periods from December to February and April to September, respectively (climate data from Tzisco Meteorological station, Servicio Meteorológico Nacional, 2017). The rainy season is centered from May to October (Fig. 4.1C) with rainfall associated with the northern position of the Intertropical Convergence Zone (ITCZ), during the boreal summer (Mestas-Núñez et al. 2007). During the boreal winter, the southern migration of the ITCZ is associated with dry condition in the region, whereas polar air masses bring light sporadic rains into the area. El Niño Southern Oscillation (ENSO) plays an important control upon interannual rainfall variability over southern Mexico (Magaña et al. 2003). ENSO produces spatially variable effects in the precipitation across Mexico, although the general pattern can be summarized as a reduction of rainfall, especially in regions characterized by strong convection (Bhattacharya & Chiang 2014). In the region of Montebello, meteorological data covering from February 1961 to December 2015 (Servicio Meteorológico Nacional, 2017) suggest that El Niño years are associated with a longer and more intense dry season and a drier wet season (Apéndice 4.3). Additionally, during El Niño years minimum and maximum temperature from February to May increase between 1 and 2 °C, causing higher evapotranspiration, and therefore more stressful conditions for

biological communities. During La Niña years, the most evident change in the precipitation regime is a drier wet season, whereas minima and maxima monthly temperatures decrease slightly (Apéndice 4.3).

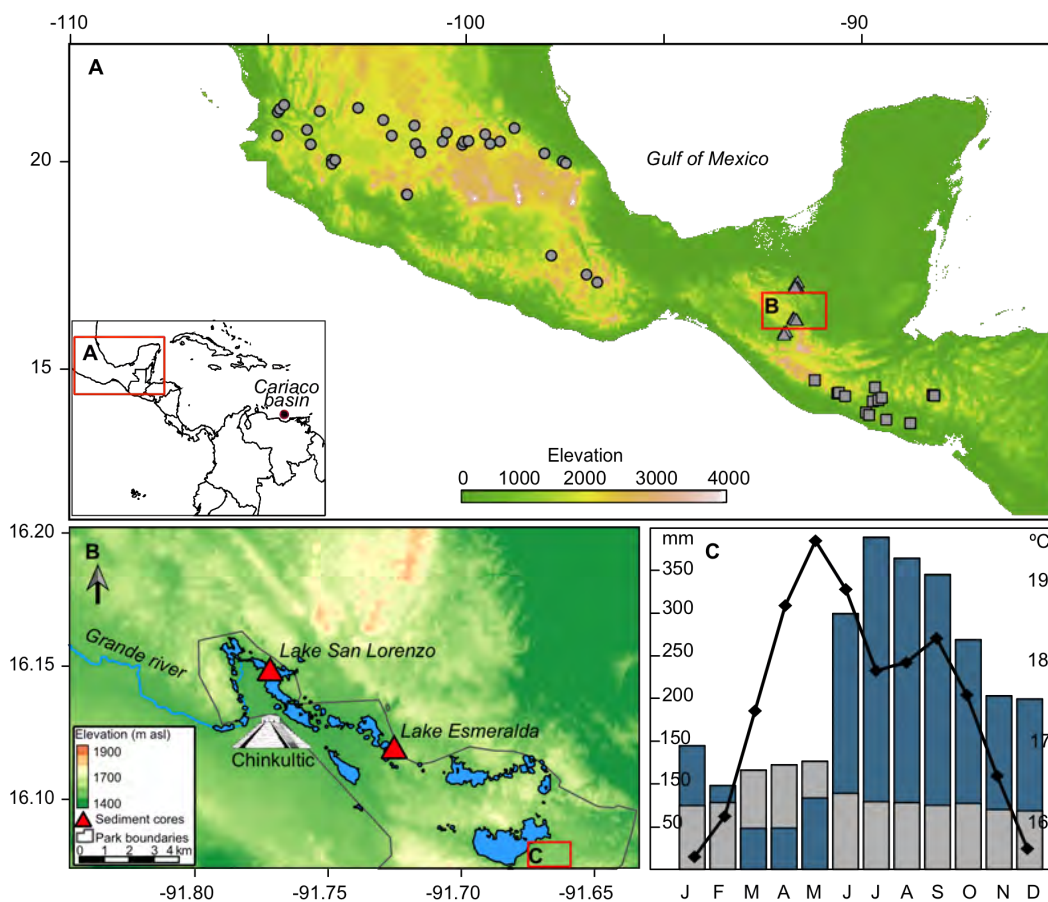


**Figure 4.1.** **A.** Lakes sampled for modern pollen in Central of Mexico (circles), and the highlands and middle elevations of Central America (rectangles) and Chiapas (triangles). **B.** Lakes San Lorenzo and Esmeralda in Lagunas de Montebello National Park. **C.** Monthly precipitation (blue bars), potential evapotranspiration (grey), and monthly mean temperature (black line) of Lagunas de Montebello National Park (data from Tziscoac Meteorological Station, Servicio Meteorológico Nacional, 2017).

The climate, geographic location, and diverse topography of the area have favored the establishment of forests composed of a mixture of coniferous and broadleaf species (Ramirez-Marcial et al. 2001). Although the mosaic of regional vegetation types is highly diverse, it can be described generally by three main vegetation types: pine forest, *Pinus-Quercus-Liquidambar* forest, and MCF (Breedlove 1981; Rzedowski 2006). Pine forests are common in disturbed areas or areas subjected to extreme temperatures, intense solar radiation, and/or low soil moisture (Ramírez-Marcial 2003). *Pinus-Quercus-Liquidambar* forests are a mixture of pine and broadleaf elements, dominated by these genera, together with *Clethra macrophylla* (Carlson 1954). MCF remnants are dominated by broadleaf species and are located in the northeastern extreme of the National Park. Their distribution is driven largely by soil moisture availability and human impact. These factors restrict MCF to areas with steep topography and slopes that receive little direct sunlight and are subject to minimal human disturbance. These forests are rich in understory broad-leaved trees species, with dominance of *Podocarpus matudai*, *Turpina tricomuta* and *Prunus brachybotria* (Ramirez-Marcial et al. 2010). All these vegetation types have been influenced by the long history of human activities in the region, which created substantial patches of open vegetation and regrowth.

#### *4.2.1. Settlement history*

Maya communities from the lowlands seem to have colonized the highlands of Chiapas between the Late Preclassic and the Early Classic (from 2,200 to 1,500 cal yr BP, see Maya chronostratigraphy in Fig. 4.7), reflecting a settlement pattern characterized by an almost total abandonment of valleys and colonization of the mountains (Adams 1961).

Nevertheless, there is evidence of Preclassic settlements along the neighboring Grijalva River (Adams 1961; Bryant & Clark 1983; Bryant et al. 2005) that probably exerted early influence in the region of Montebello. The landscape heterogeneity of the Montebello region, characterized by hills, flood plains and a large number of lakes, likely made it an attractive setting for human settlement. Indeed, the construction of Chinkultic acropolis (Fig. 4.1) indicates a considerable increase in the human population of the region (Ferguson & Adams 2001; Bryant et al. 2005). Chinkultic was a highland city that served as a gateway for trade with Mayas of lowland Chiapas, Guatemala, El Salvador, and the Pacific coast (Navarrete 2006). Built ca. 2,200 cal yr BP, the city was abandoned ca. 1,500 cal yr BP and reoccupied by ca. 1,200 cal yr BP (Maya Late Classic). Although the population declined ca. 900 cal yr BP, the city remained occupied well into the Postclassic, until 600 cal yr BP (Navarrete 2006). At the time of the Spanish conquest in the early 1500s, the highlands of Chiapas were sparsely inhabited, with most of the population distributed in isolated satellites towns that surrounded ancient indigenous villages (Bryant & Clark 1983). In modern times, despite the protected status of the area, heavy immigration of people from other areas of Mexico and Central America has led to an expansion of urbanized areas (UNHCR 2001; Ramirez-Marcial et al. 2010).

### 4.3. Material and methods

#### 4.3.1. Fossil records

Sediment sequences were retrieved from two lakes in the Lagunas de Montebello National Park. Lake San Lorenzo is a large (180 ha), shallow ( $z_{\max}$  11 m) water body located on a karstic plain at an elevation of 1454 m asl, and receives sediment and water discharge from the Grande River (Alcocer et al. 2016). Its origin is likely associated with the incision-deposition dynamics of the river, and it is therefore surrounded by extensive depositional flatlands currently used for agriculture. Lake Esmeralda is a small (1ha) and shallow ( $z_{\max}$  3.6 m), and is located in the southern mountains of the National Park at an elevation of 1473 m asl, ~ 6 km from Lake San Lorenzo (Fig. 4.1). Lake Esmeralda is of karstic origin and is characterized by steep walls and a flat bottom (Alcocer et al. 2016).

A core was retrieved from the central, deep area in each lake. Cores were collected from a raft, using a modified Livingston piston corer (Colinvaux et al. 1999a). Sediment cores of 670 cm and 166 cm long were retrieved from Lakes San Lorenzo (core LIQ13) and Esmeralda (core ESM12), respectively. Both cores were transported to the laboratory, longitudinally split, and stored at 4 °C prior to analysis. Chronologies were established with AMS radiocarbon dates on four samples from each core. Dating was performed on micro-charcoal and terrestrial plant macro-remains at Beta Analytic, Inc., Miami (Table 4.1). Hand-picked charcoal and macro-remains was preferred over bulk sediments to avoid possible hard water effects. Radiocarbon dates were calibrated using IntCal13 (Reimer et al. 2013), and Bayesian age-depth models were built using Bacon (Blaauw & Christen 2011). All ages are expressed in calibrated years before present (cal yr BP hereafter).

**Table 4.1.** Radiocarbon dates and calibrated ages for samples from cores LIQ13 and ESM12, pMC: percent modern carbon, for samples younger than 0 radiocarbon years BP (1950).

| Core name and Beta Analytic number | Depth (cm) | Dated Material | <sup>14</sup> C age | 2-sigma calibration cal yrs BP |
|------------------------------------|------------|----------------|---------------------|--------------------------------|
| <b>Lake San Lorenzo core</b>       |            |                |                     |                                |
| <b>LIQ13</b>                       |            |                |                     |                                |
| 409556                             | 53.7       | Charcoal       | 106.2 +/- 0.3 pMC   | -47 to -50                     |
| 423226                             | 332        | Charcoal       | 640 +/- 30          | 553 to 610                     |
| 437076                             | 561        | Charcoal       | 2010 +/- 30         | 1885 to 2009                   |
| 372420                             | 660        | Plant remains  | 3200 +/- 30         | 3366 to 3469                   |
| <b>Lake Esmeralda core</b>         |            |                |                     |                                |
| <b>ESM12</b>                       |            |                |                     |                                |
| 407437                             | 28         | Plant remains  | 630 +/- 30          | 552 to 613                     |
| 437075                             | 74         | Plant remains  | 1340 +/- 30         | 1234 to 1305                   |
| 407438                             | 117        | Charcoal       | 1670 +/- 30         | 1523 to 1628                   |
| 403912                             | 161        | Wood           | 2250 +/- 30         | 2156 to 2267                   |

For palynological analyses 1-cm<sup>3</sup> subsamples were taken on average every 4 and 10 cm for cores ESM12 and LIQ13, respectively. Thus, we analyzed a total of 52 samples from core ESM12 and 40 samples from core LIQ13. Samples were prepared following standard protocols (Faegri & Iversen 1989). Pollen grains were counted in each sample under an optical microscope at 400x and 1000x magnification. Counts were carried out until a pollen sum of 200 grains was obtained, and all pollen counts were transformed to percentages of the pollen sum (Birks & Gordon 1985). Because they are often overrepresented, Cyperaceae, Moraceae, *Pinus*, and *Quercus* were counted, but excluded from the pollen sum (after Correa-Metrio et al. 2011).

A 1-cm<sup>3</sup> sediment sample from each depth analyzed for pollen was processed for charcoal analysis. Following standard techniques, microscopic charcoal particles were manually separated and photographed using a stereomicroscope (Clark 1988). Subsequently, the number of pixels covered by charcoal particles was counted using ImageJ (Rasband

2005), and charcoal was expressed as area normalized to volume ( $\text{mm}^2/\text{cm}^3$ ). Concentrations of Ca, Fe, Rb, Sr, Ti, and Zr were measured every 1 cm in both cores using a handheld X-Ray fluorescence (XRF) analyzer (Niton XL3t), totaling 670 samples for LIQ13 and 166 samples for ESM12.

#### 4.3.2. *Modern pollen*

We assembled a modern pollen dataset composed of the pollen spectra from mud-water interface sediment samples collected in 73 lakes. Sampled locations covered a range of mountain environments from 400 to 2000 m asl, in central and southern Mexico (34 and 25 samples, respectively) and northern Central America (14 samples), including sites from Guatemala, Honduras, and El Salvador (Fig, 4.1). All modern datasets are published (Correa-Metrio et al. 2011 for northern Central America; Correa-Metrio et al. 2013 for Central Mexico; Franco-Gaviria et al. 2018a for Chiapas and northern Central America). We generated an *a priori* classification of samples into Central Mexico (CM), highlands (HL, > 1400 m asl) and middle elevations (ME, 400-1400 m asl) of Central America and Chiapas. Each site represented in the modern pollen dataset was described in terms of its regional modern climate and human impact. Climate variables (mean diurnal range, MDR; isothermality, IST; and annual precipitation, APP) were obtained from WorldClim (Hijmans et al. 2005), whereas human influence was assessed using the global Human Influence Index (HII), ranging from zero for fully pristine areas, to 64 for totally urbanized regions (Sanderson et al. 2002).

### 4.3.3. Numerical analysis

Modern samples and fossil pollen data from both cores were analyzed together using non-metric multidimensional scaling (NMDS). NMDS projects multivariate data along latent axes based on distance among samples, while preserving the underlying dissimilarity structure of the original dataset (McCune et al. 2002). Therefore, samples with similar scores are expected to have similarities in terms of both taxon composition and structure of the pollen assemblage. The NMDS was based on the Bray-Curtis dissimilarity index and was constructed in three dimensions. Whereas Bray-Curtis dissimilarity has been proven to be monotonically related to ecological distance (Faith et al. 1987), the use of three dimensions substantially reduces the stress, allowing a more natural ordination of samples. The scores of the NMDS were used to infer vegetation development through time and the relationships between modern and fossil pollen samples. Distributions of samples along the three NMDS axes were summarized for both modern and fossil pollen through probability density functions (PDF) of their scores (Silverman 1986). PDFs for the modern pollen dataset were constructed, separating samples by provenance, *i.e.* CM, HL, ME.

The interpretation of the underlying environmental structure of the NMDS ordination was based on multiple regressions of the scores of modern samples against the environmental attributes of the modern sites they represent. Sample scores along the three axes were regressed against MDR, IST, APP, HII, and geographic variables to produce a model that was subjected to step-wise backward variable selection (Bolker 2008). The interpretation of the ordination was then based on the best and most significant model. The modern analogue technique (Overpeck et al. 1985) was used to reconstruct HII through time, although the distance between modern and fossil pollen assemblages was calculated

using the Euclidean metric on ordination scores instead of the original dataset (Caballero-Rodríguez et al. 2017). The modern pollen assemblage showing the minimum distance to a given fossil sample was considered to be the most likely analog. All numerical analyses were produced using R (R Core Team 2017), especially the packages *vegan* (Oksanen et al. 2017) and *MASS* (Venables & Ripley 2002).

## **4.4. Results**

### *4.4.1. Chronology*

Core LIQ13 spans the last 3400 years (Table 4.1). The core shows a low sedimentation rate (~0.11 cm/yr) between the base of core (670 cm) and 350 cm depth, and higher values (~0.47 cm/yr) between 350 cm and the surface (Fig. 4.2A). Core ESM12 yielded a basal age of 2800 cal yr BP (Fig. 4.2B), and displayed a uniform, low mean sedimentation rate throughout the core (~0.065 cm/yr).

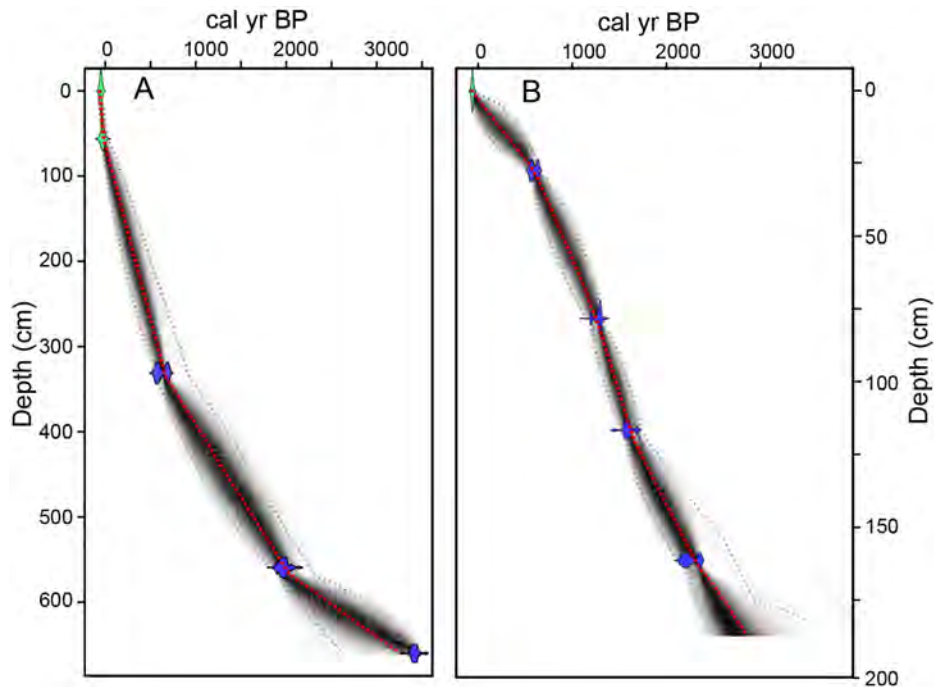


**Figure 4.2.** Age-depth models for the sediment cores from Lakes San Lorenzo (A. core LIQ13) and Esmeralda (B. core ESM12). Calibrated radiocarbon ages are in blue, whereas the gray scale indicates all likely age-depth models. Grey stippled lines show 96% confidence intervals, with the red curve indicating the accepted model.

#### 4.4.2. Fossil pollen

The fossil pollen spectrum of core LIQ13 was composed of 113 taxa (Fig. 4.3). At the bottom of the record (3,400-3,200 cal yr BP), pollen spectra were characterized by high abundances of Cyperaceae and *Pinus*. From 3,200 to 2,400 cal yr BP, arboreal elements became abundant, mainly *Pinus* (up to 200%), *Quercus* (22-68%), *Myrica* (5-12%) and *Alnus* (2-8%). A short period of dominance of herbaceous taxa such as *Ambrosia*, Asteraceae, and Poaceae is evident ca. 2,800 cal yr BP. Also, ca. 2,500 cal yr BP, *Alchornea*, *Hedyosmum*, and *Liquidambar* show important peaks. Between 2,400 and 1,500 cal yr BP, pollen spectra were characterized by increases in Poaceae (15-32%), *Ambrosia* (2-23%), Asteraceae (1-7%), and Amaranthaceae (2-3%), at the expense of arboreal

elements. Indeed, *Pinus* (40%), *Quercus* (18%), *Myrica* (3%), and *Alnus* (2%) fell to their lowest percentages during this time period. *Zea mays* pollen first appeared in the record at ca. 2100 cal yr BP, along with relatively high percentages of Cyperaceae (~40%). From 1500 to 600 cal yr BP, *Pinus* reached its maximum abundance (657%), and gradual increases were evident for *Alchornea*, *Alnus*, *Hedyosmum*, and *Quercus*. Other arboreal elements like *Liquidambar*, *Podocarpus*, and *Ulmus* became persistent from 1,200 cal yr BP onward. Herbaceous taxa Amaranthaceae, Asteraceae, and Poaceae showed gradual decreases, while *Ambrosia* and *Z. mays* were absent. Throughout the last 600 years, *Pinus*, *Ilex*, *Hedyosmum*, and *Quercus* showed gradual decreases, in antiphase with increasing *Liquidambar*, *Trema*, *Celtis*, *Myrica*, and Melastomataceae, that reached their maximum percentages. Also, Asteraceae and *Z. mays* were persistent through this time period, whereas *Ambrosia* and Amaranthaceae remained below 3 %.

The ESM12 record can be divided into four zones characterized by distinct pollen assemblages (Fig. 4.3). From 2,800 to 2,100 cal yr BP, the vegetation was characterized by arboreal elements such as *Pinus* (57-700%), *Quercus* (10-192%), *Myrica* (2-39%), Bignoniaceae (1-21%), and *Ilex* (1-13%). Also, Cyperaceae showed high abundances (59-85%), reaching their maximum at ca. 2,600 cal yr BP. Throughout this time interval, *Alchornea*, *Centropogon*, *Liquidambar*, and *Hedyosmum* were also present in abundances < 8%. Between 2,100 and 1,500 cal yr BP, *Pinus*, *Quercus*, *Ilex*, Bignoniaceae, and Cyperaceae gradually declined, reaching abundances below 3%. In contrast, *Myrica* (14-58 %), *Ambrosia* (0-12%), Asteraceae (2-19%), and Poaceae (3-40%) showed increases. From 1500 to 600 cal yr BP, *Ambrosia* and Asteraceae disappeared, while Poaceae showed a gradual decrease from 40 to 8%. These taxa were replaced by *Quercus* (85%), *Myrica* (30%), *Hedyosmum* (15%), and *Alchornea* (10%), whereas Cyperaceae was present at

moderate percentages (~20%). Other forest elements such as Bignoniaceae, *Celtis*, *Hedyosmum*, *Liquidambar*, Melastomataceae, and *Ulmus* rebounded at ca. 1,200 cal yr BP, with intermediate abundances (up to 10%). From 600 cal yr BP to present, pollen spectra were dominated by *Liquidambar* (~3-32%), *Pinus* (68-400%), *Quercus* (15-82%), Bignoniaceae (4-10%), *Celtis* (2-11%), and *Myrica* (6-16%). Although herbaceous taxa were poorly represented throughout this time period, Poaceae (8-21%) exhibited a gradual increase.

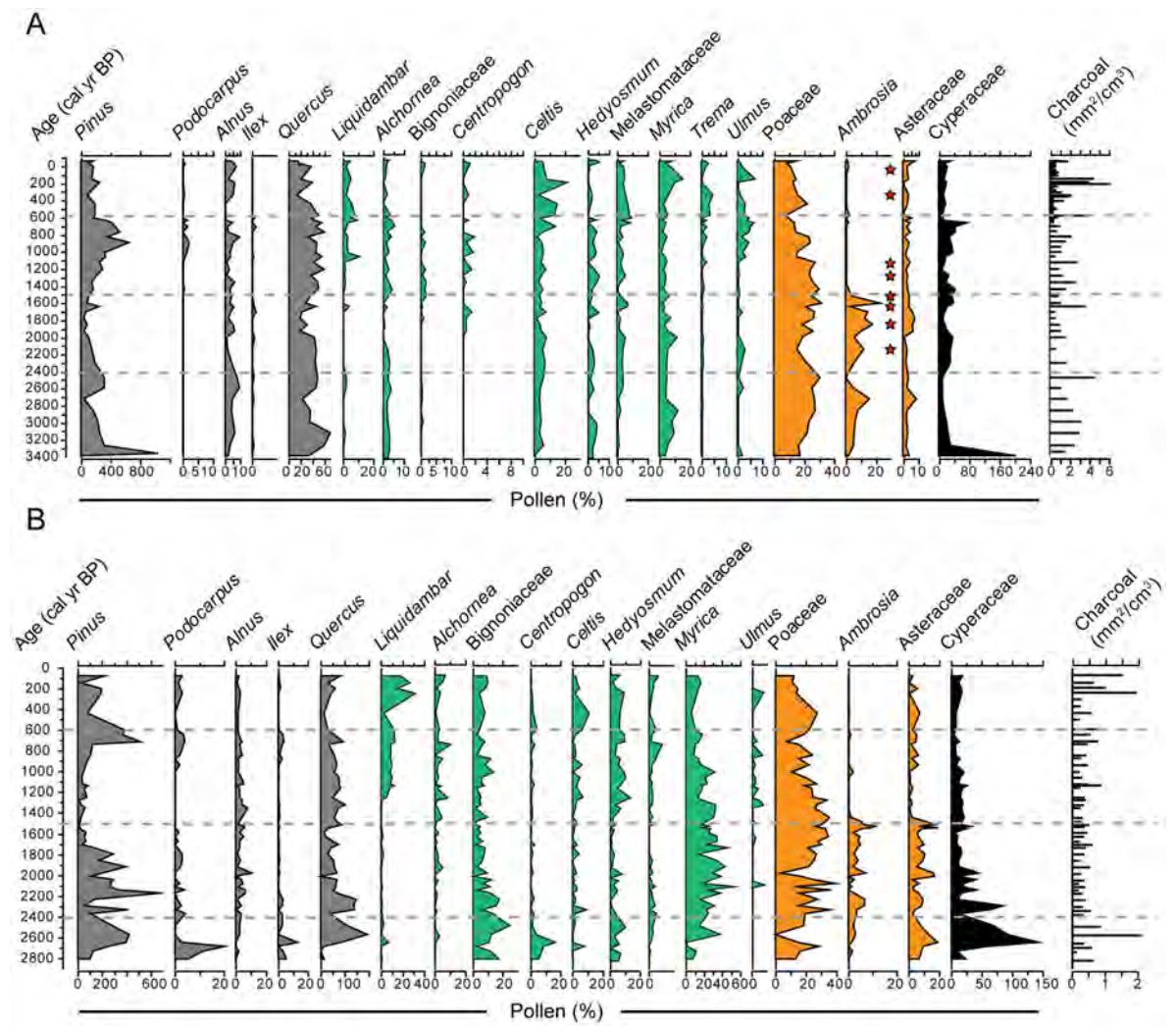


**Figure 4.3.** Simplified pollen diagrams and charcoal concentration of fossil samples from the sediment sequences of Lakes San Lorenzo (A. core LIQ13) and Esmeralda (B. core ESM12). In core LIQ13 (A), red stars indicate presence of *Zea mays* pollen.

#### 4.4.3. Charcoal and geochemistry

Charcoal concentrations in core LIQ13 showed two main stages: i) low and stable concentrations ( $< 2 \text{ mm}^2/\text{cm}^3$ ) from 3,400 to 600 cal yr BP, and ii) high and variable concentrations (up to  $6 \text{ mm}^2/\text{cm}^3$ ) from 600 cal yr BP to present (Fig. 4.3). Although charcoal concentrations were generally low, peaks were evident at ca. 2,500, 1,600, and 1,100 cal yr BP. Small particles dominated the record from 3,400 to 1,000 cal yr BP, whereas bigger particles were important from 1,000 cal yr BP to present (Apéndice 4.4). Core ESM12 also showed two contrasting periods: i) low and relatively stable charcoal concentrations ( $< 1 \text{ mm}^2/\text{cm}^3$ ) from 2,800 to 600 cal yr BP, and ii), relatively high ( $> 1 \text{ mm}^2/\text{cm}^3$ ) concentrations from 600 cal yr BP to present. During this time interval, charcoal peaks were evident at ca. 2,500, 1,100, and 700 cal yr BP (Fig. 4.3). Small charcoal particles (areas  $< 0.05 \text{ mm}^2$ ) dominated the entire ESM12 record (Apéndice 4.4).

Core LIQ13 showed Ca, Fe, Rb, Sr, Ti, and Zr concentrations that were statistically adequate (repeated measurements were consistent) and continuous throughout the record. Ca and Sr showed similar trends that were in antiphase with Fe, Rb, Ti, and Zr (Apéndice 4.1 y 4.5). High concentrations of Ca and Sr were found between 3,400 and 3,000 cal yr BP, 2600 and 2400 cal yr BP and between 1,500 and 700 cal yr BP. Their lowest concentrations were found between 3,000 and 2,600 cal yr BP, between 2,400 and 1,500 cal yr BP, and from 700 to present. In core ESM12, only Ca (97% of samples), Fe (97%), Sr (97%), and Zr (95%) were consistently and continuously detected by the XRF. In this core, Ca and Sr showed a similar pattern, in antiphase with Fe and Sr (Apéndice 4.1 y 4.5). Ca and Sr showed high concentrations between 2800 and 1400 cal yr BP, decreasing toward present.

Fe and Zr showed their highest concentrations in the bottom of the record, and low concentrations after 2,500 cal yr BP.

#### 4.4.4. Modern pollen

The modern pollen dataset was composed of 250 taxa (Fig. 4.4). Samples from CM were mainly dominated by *Pinus*, *Quercus*, and *Alnus*, although some of them showed high percentages of herbaceous taxa (e.g. *Ambrosia*, Asteraceae, and Poaceae). Pollen spectra from HL were dominated by a mixture of temperate (e.g. *Ilex*, *Liquidambar*, *Pinus*, *Quercus*, and *Myrica*) and tropical (e.g. *Alchornea*, *Celtis*, Moraceae, and *Psychotria*) taxa. In ME samples, *Celtis*, Moraceae, Melastomataceae, and *Trema* were the most frequent pollen taxa, often coexisting with *Ilex*, *Myrica*, and *Quercus*. A second type of pollen assemblage was observed in the ME samples, characterized by the dominance of arboreal taxa such as *Bursera*, *Cordia*, Moraceae, and *Pinus*, associated with herbaceous taxa such as *Ambrosia* and Poaceae. Overall, herbaceous taxa were also found in ME locations, although they had lower representation compared with samples from CM.

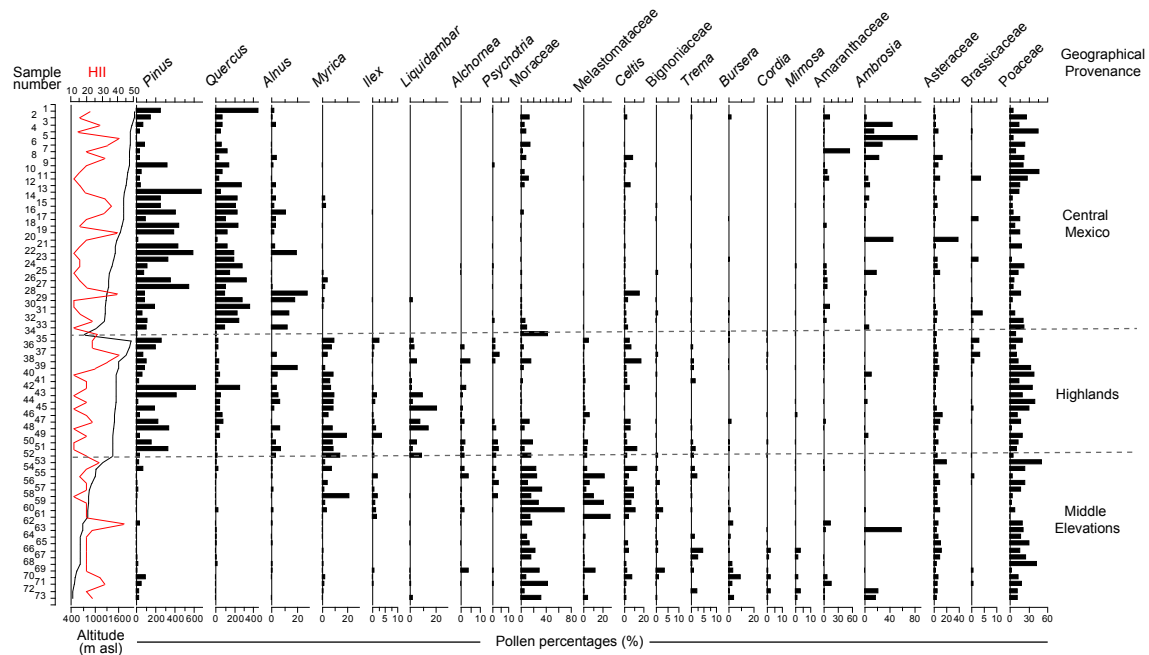


**Figure 4.4.** Simplified pollen diagram of mud-water interface samples from 73 lakes in Central of Mexico, highlands and middle elevations of Central America and Chiapas. The human impact index and altitude of sampled locations is shown in the leftmost column.

#### 4.4.5. Ordination of pollen samples and reconstruction of HII

The three-dimensional NMDS ordination for modern and fossil pollen assemblages produced a convergent solution with a stress of 0.1 (Fig. 4.5). The ordination of modern samples in the bivariate space defined by Axes 1 and 2 of the NMDS showed some overlapping among the distributions of samples from CM, HL, and ME (Fig. 4.5). These groups of samples, however, showed clear clustering according to their provenance. NMDS Axis 3 showed little dispersion and samples from all provenances were rather mixed. PDFs of sample scores along NMDS Axis 1 showed that samples from HL were more variable than those from ME, which in turn were more variable than those from CM (Fig. 4.5D). Along Axis 2, PDFs of sample scores showed a gradual turnover, from CM located towards the negative end of the axis, to HL in the center of the axis, to ME mostly on the positive

side. PDFs of Axis 3 also showed differential modes for each region represented by the modern sampling, but their dispersion was substantially lower than those of Axes 1 and 2.

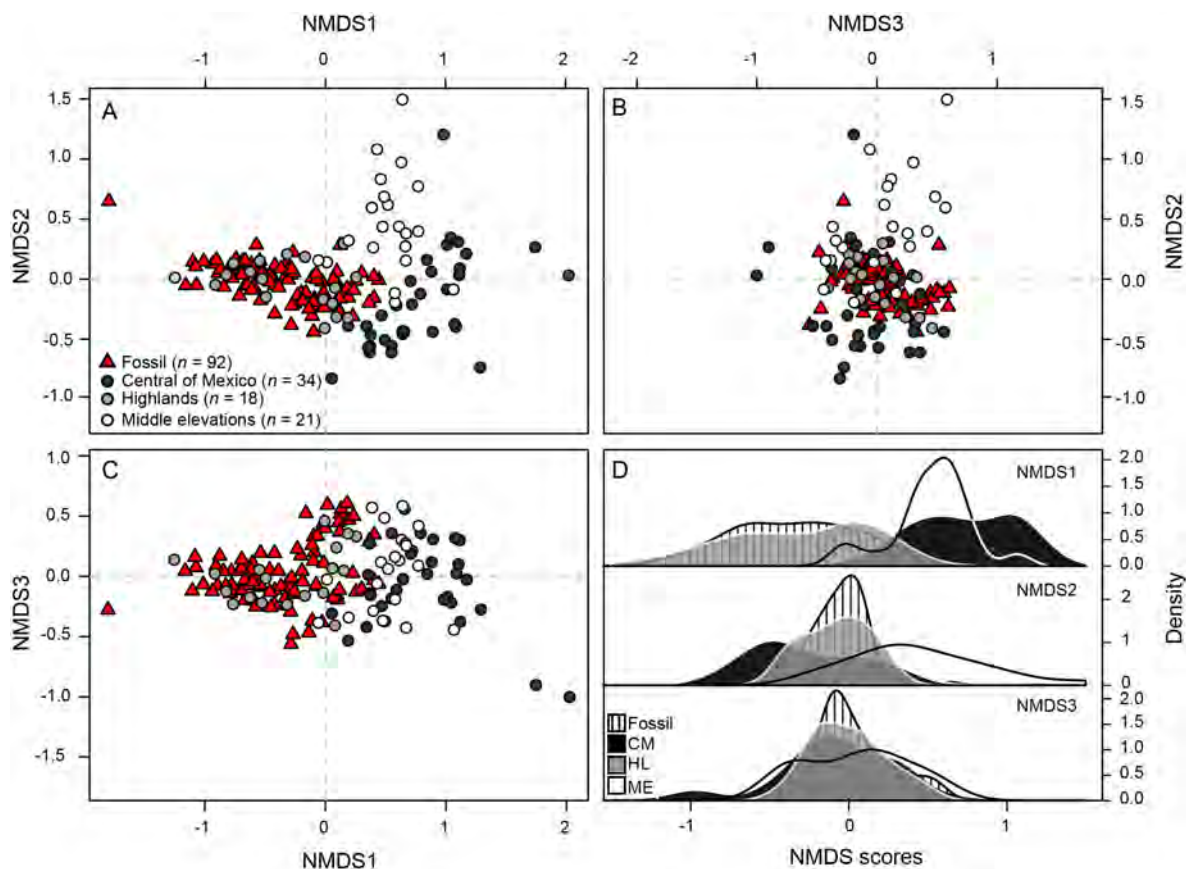


**Figure 4.5.** Non-metric multidimensional scaling (NMDS) ordination of modern and fossil pollen samples. **A.** NMDS Axis 1 vs NMDS Axis 2. **B.** NMDS Axis 3 vs NMDS Axis 2. **C.** NMDS Axis 1 vs NMDS Axis 3. **D.** Probability density functions (PDFs) of NMDS sample scores discriminated by sample provenance.

NMDS scores for the LIQ13 record showed values between -1.81 and 0.44 for Axis 1. Negative scores were obtained from 3,400 to 2,000 cal yr BP, and from 1,500 cal yr BP to present, whereas positive scores characterized samples from the time period between 2,000 and 1,500 cal yr BP. Scores along Axis 2 ranged from -0.08 to 0.66, averaging 0.2. Along Axis 3, scores were relatively constant and ranged from -0.38 to 0.01. NMDS scores for the ESM12 record ranged from -1.17 to 0.40 along Axis 1, with predominance of

negative and near-zero values from 2,500 to 1,700 cal yr BP, and from 1,200 cal yr BP to present. A short period of positive values occurred from 1,700 to 1,200 cal yr BP. Negative and near-zero scores dominated along Axis 2, and positive, stable values characterized the distribution of samples along Axis 3.

Although NMDS scores of fossil samples were variable (Fig. 4.5), they were more constrained than scores of modern samples from the region (HL and ME). PDFs of Axis 1 scores for fossil samples showed they had more affinity with modern ME and HL locations than with CM. This pattern was seen in the distribution of fossil samples in the biplot produced by Axis 1 and 2. In terms of NMDS Axes 2 and 3, fossil samples showed less variability than any group of modern samples, with scores centered on the origin of the axes.

**Table 4.2.** Multiple regressions to explain the NMDS scores as a function of independent variables. In all cases,  $NMDS = X\beta$ , where X corresponds to the explanatory variables selected (Biogeographical provenance from Central Mexico (CM), Highlands (HL), and Middle Elevations (ME) of Central America and Chiapas, Latitude, Longitude, Human Influence Index (HII), Annual Precipitation (APP), Mean Diurnal Range (MDR), Altitude, and Isothermality (IST)), and  $\beta$  are the estimated coefficients associated with each model.

| Explanatory variable | Response variable |          |         |          |         |          |
|----------------------|-------------------|----------|---------|----------|---------|----------|
|                      | NMDS 1            |          | NMDS 2  |          | NMDS 3  |          |
|                      | $\beta$           | p-value  | $\beta$ | p-value  | $\beta$ | p-value  |
| Intercept (Zone A)   | 2.84              | —        | -3.28   | < 0.0001 | -1.73   | < 0.01   |
| Zone B               | —                 | —        | 0.8497  | < 0.0001 | 0.5099  | < 0.001  |
| Zone C               | —                 | —        | 1.3452  | < 0.0001 | 0.5555  | < 0.0001 |
| Latitude             | 0.2721            | < 0.0001 | 0.1532  | < 0.0001 | 0.1376  | < 0.0001 |
| Longitude            | 0.0737            | < 0.01   | —       | —        | —       | —        |
| HII                  | 0.0246            | < 0.001  | —       | —        | -0.0091 | < 0.01   |
| APP                  | -0.0002           | < 0.01   | —       | —        | —       | —        |
| MDR                  | —                 | —        | —       | —        | -0.0582 | < 0.01   |
| Altitude             | —                 | —        | —       | —        | —       | —        |
| IST                  | —                 | —        | —       | —        | —       | —        |

Statistical significance of predictors in the multiple regressions of NMDS scores as a function of environmental attributes (Table 4.2) showed that Axis 1 responded positively to latitude, longitude, and HII, and negatively to APP. Axis 2 showed a positive relationship with latitude and biogeographic provenance. Axis 3 scores were positively related to latitude and biogeographic provenance, and negatively to HII and MDR.

In the LIQ13 record, the reconstructed human influence index (HII) values from 3,400 to 1,500 cal yr BP were high (generally > 25) (Fig. 4.7). From 1,500 to 500 cal yr BP, reconstructed HII values were between 15 and 20. The time period from 500 cal yr BP to present was characterized by high values at the beginning and a progressive drop towards present. The ESM12 core, in contrast, showed a relatively stable HII record, with intermediate-to-low values (25-15) during the last 2800 years.

## **4.5. Discussion**

### *4.5.1. Pollen assemblages and elemental geochemistry: the environmental signal of the sediments*

#### *4.5.1.1. Pollen assemblages and dimensional rescaling*

The high taxon richness found in the modern pollen spectra reflects the spatial scale of the sampling, which encompasses two biogeographic realms represented by at least four provinces (Campechean, Central American, Guerreran, and Madrean-Cordilleran, after Udvardy, 1975). Taxon richness reported in other studies, conducted at smaller geographic scales from the same region, has been consistently lower (65 taxa in Rodgers & Horn 1996; 96 taxa in Islebe & Hooghiemstra 1997; 110 taxa in Domínguez-Vásquez et al. 2004; 90 taxa in Bhattacharya et al. 2011). This high taxonomic richness offers a broader spectrum

for the potential expression of the environmental conditions and ecological processes associated with vegetation. The most noticeable signal of ecological turnover in the modern pollen spectra was manifested in the latitudinal/altitudinal gradient that structures the Nearctic-Neotropical vegetation transition (Rzedowski, 2006). Thus, there is a progressive change from dominance of *Alnus*, *Pinus*, and *Quercus* in samples from Central Mexico, to *Alchornea*, *Bursera*, *Celtis*, *Liquidambar*, Melastomataceae, Moraceae, and *Psychotria* from samples collected in Chiapas and Central America (Fig. 4.4). This turnover pattern has been documented in many vegetation studies (Nixon 2006; Rzedowski 2006; Graham 2010), implying a  $\gamma$ -diversity imprint on the regional pollen spectra.

Coarse vegetation types were also identified by the pollen spectra. Sites from CM were characterized by *Pinus*, *Quercus*, and *Alnus*, vegetation elements typically representative of mixed *Pinus-Quercus* forest (Correa-Metrio et al. 2012b). In contrast, ME locations were characterized by taxa typical of tropical montane forest (e.g. Bignoniaceae, Melastomataceae, Moraceae, *Myrica*, and *Trema*). Samples from HL of Chiapas were characterized by *Alchornea*, *Ilex*, *Liquidambar*, *Myrica*, *Psychotria*, and *Quercus*, vegetation elements reportedly belonging to MCF (Rzedowski 2006; Correa-Metrio et al. 2011). Nevertheless, pollen spectra from this region also showed high abundances of *Pinus*, reflecting the Nearctic influence on the composition of regional vegetation (Rzedowski 2006). Thus,  $\beta$ -diversity of parental vegetation is also reflected in our modern pollen dataset. Disturbance patterns in pollen assemblages are probably expressed through high abundances of *Ambrosia*, Amaranthaceae, and Asteraceae, taxa that increase in places with low forest cover and high human influence (Franco-Gaviria et al. 2018a).

NMDS ordination (Fig. 4.5 and Apéndice 4.6) offered additional evidence of pollen spectra reliably representing modern vegetation, and therefore environmental conditions. According to the ordination of taxa projected on the ordination of samples (Apéndice 4.6), NMDS Axis 1 was associated with forest cover, with arboreal (non-arboreal) elements ordinated towards the negative (positive) end of the axis. Given their Nearctic nature (Udvardy 1975), samples from HL and CM shared a substantial amount of taxa that were also dominant in their pollen spectra. They, however, had contrasting scores along NMDS Axis 1 (Fig. 4.5), suggesting an important effect of pollen relative abundances on the ordination. Whereas non-arboreal elements were more common in CM, samples from HL had a higher abundance of arboreal elements (Fig. 4.5 and Apéndice 4.6). This pattern emerges from the fact that although they have similar floras, these two regions show important differences in both precipitation (~2500 and 800 mm/year for HL and CM, respectively) and HII (~21 and 25 HII values for HL and CM, respectively) that result in simpler vegetation cover in CM. Samples from ME had mostly positive Axis 1 scores, with little dispersion, suggesting a mixture of locations dominated by arboreal elements with highly disturbed locations. Overall, as reported in other studies (Bush et al. 2001; Correa-Metrio et al. 2011; Caballero-Rodríguez et al. 2017), the first axis of the ordination represents a dense-forest to open-vegetation gradient.

Taxa ordination along NMDS Axis 2 showed a separation of Nearctic (negative end) and Neotropical elements (positive end), suggesting an association with vegetation biogeography. Accordingly, samples from CM and HL yielded Axis 2 scores that varied from the negative side to around the origin of the axis (Fig. 4.5). Indeed, the PDFs of Axis 2 showed a gradual turnover of pollen spectra from CM towards the negative side of the axis, to HL around the center, to ME mostly to the positive side. This turnover pattern is

commonly associated with regional ( $\beta$ - to  $\gamma$ -) diversity, represented by modern pollen samples (Bush et al. 2001; Correa-Metrio et al. 2011). In terms of NMDS Axis 3, both taxa and samples were rather tightly clustered and therefore its ecological meaning will not be discussed. Nevertheless, the inclusion of this axis substantially diminished the stress of the ordination, from 0.18 to 0.11, demonstrating its usefulness for producing a relatively relaxed ordination where pollen spectra can express and associate more freely.

Latitude of samples showed a positive significant relationship with all NMDS axes (Table 4.2), reinforcing the idea that pollen spectra reflect the floristic gradients associated with the regional biogeography and climate gradients. NMDS Axis 1 was also significantly related to longitude, proving that, as reported for other regions (Bush et al. 2001; Weng et al. 2004; Felde et al. 2014; Zheng et al. 2014), pollen assemblages provide evidence of spatial expression of environmental variables. As suggested by our *a priori* interpretation of Axis 1, it was related to HII and APP, variables intimately linked to vegetation structure and vigor. Indeed, given that these two variables reflect similarly in pollen spectra, they have been reported as potential sources of bias in paleoclimate reconstructions (Li et al. 2014; Caballero-Rodríguez et al. 2017). According to the relationships between Axis 2 and environmental variables, the ordination along this axis was driven by geographic position and provenance of samples.

#### 4.5.1.2. Geochemistry

Fe, Rb, Ti, and Zr all belong to the terrigenous fraction of the sediments and were positively correlated with one another (Apéndice 4.6). These elements are sourced from allogenic minerals and vary directly with the coarse-grained fraction of the sediments, and

therefore indicate rainfall and basin runoff (Haug et al. 2001). High correlations between mobile (e.g. Fe and Rb) and insoluble (e.g. Ti and Zr) elements ( $r > 0.7$ ,  $p = 0.001$ ) in our sediment records suggest low diagenetic effects from sediment-water interactions (Haug et al. 2001; Kylander et al. 2011). Thus, it is reasonable to assume that the elemental compositions of our sediment records were inherited mainly from the regional regolith, and Fe/Zr ratios would be informative regarding potential changes in provenance of the sediments (Konfirst et al. 2011). These ratios were high and stable in both cores (Fig. 4.6), indicating relatively constant sediment sources and small changes in the diagenetic processes at the bottom of the lakes.

Authigenic (Ca and Sr) and terrigenous elements were negatively correlated in both sediment cores (Apéndice 4.1), suggesting a climatic signal from both groups. Ca, which typically reflects carbonates ( $\text{CaCO}_3$ ) in the sediments (Eugster & Hardie 1978), was the most abundant element in both cores (LIQ13 average 9.4 %, and ESM12 average 6.5%). Carbonates, however, could be of authigenic or terrigenous origin, a distinction that has major implications for interpretation of the record. Whereas authigenic carbonates are typically associated with water level fluctuations, ostracod and gastropod shells, or bio-induced precipitation caused by photosynthetic  $\text{CO}_2$  uptake, detrital carbonates indicate erosive processes in the basin. Calcifying organisms fix Sr along with Ca, implying that the ratio between these two elements could be used as a marker of carbonate origin (Zaragosi et al. 2006). Although displaying high-frequency variability, the Ca/Sr ratio along core LIQ13 (Fig. 4.6) did not show a systematic trend, suggesting that Ca in this lake is mainly derived from biogenic  $\text{CaCO}_3$ , associated with low lake levels (Hodell et al. 2008). Core ESM12 showed a systematic trend in the Ca/Sr ratio, suggesting that Ca sources varied through time. Lake Esmeralda is a small lake surrounded by relatively steep hillsides that might

have contributed with carbonates during specific time intervals. Therefore, we consider that the geochemical signal associated with carbonates in the core ESM12 is likely local and less consistent than the regional signal of LIQ13. The evidence points to local processes having a non-stationary effect on the composition of the sediments of core ESM12. Because of this finding and the patchiness of the elemental record of core ESM12 caused by below detection limit concentrations, we based our climatic interpretation on the geochemical record of core LIQ13. Furthermore, Ti/Sr and Ti records from core LIQ13 showed the same trend over time (Fig. 4.6), reinforcing the conservative behavior of Ti with respect to dissolution processes (Kylander et al. 2011).

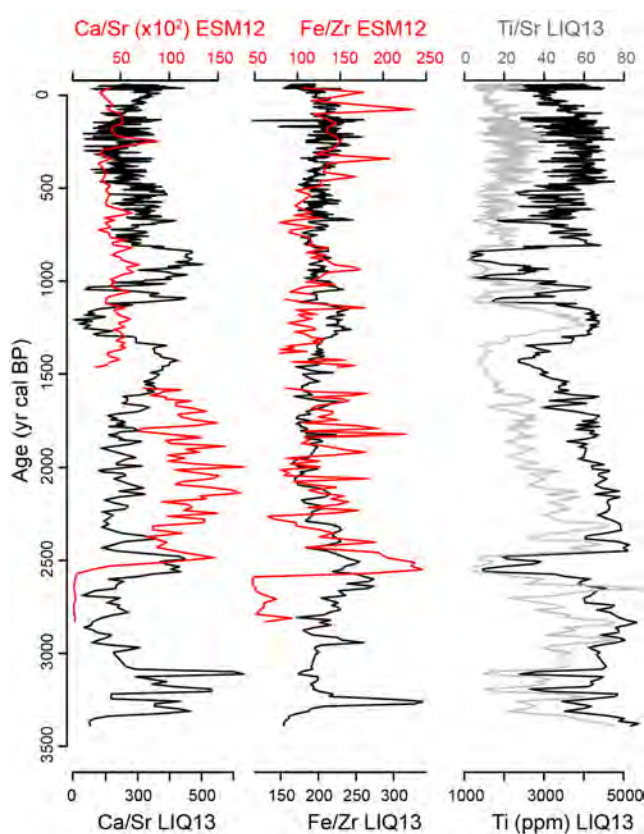


**Figure 4.6.** Geochemical measures in the sediment sequences from Lakes San Lorenzo (core LIQ13) and Esmeralda (core ESM12). **A.** Ca/Sr ratio for both cores. **B.** Fe/Zr ratio for both cores. **C.** Ti/Sr ratio and Ti concentration along core LIQ13.

#### 4.5.2. Late Holocene environmental changes in the highlands of Chiapas

The pollen records indicate shifting relative proportions of forest and open vegetation through time. These inferred vegetation changes provide insights into the interplay between climatic and anthropogenic factors through time. High dynamism is a feature of most biological associations, and transitions between environmental states are rarely discrete (Delcourt & Delcourt 1991). However, we divided the environmental history of the Chiapas highlands into four stages to facilitate the description and understanding of environmental conditions reflected in our sediment records.

##### **Stage 1, 3,400 – 2,500 cal yr BP (Early-Middle Preclassic)**

High abundances of Cyperaceae pollen at the bottom of the cores (Fig. 4.3) could indicate young and shallow lakes (Bush 2002b). The bottom of core LIQ13 had high abundances of *Concentrycistis* sp., an alga typically associated with fluvial environments (Christopher, 1976). Given the location of Lake San Lorenzo, it was likely part of the river, which became a depositional environment ca. 3,400 cal yr BP. Cores from both lakes show low pollen concentrations and dominance of *Pinus* in their bottoms. Given the structure of *Pinus* pollen grains, it is particularly resistant to oxidation, resulting overrepresented when sediments are deposited under low lake stands (Hall 1981). Additionally, given its anemophilous pollination syndrome, *Pinus* is well known for its regional overrepresentation in pollen assemblages produced by high pollen production and long-distance dispersal (Islebe and Hooghiemstra, 1995; Correa-Metrio et al. 2011, 2013).

Until ca. 2,400 cal yr BP, both pollen records were dominated by taxa characteristic of *Pinus-Quercus* forest and open vegetation. These elements were both represented in the

pollen spectra, which suggested vegetation composed of herbs and shrubs, and sparse arboreal elements. This pattern is consistent with the dominance of open vegetation reported for other areas across Mesoamerica, which has been attributed mostly to human disturbance (Curtis & Hodell 1996; Leyden 2002; Dull 2004a). Our estimation of HII indicates intermediate disturbance levels through this time period, in agreement with earlier interpretations. Our charcoal and Ti records indicate recurrent regional droughts, which probably also played an important role in maintaining disturbance-associated vegetation. High charcoal concentrations dominated by small particles suggest recurring regional fires (Fig. 4.7), which could have helped maintain the dominance of pyrophyllous *Pinus* and *Quercus* species (González-Espinosa et al. 1991; Dull 2004a). Low Ti concentrations suggest recurrent droughts that were synchronous with high-frequency Ti variability in the marine record from the Cariaco Basin (Haug et al. 2001, Fig. 4.7). Dry and variable conditions were reported for the Northern Hemisphere between 4,000 and 2,400 cal yr BP (Haug et al. 2001), a pattern that resulted from the southward shift of the ITCZ and intensification of the El Niño activity (Moy et al. 2002).

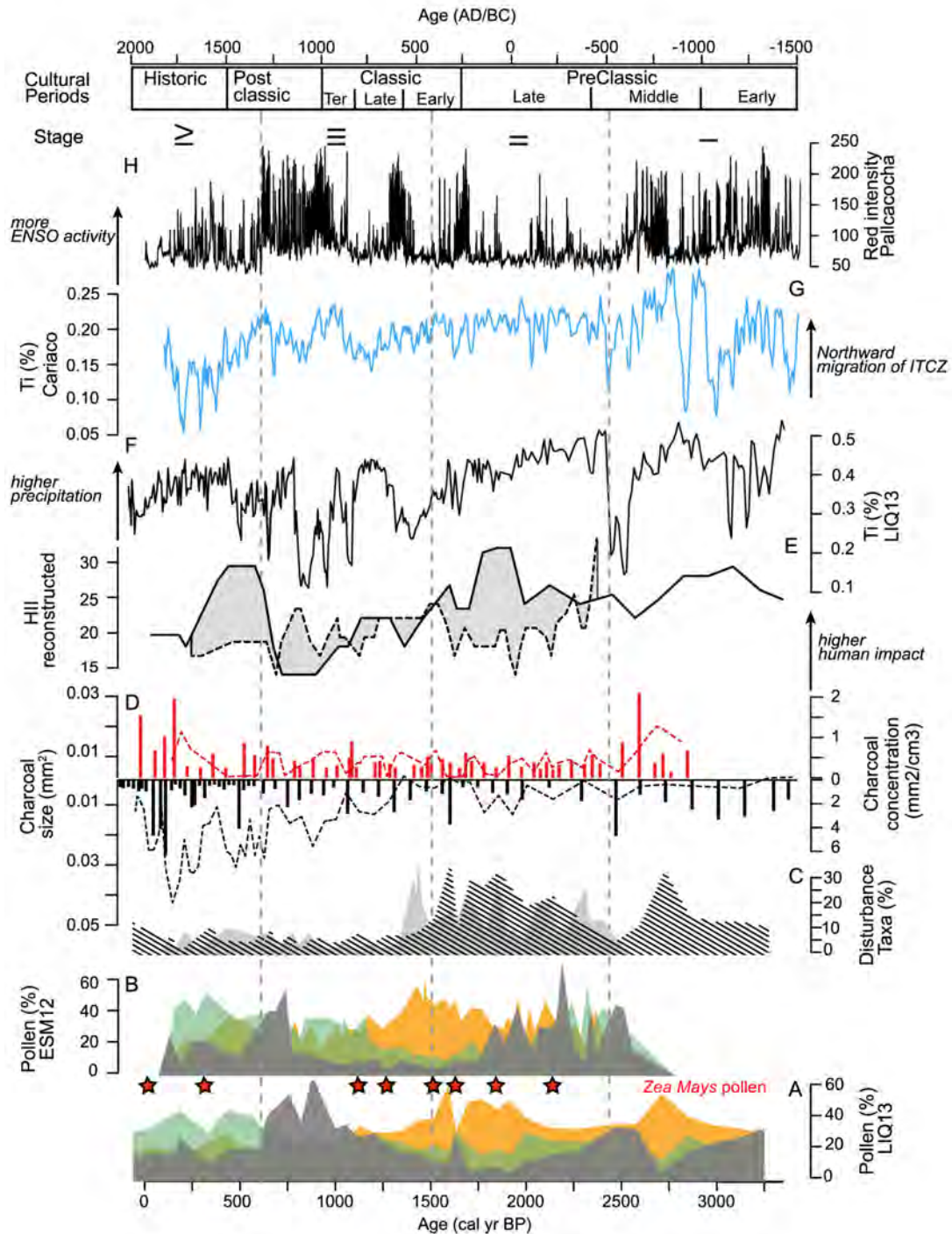


**Figure 4.7.** Environmental history of Lagunas de Montebello National Park. The Maya chronostratigraphy is shown in the top of the figure (after Sharer & Traxler 2006). Percentages of *Pinus* ( $\times 10^{-2}$ ) (gray area), taxa associated with montane cloud forest (green area), and open vegetation (orange area) for cores LIQ13 (A) and ESM12 (B); presence of *Zea mays* pollen is indicated with red stars. C. Percentages of disturbance taxa for ESM 12 (gray area) and LIQ13 (dashed area). D. Total charcoal concentration along ESM12 (red

bars) and LIQ13 (black bars), and median of charcoal size for the same cores (dashed red and black lines for cores ESM12 and LIQ13, respectively). **E.** Human influence index (HII) reconstructed for ESM12 (dashed line) and LIQ13 (black line). **F.** Titanium concentration, in dry weight %, along core LIQ13. **G.** Titanium weight % in marine sediments of the Cariaco Basin, off northern Venezuela (Haug et al. 2001). **H.** Red color intensity in the sediments of Lake Pallcacocha, Ecuador (Moy et al. 2002).

## **Stage 2, 2,400 – 1,500 cal yr BP (Late Preclassic – Early Classic)**

This period was characterized by a substantial increase in disturbance taxa (e.g. *Ambrosia*, Asteraceae, and Amaranthaceae) at the expenses of arboreal elements (Fig. 4.7). Repeated occurrences of *Z. mays* pollen since ca. 2,200 cal yr BP in the LIQ13 record suggest a period dominated by agricultural activities on the alluvial plains. This finding was expected, as *Z. mays* pollen has been reported in the Maya region between 7,000 and 4,500 cal yr BP (Goman & Byrne 1998; Pope et al. 2001; Dull 2004b; Wahl et al. 2006). This period in core LIQ13 is also characterized by the highest reconstructed values of HII (Fig. 4.7), suggesting strong human impact associated with the increase of agricultural activities. Nevertheless, the absence of *Z. mays* and low reconstructed HII values for core ESM12 are testimony to the high spatial heterogeneity of human occupation and disturbance patterns. This heterogeneity was likely associated with local peculiarities of the landscape. Whereas Lake San Lorenzo is surrounded by slopes of  $\sim 2^\circ$  that probably favored agriculture, Lake Esmeralda is located in the mountains and is surrounded by slopes of  $\sim 50^\circ$ .

Although the pollen data suggest deforestation associated with agricultural activities, there was little evidence of fires during this period (Fig. 4.7). Fire suppression could be the result of lower fire likelihood because of substantial biomass reduction, and/or a change in the way people managed natural resources. Anthropogenic land clearance may have reduced biomass and therefore fuel (firewood) for burning (Anderson & Wahl 2016).

Indeed, through this time period, *Pinus* representation in the pollen spectra was reduced substantially compared with other arboreal elements, coinciding with the construction and development of the Chinkultic acropolis near Lake San Lorenzo (Bryant & Clark 1983; Ferguson & Adams 2001; Palka 2014). Archeological evidence suggests that Maya communities selectively used pines for construction and fuel, with vast quantities needed to burn limestone and produce stucco (McNeil et al. 2010; Hansen et al. 2011). On the other hand, as societies evolved more sophisticated agro-engineering strategies, they tend to suppress fire as a vegetation management tool (Ellis et al. 2013; Bush et al. 2016).

The highest input of terrigenous elements in the record was found during this period (Fig. 4.7), coinciding with both an increase in the regional moisture (Curtis et al. 1996, 1998; Goman and Byrne, 1998; Vazquez-Molina et al. 2016) and probably, more intense regional erosion caused by vegetation clearance. Evidence of deforestation, agricultural activities, and monumental constructions through this time period was reported for other areas of the Maya region (Curtis & Hodell 1996; Islebe et al. 1996; Goman & Byrne 1998; Lozano-Garcia et al. 2007; Lentz & Hockaday 2009). Our results thus indicate regional expansion of agricultural practices and intensive landscape manipulation in Mesoamerica from ca. 2,400 to 1,500 cal yr BP. Although the late Holocene in the Northern Hemisphere Neotropics has been characterized by a gradual diminution of moisture availability (Haug et al., 2001), this period was characterized by relatively mild conditions, probably associated with the reported decrease in El Niño frequency (Fig. 4.7, Moy et al., 2002). The lack of recurring El Niño events, which manifests in the region as severe droughts (Magaña et al. 2003; Douglas et al. 2015), probably favored the establishment of regular seasonality, which in turn favored the agricultural activities.

**Stage 3, 1,500 – 600 cal yr BP (Early Classic - Postclassic)**

The beginning of this period was characterized by a substantial diminution of disturbance taxa and total absence of *Z. mays* in both records (Fig. 4.3 and Fig. 4.7), suggesting an agricultural abandonment of the region. This timing coincided with the “Maya Hiatus”, defined as a break between the Early and Late Classic periods that was characterized by a decline of Maya population (Webster et al. 2007). Similar documented vegetation shifts have been identified in palynological records from the highlands of Mesoamerica (Dull 2004a; Velez et al. 2011). The decrease in disturbance taxa and decline of human activities in our study area is also supported by the lower reconstructed HII value, particularly in the record from Lake San Lorenzo (Fig. 4.7). The reduction of disturbance taxa was accompanied by establishment of forest dominated by *Quercus*, *Alchornea*, and *Pinus* (Fig. 4.3). These two latter genera are usually present in the early stages of forest ecological succession because they possess many species that are heliophilous trees that grow in forest gaps (González-Espinosa et al. 1991; Marchant et al. 2002). Thus, their dominance of the pollen spectra between 1,500 and 1,200 cal yr BP probably represents the initial stages of the post-disturbance ecological succession, which led subsequently to the establishment of the regional MCF at ca. 1,200 cal yr BP.

Establishment of the modern forests in the region was clearly expressed by a substantial and relatively abrupt increase in MCF elements ca. 1,200 cal yr BP (mostly *Liquidambar*, *Hedyosmum*, *Celtis*, Melastomataceae, and *Ulmus*). The absence of *Z. mays*, low representation of disturbance taxa (< 10%), and the lowest reconstructed HII value suggest that between ca. 1,200 and 600 cal yr BP (Fig. 4.7), the region was little affected by anthropogenic activities. The abandonment of the nearby Las Margaritas archeological site (~30 km from Montebello National Park [Álvarez, 1993]) at ca. 1,000 cal yr BP, offers

additional support to our interpretation of a low human pressure on the regional forest resources. Synchronous abandonment of Montebello and Las Margaritas coincides with the first in a series of severe regional droughts in the lowlands, which have been proposed as playing a role in the Terminal Classic cultural collapse of the Maya (Hodell et al. 2005; Medina-Elizalde et al. 2010; Douglas et al. 2015). Additionally, the Ti record from Lake San Lorenzo indicates a series of severe droughts throughout this time period, between 1100 and 750 cal yr BP (Fig. 4.7). Negative excursions of Ti could also be attributable to lower erosion caused by dense forest cover. However, an increase in the size of charcoal particles in the record of Lake San Lorenzo indicates a higher frequency of local fires, probably reflecting increased climatic variability derived from a re-invigorated El Niño (Moy et al. 2002).

**Stage 4**, 600 cal yr BP – present (Late Postclassic to modern times)

The last 600 years have been characterized by gradual declines of *Pinus* and *Alchornea* in both records, whereas elements indicative of MCF have expanded (Fig. 4.3). The inception of this period was characterized by declines in *Pinus* and *Alchornea*, which are ecologically opportunistic, but under milder environmental conditions are outcompeted by other taxa (González-Espinosa et al. 1991; Ramirez-Marcial et al. 2001). Declines in these taxa probably resulted from a reduction in environmental and anthropogenic pressure on vegetation, which enabled increases in *Celtis*, *Liquidambar*, Melastomataceae, and *Ulmus*. During the last 600 years, these MCF elements have been accompanied by relatively high percentages of *Pinus* and *Quercus* (Fig. 4.3). Their proximity in the NMDS to modern pollen spectra from the highlands (Fig. 4.5) indicates that modern climate and environmental conditions have prevailed in the region during the last 600 years. Today,

primary fragments of MCF persist in the area, intermingled with secondary *Pinus-Quercus* forest, pinelands and scrublands (Ramirez-Marcial et al. 2001). Cloud forests from west-central Mexico were reported as having expanded within the same time interval (Figueroa-Rangel et al. 2010), pointing to a broad pattern of wetter conditions and low human influence on the vegetation. Presence of *Z. mays*, high values of reconstructed HII, and an increase of local charcoal in the San Lorenzo record indicate that, human activity was probably spatially localized during this period. After the Maya cultural collapse, most of the remaining population persisted in isolated satellite villages around the region (Bryant and Clark, 1983; Navarrete, 2006), and probably the fluvial plain of Lake San Lorenzo offered fertile soils and access to water, constituting an ideal setting for human settlements.

Flourishing of MCF during the last 600 years was probably a consequence of higher moisture availability, as suggested by the Ti records (Fig. 4.7). The increase in moisture availability was also documented in other middle- and high-elevation records from Central Mexico and Central America (Goman and Byrne, 1998; Dull, 2004; Lozano-Garcia et al. 2007; Vázquez-Molina et al. 2016), indicating a regional process was operating. In contrast, paleoclimate records from the lowlands of the Yucatan Peninsula indicate dry conditions, associated with southward displacement of the ITCZ (Haug et al. 2001; Hodell et al. 2005). Given the elevation and geographic position of our study area, higher moisture availability was probably the result of lower evaporation (Correa-Metrio et al. 2016) and higher orographic precipitation (Vazquez-Molina et al. 2016).

## 4.6. Conclusions

Analysis of two sediment sequences from the highlands of Chiapas enabled us to distinguish between the relative contributions of climate and human activities in the development of regional vegetation. Our records showed systematic dominance of Nearctic elements during times of environmental stress (e.g. *Alnus*, *Pinus*, and *Quercus*, after Gentry 1982). In contrast, under low human and/or natural pressures, the vegetation was dominated by Neotropical taxa (e.g. *Hedyosmum*, Melastomataceae, and Moraceae, after Gentry 1982). This pattern was probably a result of Nearctic elements responding opportunistically to disturbances, whereas Neotropical elements were probably associated more with ecological succession, mediated by the expression of their environmental niches in the regional climates. Clustering of all fossil and modern samples from the region in the NMDS (Fig. 4.5D) demonstrates that vegetation in the Maya highlands remained within the envelope defined by the modern regional vegetation mosaic during the last 3,400 years. This finding implies that vegetation diversity patterns expressed in the Montebello area through time are also represented today as a consequence of the rich mosaic of environmental and ecological conditions in the region.

Ti concentrations in the sediment profiles suggest that erosion, and therefore rainfall, in the highlands was closely associated with hemispheric patterns of climate variability. The observed long-term trend towards lower precipitation from 3,400 to 600 cal yr BP coincides with the southward displacement of the ITCZ through the Holocene (Haug et al. 2001). Anthropogenic stress, superimposed on the climate-drying trend between 3,400 and 1,500 cal yr BP, drove vegetation cover in the Maya highlands, from forest to open vegetation. It is notable that during the period of maximum human occupation around Lake

San Lorenzo, Lake Esmeralda showed evidence of relatively low disturbance. Therefore, the area around Lake Esmeralda may have served as a refuge that allowed rapid plant recolonization after periods of environmental stress, including intense human activities. According to our paleoecological records, human abandonment of the area began about 1,500 cal yr BP. Nevertheless, early forest re-growth was characterized by dominance of *Pinus* and *Quercus*, probably as a result of recurrent droughts that took place in Montebello between 1,500 and 600 cal yr BP. These dry conditions together with severe recurrent droughts that have been reported for the area between 1,100 and 750 cal yr BP (Hodell et al. 2005; Medina-Elizalde et al. 2010) were likely a consequence of the invigorated El Niño that characterized this time period (Moy et al. 2002).

Amelioration of the climate stress throughout the last 600 years, which has been characterized by wetter conditions, enabled the establishment of dense forest cover dominated by MCF elements. The reconstructed vegetation dynamics of the Maya highlands during the late Holocene indicate that the MCF that today occupies the highlands of Chiapas dates back to the last 600 years. Although climate has played a critical role in determining the geographic distribution of MCF, without human abandonment its re-establishment in the highlands of tropical Mexico would have been unlikely. Different vegetation types that exist in the Maya region today were produced by natural and anthropogenic drivers, and modern regional vegetation is the product of ecological processes that acted upon a legacy of centuries of disturbances.

## **Acknowledgements**

This research was funded by Programa de Apoyo a Proyectos de Investigación e Innovación Tecnológica PAPIIT-UNAM [grant number IN107716], and National Geographic Society – Committee for Research and Exploration [grant number 9137-12]. Additional funding was provided by Programa de Investigación en Cambio Climático, PINCC-UNAM, and Consejo Nacional de Ciencia y Tecnología [grant number 256406]. We thank Gerardo Martínez for his assistance with laboratory analyses. We are grateful to Comisión Nacional de Áreas Naturales Protegidas for granting us access to the study area. Juan Carlos Beltán, Margarita Caballero, Dayenari Caballero-Rodríguez, Esmeralda Cruz Silva, Alejandra Díaz, Julián Hernández, and Yosahandy Vásquez are thanked for their assistance in the field.

## CAPÍTULO 5

### DINÁMICA DE LA VEGETACIÓN DEL HOLOCENO, VARIABILIDAD CLIMÁTICA E IMPACTO HUMANO EN LA SELVA LACANDONA, ELEVACIONES MEDIAS DE MÉXICO TROPICAL

### HOLOCENE VEGETATION DYNAMICS, CLIMATE VARIABILITY AND HUMAN IMPACT AT THE LACANDON FOREST, MIDDLE ELEVATIONS OF TROPICAL MEXICO

**J.F. Franco-Gaviria<sup>1\*</sup>, A. Correa-Metrio<sup>2</sup>**

1. Posgrado en Ciencias de la Tierra, Universidad Nacional Autónoma de México,

Coyoacán, Ciudad de México, México 04510.

2. Instituto de Geología, Universidad Nacional Autónoma de México, Coyoacán, Ciudad de

México, México 04510.

*Artículo en preparación*

## Resumen

Durante la última década, las reconstrucciones ambientales en las tierras bajas mayas han proliferado. Sin embargo, poco se conoce acerca de las dinámicas ambientales en las elevaciones medias, una región que probablemente jugó un papel clave ofreciendo refugio a las poblaciones naturales y humanas durante periodos de transiciones ambientales críticas. En este trabajo se presenta el análisis sedimentario de un núcleo de 9,500 años recuperado en el Lago Ocotitalito (920 m s.n.m.), al sureste de México. Se llevaron a cabo análisis geoquímicos y de polen en las secuencias sedimentarias para evaluar el clima regional y la dinámica de la vegetación. El registro paleoambiental revela una alta disponibilidad de humedad durante el Holoceno temprano, lo cual favoreció el establecimiento del bosque húmedo tropical en la región. Entre 8,200 y 6,000 AP, se presentó una transición abrupta hacia condiciones secas pero con un bajo impacto en los bosques, los cuales se caracterizaron por el reclutamiento de especies clave, conservando la estructura de la vegetación. De 6,000 a 4,000 AP, dominaron condiciones secas y altamente variables, las cuales se reflejaron en el incremento de incendios y pérdidas importantes de la cobertura forestal. Entre 4,000 y 1,600 AP, persistieron condiciones climáticas variables asociadas a un mayor impacto humano en la región. Estas condiciones favorecieron el incremento de vegetación abierta a expensas de pérdidas sustanciales de la cobertura forestal. Los últimos 1,600 años se caracterizaron por la recuperación del bosque, que inició con la ocupación temprana de especies oportunistas como *Pinus* que dieron lugar al establecimiento de la vegetación moderna ca. 800-700 AP. Dicha recuperación fue el resultado de una disminución del estrés antropogénico y climático. También, la evidencia sedimentaria mostró que las dinámicas ambientales y de la vegetación durante el Holoceno temprano y medio fueron probablemente el resultado de cambios en el clima regional. Posteriormente,

los disturbios antropogénicos que caracterizaron el Holoceno tardío actuaron como catalizadores de los efectos negativos de la inestabilidad climática sobre la vegetación. El registro paleoclimático sugiere que entre el Holoceno temprano y medio, el sistema climático de las elevaciones medias de Chiapas fue altamente variable y pudo estar asociado con cambios en la temperatura del Océano Atlántico, expresados a través de los desplazamientos latitudinales de la Zona de Convergencia Intertropical. En escalas de tiempo más cortas (Holoceno medio-tardío), es probable que el aumento en la frecuencia de la actividad de El Niño haya introducido una alta variabilidad climática regional.

**Palabras clave:** Selva Lacandona, Holoceno, disturbios, Maya, variabilidad climática, paleoecología

### **Abstract**

Environmental reconstructions of the Maya lowlands have proliferated during the last decade. Little is known, however, about environmental dynamics of mid elevation ranges, a region that probably played a critical role in providing refugia for natural and human populations during times of critical environmental transitions. Here we report the sedimentary analysis of a 9,500 year-old core retrieved from Lake Ocotulito (920 m asl), southeastern Mexico. Geochemistry and pollen analyses on the sedimentary record were used to evaluate regional climate and vegetation dynamics. The record reveals high moisture availability during early Holocene, which favored the development of dense tropical rainforest. An abrupt transition toward dry conditions occurred between 8,200 and 6,000 BP, forest structure remained whereas their composition changed substantially from tropical to montane forests. From 6,000 to 4,000 BP, dry and highly variable conditions took place, reflected on intense fires and significant losses of forest cover. A climate highly

variable and strong human impact from 4,000 to 1,600 BP, favored the increase of open habitats in the region. The last 1,600 years were characterized by forest recovery, beginning with the early occupation of *Pinus* and the subsequent establishment of modern vegetation dominated by montane elements at ca. 800-700 BP, at a time when environmental conditions were relatively mild. The sedimentary evidence showed that environmental and vegetation dynamics from early to mid-Holocene were likely the result of climate changes at different geographic scales. Additionally, anthropogenic disturbances during the late Holocene acted as a catalyst for the negative effects of climatic instability over vegetation. Moreover, the paleoclimatic reconstruction suggests that during the early to middle Holocene, the climate system in the middle elevations of Chiapas was highly variable and probably associated with Atlantic Ocean dynamics, expressed through the latitudinal displacements of the Intertropical Convergence Zone. At shorter time scales (middle-late Holocene), it is likely that increased frequency of El Niño activity introduced high regional climate variability.

**Keywords:** Lacandon forest, Holocene, natural and anthropogenic disturbances, Maya, climate variability, paleoecology

## 5.1. Introduction

The Lacandon forest, southeastern mountains of the State of Chiapas, Mexico, represents one of the largest areas of tropical forest in Mexico (Arriaga et al. 2000). It lies on the northeastern flank of the Sierra Madre de Chiapas mountain range, facing the lowlands of the Yucatan Peninsula. Its geographic location and physiography offer conditions that promote high biodiversity: a mixture of biogeographic realms over steep environmental

gradients. Tropical vegetation elements from Central America and the Yucatan Peninsula intermingle with components from the more temperate vegetation that dominates the highlands of Chiapas (Rzedowski 2006). These taxa interact along steep environmental gradients that facilitate species migration and fast response to climate change (Bush 2002). At larger spatial and temporal scales, vegetation and climate have been highly responsive to changes in global climate, and possibly, to pervasive human occupation from mid to late Holocene (Leyden 1995; Curtis et al. 1998; Domínguez-Vásquez & Islebe 2008; Hodell et al. 2008; Correa-Metrio et al. 2012b).

The late Quaternary environmental history in the lowlands nearby the Lacandon forest has been characterized by a high millennial-to-centennial-scale climate and vegetation variability. The deglaciation in the Guatemalan lowlands of Petén, some 150 km from the Lacandon forest, was characterized by severe droughts and sparse vegetation (Correa-Metrio et al. 2012a). At ca. 10,500 BP (calibrated years before present hereafter), forests dominated by thermophilous flora that do not seem analogue to modern vegetation appeared in the area (Leyden 1984; Hillesheim et al. 2005; Correa-Metrio et al. 2012a). These forests apparently dominated the region between the inception of the Holocene and ca. 8,000 BP (Islebe et al. 1996; Correa-Metrio et al. 2012a). At ca. 8,000 BP, a regional expansion of forests began and dominated the region until the appearance of disturbance elements between 6,000 and 5,000 BP (Curtis et al. 1998; Wahl et al. 2016b). Open and disturbed vegetation probably associated with anthropogenic activities prevailed in the area from the middle Holocene to ca. 1,000 BP, when the Maya cultural collapse took place (Hodell et al. 2001; Domínguez-Vásquez & Islebe 2008). Overall, vegetation in the Maya lowlands through the Holocene has been a highly dynamic system operated by multiple drivers. Nevertheless, there is still no certainty regarding the history of the middle

elevations, where orographic moisture may have ameliorated the deleterious effect of extreme climates on local and regional vegetation.

From the middle to the late Holocene, anthropogenic disturbances have exerted significant pressure on the regional ecosystems of the Maya lands especially during the Preclassic and Classic Maya cultural periods (Leyden 2002; Anselmetti et al. 2007; Franco-Gaviria et al. 2018b). This pressure has manifested mainly through deforestation and substantial increases in soil erosion. This pattern of forest deterioration reverted after the Maya cultural collapse around 1,000 BP, and indeed, the post-hispanic period has been characterized by a substantial recovery of the vegetation (Curtis et al. 1998; Domínguez-Vásquez & Islebe 2008; Wahl et al. 2016b; Franco-Gaviria et al. 2018b). However, little is known about the extent of people's role in shaping modern vegetation. Are modern forests the legacy of thousands of years of human occupation?. If so, modern forests would appear in the fossil record synchronously or after vegetation associated with pervasive occupation. Another idea proposed in mayan research is the hypothesis that an almost entire clearing of the landscape through the Maya time led to changes in hydrological cycle (Leyden 2002).

Hundreds of lakes lie on the northeastern karstic flank of the Central American cordillera, offering an exceptional opportunity to document vegetation and climate changes through time. We used pollen, charcoal, and geochemical evidence from a sedimentary record from the middle elevations of tropical Mexico to answer the following questions: i) did climatic and vegetation dynamics in middle elevations of tropical Mexico parallel those of the lowlands? ii) What was the extent of human alteration on vegetation during the mid Holocene?; and iii) are forests that occupy the Lacandon forest today of anthropogenic origin?

## 5.2. Materials and methods

### 5.2.1. Study area

Lake Ocotitalito is located in the northern limit of the Lacandon forest, eastern mountains of Chiapas, Mexico (16.95° N, 91.60° W, Fig. 5.1), at an elevation of 920 meters above sea level (m asl hereafter). The area consists of a karstic relief of Cretaceous origin that structures a series of valleys and streams at altitudes ranging from 100 to 1,800 m asl. Slopes and hills adjacent to alluvial plains have been shaped on lutite and sandstone of Tertiary origin (Vasquez & Ramos 1992; Tejada-Cruz et al. 2009). The dominant climate is warm sub-humid with annual mean temperature and annual precipitation of 22 °C and 1932 mm, respectively. The regional moisture availability is modulated by the seasonal migration of the Intertropical Convergence Zone (ITCZ) and seasonal size changes of the Atlantic Warm Pool (AWP) (Magaña et al. 1999; Wang et al. 2006). Thus, the northerly position of the ITCZ and the expansion of the AWP during the boreal summer bring heavy rains to the region between June and October, whereas the dry season takes place from January to May (Fig. 5.1). El Niño Southern Oscillation (ENSO) plays an important control upon interannual rainfall variability over southern Mexico (Magaña et al. 2003). In the neighboring region of Montebello, some ~90 km south from the Lacandon forest, El Niño years result in a longer and more intense dry season and a decrease of total precipitation during the wet season (Franco-Gaviria et al. 2018b). During La Niña years, the most evident change in the precipitation regime is a drier wet season, while temperatures decrease slightly. Nevertheless, the climate of zones characterized by strong convection such as the mountains of Chiapas could be insensitive to these hemispheric anomalies.

The conjunction of the regional climate with the heterogeneity of the landscape produces a mosaic of diverse vegetation types composed of a mixture of broadleaf and coniferous species. The principal modern natural vegetation types are Lower Montane Rain Forest (LMRF), Montane Rain Forest (MRF), and Pine-Oak Forest (POF) (Breedlove 1981). Regional vegetation has been influenced by a long history of anthropogenic activities that have promoted the expansion of open vegetation and regrowth at the expense of the natural vegetation (Hernández-Nava 2003). LMRF is the dominant vegetation type, spanning an elevational range from 300 to 800 m asl, dominated by broadleaf species with forest composition and physiognomy resembling short tropical rain forest. The tallest trees, mainly *Alchornea latifolia*, *Brosimum alicastrum*, *Calophyllum brasiliense*, *Pseudordia oxiphyllaria*, *Swietenia macrophylla*, and *Terminalia amazonia*, reach heights up to 30 m (Pennington & Sarukhán 2005; CONABIO 2013). MRF, also referred to as Montane Cloud Forest (Hamilton et al. 1995), is characterized by the coexistence of broadleaf and coniferous species occurring mostly on hillsides and mountain ridges at altitudes above 900 m asl with high moisture availability. Some typical species are *Clethra* spp., *Clusia* spp., *Hedyosmum mexicanum*, *Myrica cerifera*, *Podocarpus matudai*, *Ulmus Mexicana*, and various species of *Pinus* and *Quercus* (Hernández-Nava 2003; CONABIO 2013). MRF also includes deciduous and semi-deciduous trees such as *Liquidambar styraciflua* L., *Nissa sylvatica*, *Sapium* sp., and *Styrax* spp. (CONABIO 2013). POF occupies areas above 1,000 m asl, mainly on the ridges of the mountains and in areas with low soil moisture availability. This vegetation type is dominated by few species of pines (e.g. *Pinus maximinoí* and *P. oocarpa*) ranging between 15 and 40 m in height, and a smaller representation of oaks (e.g. *Quercus benthamii* and *Q. crassifolia*). Other species include *Ardisia* sp., *Eugenia* sp., and *Ilex brandegeana*. Given the extensive anthropogenic intervention of the landscape,

secondary species such as *Acacia pennatula*, *Bursera simaruba*, *Ceiba pentandra*, and *Cecropia* spp., and various species of Asteraceae and Poaceae are commonly found (Hernández-Nava 2003; Pennington & Sarukhán 2005).

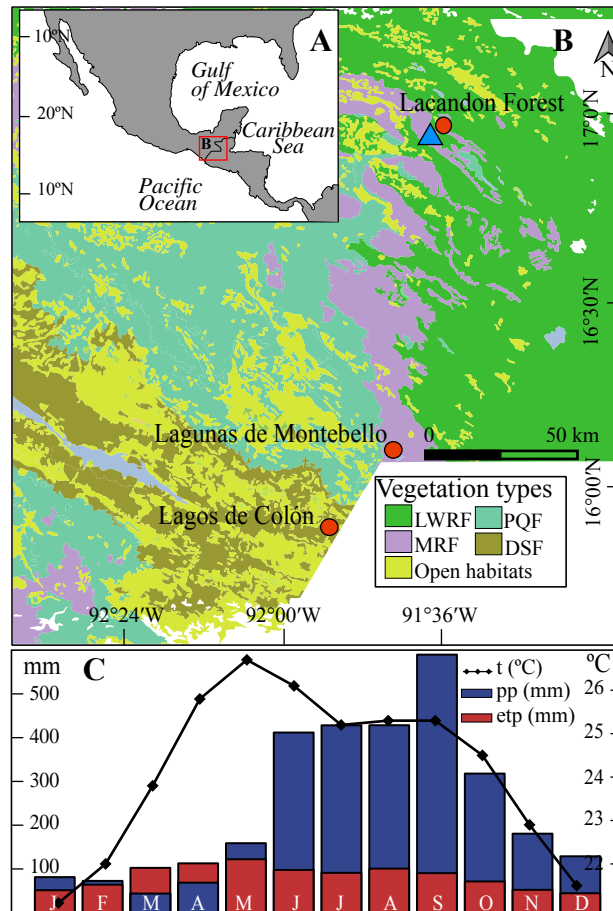


**Figure 5.1.** Study area. **A.** The localization of the Lacandon forest in southeastern Mexico. **B.** Lake Ocotolito (blue triangle), and modern samples (red circles), in the context of the vegetation types in the region. LMRF, Lower Montane Rain Forest; MRF, Montane Rain Forest; PQF, Pinus-Quercus Forest; DSF, Deciduous Seasonal Forest; and Open Vegetation (modified from CONABIO 2003). **C.** Monthly precipitation (pp, blue bars), potential evapotranspiration (etp, red bars), and monthly mean temperature (black line) of Lacandon forest (data from Lacantún meteorological station, Servicio Meteorológico Nacional, 2017).

### 5.2.2. Data collection and processing

Two sediment cores were retrieved from the deepest part of Lake Ocotitalito ( $z_{\max}$  23 m). A 540-cm-long core (OCO12-II) was retrieved using a Livingstone core and a 97-cm-long core (OCO16G-I) was recovered from the same location using a UWITEC gravity corer. Both cores were transported to the laboratory, longitudinally split, described, and stored at 4 °C. Chronologies were established using 13 AMS radiocarbon dates analyzed at Beta analytic, Inc. Miami (Table 5.1). Radiocarbon ages were calibrated through InCal13 (Reimer et al. 2013), and calibrated ages were used to build one independent Bayesian age-depth model for each core using Bacon (Blaauw & Christen 2011). All ages are expressed in calibrated years before present (BP hereafter).

**Table 5.1.** Radiocarbon dates and calibrated ages for the sedimentary record of Lake Ocotitalito.

| Laboratory sample code | Depth (cm) | Dated material   | <sup>14</sup> C age | Calibrated dates cal yr BP (2- $\sigma$ range) |
|------------------------|------------|------------------|---------------------|--|
| <b>OCO16G-I</b>        |            |                  |                     |  |
| 463259                 | 22         | Insect remains   | 270 $\pm$ 30        | 290-434  |
| 461848                 | 22         | Organic sediment | 760 $\pm$ 30        | 668-729  |
| 461849                 | 62         | Organic sediment | 1,590 $\pm$ 30      | 1,410-1,544                                    |
| 443765                 | 97         | Organic sediment | 2,090 $\pm$ 30      | 1,993-2,141                                    |
| <b>OCO12-II</b>        |            |                  |                     |  |
| 394177                 | 24         | Pollen extract   | 2,090 $\pm$ 30      | 1,993-2,141                                    |
| 405131                 | 24         | Micro-charcoal   | 2,130 $\pm$ 30      | 2,002-2,157                                    |
| 372422                 | 83         | Organic sediment | 3,230 $\pm$ 30      | 3,382-3,497                                    |
| 394178                 | 134        | Pollen extract   | 4,350 $\pm$ 30      | 4,851-4,974                                    |
| 394175                 | 195        | Micro-charcoal   | 3,380 $\pm$ 30      | 3,566-3,654                                    |
| 374153                 | 252        | Organic sediment | 6,380 $\pm$ 30      | 7,259-7,337                                    |
| 345042                 | 351        | Plant remains    | 7,260 $\pm$ 40      | 8,001-8,170                                    |
| 335994                 | 540        | Organic sediment | 8,490 $\pm$ 40      | 9,455-9,540                                    |

Pollen analysis was carried out on 146 one-cm<sup>3</sup>-sediment samples evenly distributed along time (123 and 23 samples from core OCO12-II and OCO16G-I, respectively). Samples for pollen analysis were prepared according to standard protocols (Faegri & Iversen 1989) and gravimetrically separated to concentrate pollen and spores (Krukowski 1988). Samples were analyzed at magnifications of 400X and 1000X, using a transmitted light microscope. Counts were made aiming a sum of 200 grains, excluding pollen grains of Cyperaceae, Moraceae, *Pinus*, and *Quercus*, which were counted but excluded from the pollen sum to avoid their dominance of the pollen spectra and increase the probability of finding rare taxa (after Correa-Metrio et al. 2011). All pollen data were expressed as the percentage of the pollen sum (Birks & Gordon 1985) and stratigraphically plotted. The diagram was divided into pollen zones that were defined based on visual inspection of major changes in assemblage composition and identification of relatively homogeneous pollen assemblages among time intervals. We assembled a modern pollen dataset composed of previously published pollen spectra from mud-water interface sediment samples collected in 24 lakes from the region (Correa-Metrio et al. 2011; Franco-Gaviria et al. 2018a). Sampled locations covered a range of mountain environments from 500 to 1,600 m asl, in the Lacandon forest (10 samples), Lagunas de Montebello National Park (9 samples), and Lagos de Colón (5 samples).

A 1-cm<sup>3</sup> sediment sample from each depth analyzed for pollen was processed for charcoal analysis. Microscopic charcoal particles were manually separated and photographed using a stereomicroscope (Clark 1988). Subsequently, the number of pixels covered by charcoal particles was counted using ImageJ (Rasband 2005), and charcoal was expressed as area (mm<sup>2</sup>), and standardized to volume to express it as concentration (mm<sup>2</sup>/cm<sup>3</sup>). Concentrations of Fe, Rb, Sr, Ti, and Zr were measured at 1-cm intervals

along the cores using a handheld X-Ray fluorescence (XRF) analyzer (Niton XL3t), totaling 637 samples. Concentrations of Fe, Rb, Sr, Ti, and Zr were expressed in parts per million (ppm) or percentages (%). Ti/Sr ratio was calculated to characterize detrital input to the lake, reducing possible dilution effects by carbonates, thus revealing otherwise undetectable patterns in single elemental profiles (Lowemark et al. 2011).

### *5.2.3. Numerical analysis*

Modern and fossil pollen samples were analyzed together using non-metric multidimensional scaling (NMDS). This technique projects multivariate data along latent axes preserving the underlying dissimilarity structure of the original dataset (McCune et al. 2002). Thus, samples with similar scores reflect similarities of both taxon composition and structure of the pollen assemblages. The NMDS for the data of Lake Ocotolito was based on the Bray-Curtis dissimilarity index and was constructed in three dimensions to bring stress below 0.1. Whereas sample scores were obtained directly from the ordination, taxon scores were calculated through weighted averaging of site scores. NMDS scores were used to infer vegetation development through time and the relationships between modern and fossil pollen samples. Distribution of modern samples along the two NMDS axes was differentiated by provenance (Lacandon forest, Lagunas de Montebello, and Lagos de Colón) and summarized through bivariate probability density functions (PDF) (Silverman 1986), generating envelopes (95% probability) to define the distribution of modern vegetation. Modern analogues were evaluated by the position of fossil pollen spectra in the context of the probabilistic spaces defined by modern samples. All numerical analyses were

performed using R (R Core Team 2017), especially packages *vegan* (Oksanen et al. 2017), *KernSmooth* (Wand 2015) and *MASS* (Venables & Ripley 2002).

### 5.3. Results

From 540 to 400 cm, core OCO12-II was composed of gray massive clays (Fig. 5.2B); from 400 to 100 cm, the core was characterized by light-brown sandy silt with presence of ostracod and gastropod shells; the upper 100 cm of core were characterized by brown organic silt. Core OCO16G-I was characterized by a massive structure of brown organic silt (Fig. 5.2A). According to the age-depth models, core OCO12-II spanned from ca. 9,500 to 1,900 BP, whereas core OCO16-G represented the last 2,100 years (Table 5.1 and Fig. 5.2). Core OCO12-II was characterized by sedimentation rates of  $\sim 0.12$  cm/yr from the bottom of the core to 250 cm, and  $\sim 0.05$  cm/yr, from 250 cm to the top of the record. Core OCO16G-I had a basal age of 2,100 BP and apparently a stable sedimentation rate of  $\sim 0.05$  cm/yr. Given the lithological and sedimentological homogeneity of the cores, it was not possible to construct a composite section based on stratigraphic correlations. Thus, the composite profile representing the sedimentary evidence from Lake Ocotlito was constructed based on the age models from the two analyzed cores, with the basal age of core OCO16G-I overlapping the uppermost date of core OCO12-II (Fig. 5.2C).

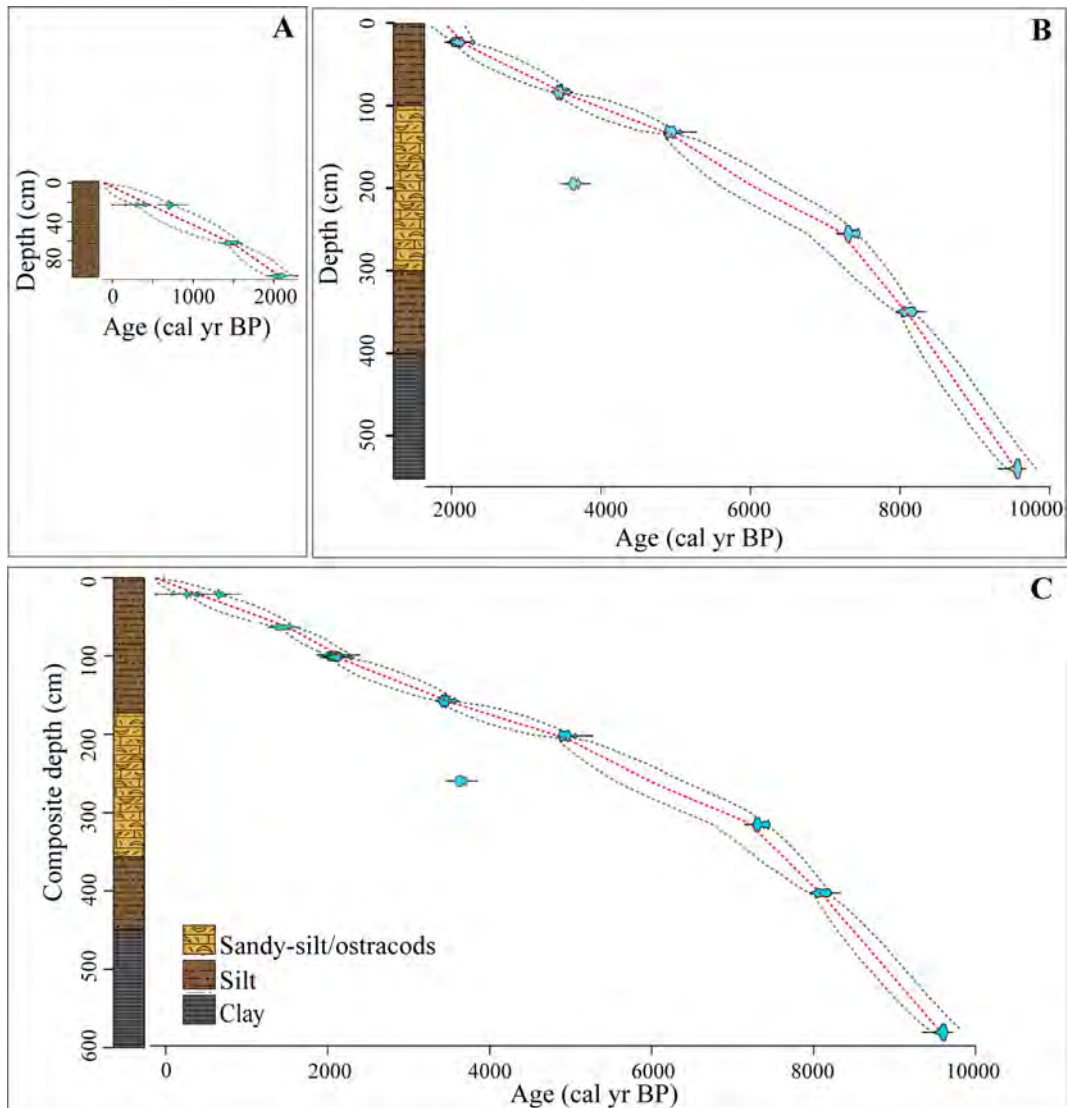


**Figure 5.2.** Lithology and Age-depth models for the sediment cores from Lake Ocotulito. **A.** Gravity core OCO16G-I and **B.** Long core OCO12-II. Calibrated radiocarbon dates in green and blue, the accepted models with their 95% confidence intervals in red and gray dashed lines, respectively. **C.** Composite section of Lake Ocotulito based on the age models **A** and **B**.

The pollen sum of at least 200 grains was reached in all samples, with pollen counts varying between 317 and 1500 grains per sample. The composite record was characterized by 128 palynological taxa, with three, 84, and 37 of them identified at species, genus, and family levels, respectively, whereas five remained unknown. Four pollen zones were

defined to facilitate the description of the pollen record (Fig. 5.3) and the main changes of the charcoal and elemental geochemistry records (Figs. 5.5 and Apéndice 5.2).

Zone I (From ca. 9,500 to 7,800 BP) the bottom of this zone (up to 9,000 BP) was characterized by high percentages of *Quercus* and *Alnus* and variable abundances of Amaranthaceae, Asteraceae, Cyperaceae, Moraceae, and *Pinus*. From 9,000 to 7,800 BP, Moraceae, Araliaceae, *Brosimum*, and *Protium* showed high percentages, with a short intermission (from 8,200 to 7,800 BP) dominated by *Quercus*, *Alnus*, *Acalypha*, and *Ilex*. Charcoal fragments were present in almost all samples in low concentrations (below 8 mm<sup>2</sup>/cm<sup>3</sup>). Elemental composition was characterized by the highest concentrations of Ti (above 2000 ppm), Rb (above 40 ppm), and Zr (above 140 ppm), in contrast to very low concentrations of Sr and Fe. Ti/Sr ratio showed the highest values along the core (above 140).

Zone II (from 7,800 to 6,000 BP) was characterized by high percentages of Bignoniaceae, Melastomatecea, *Myrica*, *Spondias*, and *Zanthoxylum*. Through this time interval, there were also progressive decreases of Moraceae and *Quercus*. Microcharcoal concentrations remained low. Ti, Rb, and Zr showed an abrupt decrease, whereas Sr increased substantially, reaching values above 60 ppm. Additionally, Peaks of Fe predated Sr increases and Ti/Sr showed a substantial decrease.

Zone III (from 6,000 to 4,000 BP) was dominated by Poaceae, Asteraceae, and *Ambrosia*, whereas arboreal taxa showed substantial decreases. *Pinus* and *Quercus* showed high percentages. *Zea mays* resulted represented at ca. 5,000 BP by a pollen grain. Charcoal concentrations in this zone increased substantially reaching values above 10 mm<sup>2</sup>/cm<sup>3</sup>. Elemental record showed a prevalence of high concentrations of Sr and low values of Ti, Rb, Zr, and Ti/Sr.

Zone IV (from 4,000 to 1,600 BP) was characterized by pollen spectra showing an abrupt decline of *Pinus* and *Quercus*, whereas *Ambrosia*, Asteraceae, and Poaceae remained abundantly represented. Through this zone *Z. mays* became more abundant and persistent. Under the dominance of herbaceous taxa, charcoal concentrations were high and variable, with several peaks above 12 mm<sup>2</sup>/cm<sup>3</sup>. This zone was characterized by a substantial decreasing in Sr, whereas Ti, Rb, and Zr increased slightly. Ti/Sr ratio showed high and variable values.

Zone V (from 1,600 to top of the composite record) was characterized by the maximum abundance of *Pinus* (500 %), whereas *Alchornea*, Melastomataceae, Moraceae, *Myrica*, and *Ulmus* increased gradually, dominating the pollen spectra of the last 600 years. Beginning this period, herbaceous taxa decreased substantially, with *Ambrosia* disappearing from the record. Poaceae and *Z. mays* pollen decreased abruptly at ca. 800 BP. Charcoal concentrations remained high and variable from the beginning of this time period to ca. 800 BP, when decreased substantially reaching values below 3 mm<sup>2</sup>/cm<sup>3</sup>. Elemental composition and Tr/Sr ratio showed a substantial decrease in this zone, despite a peak of Sr between 1,600 and 1,100 BP. Also, all elements increased to the top of the record.

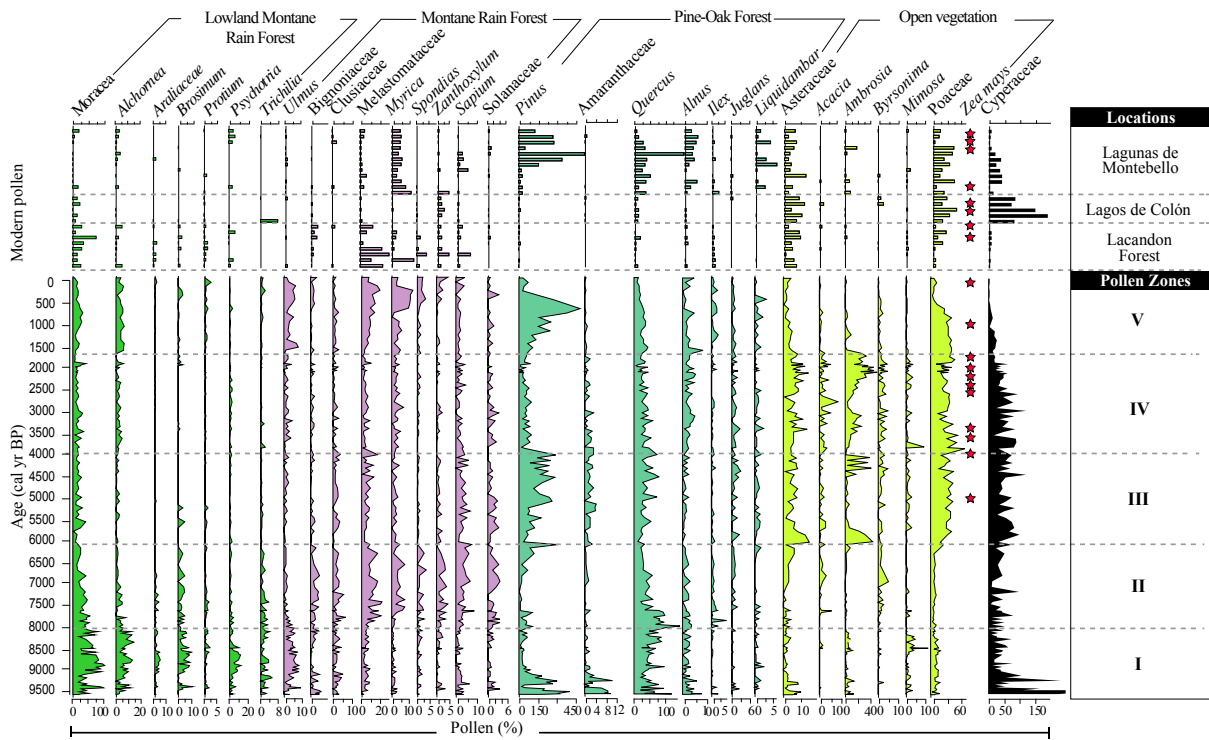


**Figure 5.3.** Simplified pollen diagram of regional modern pollen samples and fossil samples from the sediment sequence of Lake Ocotitalito. Red stars indicate presence of *Zea mays* pollen.

### 5.3.1. Modern pollen

The modern pollen dataset was composed of 123 taxa (Fig. 5.3). Samples from Lagunas de Montebello National Park were mainly dominated by taxa associated with temperate environments (e.g. *Liquidambar*, *Myrica*, *Pinus*, and *Quercus*) with some tropical elements (e.g. *Alchornea* and *Psychotria*). Pollen spectra from Lagos de Colón were dominated by taxa associated with deciduous and semi-deciduous forests (e.g. *Acacia*, *Bursera*, *Byrsonima*, *Spondias*, and *Zanthoxylum*), and herbaceous taxa, mainly Asteraceae and Poaceae. Samples from the Lacandon forest were dominated by *Brosimum*, Moraceae, Melastomataceae, *Trema*, and *Zanthoxylum*, often co-occurring with *Ilex*, *Myrica*, and *Quercus*. Overall, herbaceous taxa were found in all localities, although they are less

represented in samples from Lacandon forest as compared with those from Montebello and Lagos de Colón.

### 5.3.2. Ordination of pollen samples

The three-dimensional NMDS ordination of modern and fossil pollen assemblages produced a convergent solution with a stress of 0.097 after 34 iterations (Fig. 5.4). Fossil samples from pollen zones I, II, and III had negative scores on NMDS Axis 1, while zones IV and V showed transitioning scores from the negative to the positive ends of NMDS Axis 1. NMDS Axis 2 produced a clear separation of fossil pollen zones I and II in the positive extreme, while zones III, IV, and V were ordinated towards the origin and the negative side of the axis (Fig. 5.4A). The space occupied by modern samples by localities was summarized as the central 95% probability of the PDFs estimated per site (Appendix 6.1), resulting differentiated along the first two axes of NMDS and occupying a space similar to that of fossil samples (Fig. 5.4). The overlapping probability among the PDFs that characterized the three regions was 0.005, while the probability of intersection between pairs of envelopes were of 0.183 for Lagos de Colón and Landon Forest, 0.038 for Lagos de Colón and Montebello, and 0.004 for Montebello and Lacandon forest (Appendix 6.1). Fossil samples from zones I and II were mostly associated with modern samples from the Lacandon forest, especially with relatively well-preserved locations such as Nahá, Metzabok, and Chanzip. Samples from zones III and IV were mostly associated with more disturbed locations mostly from largos de Colón and Lagunas de Montebello (*e.g.* Kichayil, and Gemelas). Samples covering the last 1,600 BP were broadly distributed along NMDS

Axis 1, clustering with samples from Lagunas de Montebello from 1,600 to 800 BP and Lacandon forest for the last 800 years.

NMDS weighted-averaged scores for taxa produced an ordination where taxa were clearly separated along the two first NMDS axes (Fig. 5.4B). *Hymenaea* (-1.2), Araliaceae (-0.78), *Protium* (-0.76), *Brosimum* (-0.67), *Trema* (-0.63), and Moraceae (-0.41) resulted ordinated on the negative end of Axis 1 (scores in parenthesis). Clusiaceae (-0.07), *Myrica* (-0.06), *Alnus* (-0.008), and *Quercus* (0.03) were ordinated around the origin of Axis 1, whereas *Pinus* (0.74), *Liquidambar* (0.62), and Amaranthaceae (0.44) resulted on the positive side. Along NMDS Axis 2, *Z. mays* (-0.87), *Ambrosia* (-0.75), Poaceae (-0.47), and Asteraceae (-0.46). *Pinus* (-0.01), *Eugenia* (-0.01) were ordinated on the negative end, whereas *Sapium* (0.04), *Bursera* (0.06) and *Ilex* (0.09) obtained scores close to zero. Araliaceae (0.71), *Brosimum* (0.69), Lecythidaceae (0.52), and Moraceae (0.42) resulted on the positive end of this axis.

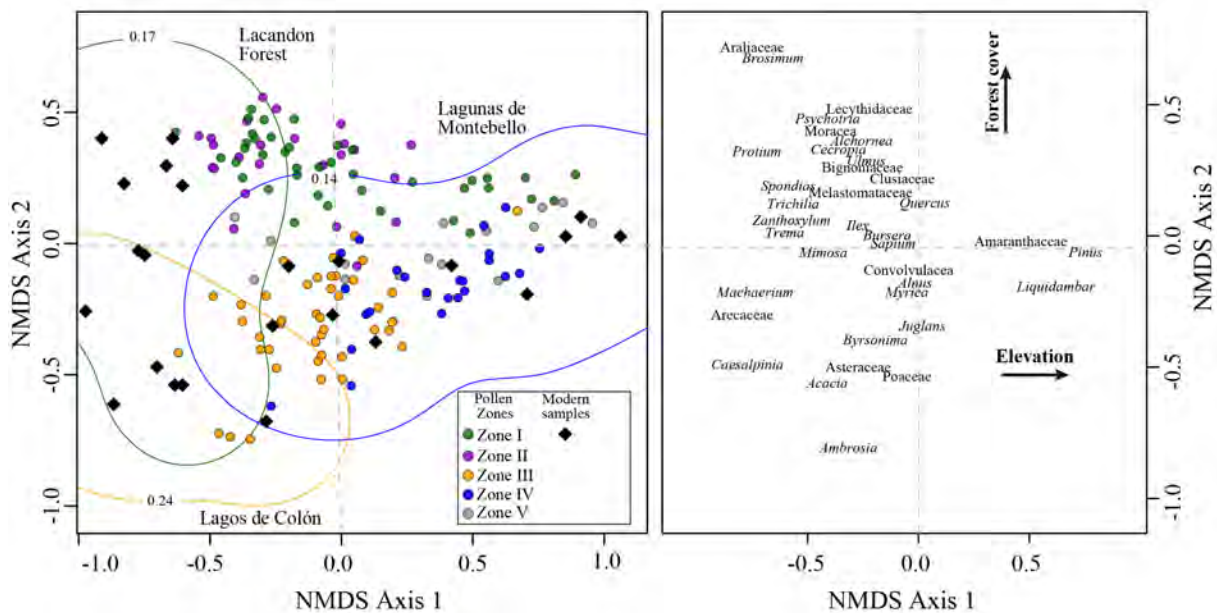


**Figure 5.4.** Non-metric multidimensional scaling (NMDS) ordination of fossil pollen samples from Lake Ocotitalo and modern samples from the region. **A.** Ordination of samples; color lines represent the modern samples distributions, which were estimated by bivariate probability density functions with a 95% confidence. Fossil samples are color coded into five pollen zones periods that represent major vegetation changes through the record. **B.** Species ordination based on weighted averages of sample scores.

## 5.4. Discussion

### 5.4.1. The sedimentary signal of Lake Ocotitalo

#### *The pollen signal in the sediments of Lake Ocotitalo*

Coarse vegetation types were identified by the composition and structure of modern pollen spectra, a fact reflected in the NMDS ordination (Figs. 5.3 and 5.4). Sites from Lagunas de Montebello were characterized by pollen spectra dominated by *Pinus*, *Quercus*, *Alnus*, and *Liquidambar*, typically representative of POF (Correa-Metrio et al. 2011; Franco-Gaviria et al. 2018a). In contrast, locations from the Lacandon forest were characterized by a combination of taxa typical of LMRF and MRF (Figuroa-Rangel et al. 2010; Correa-

Metrio et al. 2011). Asteraceae, Poaceae, and *Z. mays* pollen were also found in samples from the Lacandon forest associated with relatively open habitats that characterize areas outside of the protected reserve. Samples from Lagos de Colón contained mostly herbaceous elements and pollen from deciduous shrubs and trees, vegetation elements typical of disturbed areas and tropical deciduous forest (Correa-Metrio et al. 2011).

Samples ordination along NMDS Axis 1 showed a clear separation of samples from high elevations of the Lagunas de Montebello in the central and positive side and samples from middle elevations of the Lacandon forest and Lagos de Colón in the negative extreme (Fig. 5.4A). Accordingly, tropical taxa (e.g. Araliaceae, *Brosimum*, *Protium*, and *Caesalpinia*) and temperate taxa (e.g. *Alnus*, *Quercus*, *Pinus* and *Liquidambar*) were separated along NMDS Axis 1 (Fig. 5.4B), indicating that this axis is strongly related to the analyzed elevation gradient. Thus, this axis represents a temperature gradient from warm to cold conditions. Overall, as reported in other studies (Bush & Colinvaux 1990; Correa-Metrio et al. 2011; Franco-Gaviria et al. 2018a), the first axis of the ordination also represents a temperature gradient. The ordination along NMDS Axis 1 also shows a compositional difference between Lacandon forest and Lagunas de Montebello. A marked difference in habitats exists in the mountains of Chiapas at places where clouds form. At elevations above 1,400 m asl where the Lagunas de Montebello lies is likely condensed moisture that forms clouds remains on the surface as ground-level cloud. This directly influences the growth of MRF or montane cloud forest (Bruijnzeel et al. 2011). Consequently, pollen spectra from the Lagunas de Montello are dominated by MRF taxa (e.g. *Liquidambar*, Melastomataceae, *Myrica*, *Quercus*, and *Sapium*) (Figs. 5.3 and 5.4). Differently, much of the Lacandon forest lies in elevations below 1,000 m asl and largely dominated by lowlands tropical elements due in part to its proximity to the lowlands of

Yucatan Peninsula. Therefore, this altitudinal limit (around 1,400 m asl) of potential establishment of montane cloud forest sets a physiological limit that is reflected in the pollen spectra.

Samples and taxa ordination along NMDS Axis 2 suggest that this axis is associated with a forest cover gradient. Sites characterized by dense forests such as the Lacandon forest were arranged on the positive extreme, whereas sparse vegetation sites from Lagunas de Montebello and Lagos de Colón were ordinated around the origin and negative side. This pattern reflects on the ordination of taxa, with arboreal taxa associated with large canopies and low levels of disturbance (*e.g.* Araliaceae, *Brosimum*, Lecythidaceae, and Moraceae) ordinated on the negative side as opposed to non-arboreal taxa (*e.g.* Asteraceae, Poaceae, and *Ambrosia*) ordinated on the positive side of the axis (Marchant et al. 2002; Franco-Gaviria et al. 2018a). Commonly, open vegetation is highly influenced by disturbances, either anthropogenic and natural (Franco-Gaviria et al. 2018a).

The apparent distinction of modern pollen spectra from the defined regions was supported by their differentiation in the ordination (Fig. 5.4A). According to the modern PDFs, the probability of overlap of the modern envelope between the three regions was very low (0.005, Apéndice 5.1), reflecting the ability of pollen spectra to represent regional generalities of the vegetation. Nevertheless, higher overlap probabilities (Appendix 6.1) between pair-wise regional PDFs clearly reflects natural continuous vegetation turnover. Whereas vegetation turnover takes place gradually and some taxa are cosmopolitan within the studied area (*e.g.* *Pinus* and *Quercus*, (Rzedowski 2006)), the taxonomic resolution of pollen data further blurs the signal (Correa-Metrio et al. 2011). Additionally, human-induced vegetation simplifies ecosystems and introduced more difficulties to distinguish more specific vegetation associations (Franco-Gaviria et al. 2018a).

Overall, samples and taxa ordination along NMDS axes provide an approximation to climate and forest cover conditions along the time through NMDS Axes 1 and 2 of fossil samples (Fig. 5.5). Clustering of most fossil and modern samples from the region in the NMDS (Fig. 5.4) indicates that through the Holocene vegetation in the Lacandon forest remained within the envelope defined by the modern regional vegetation mosaic. In a lower proportion, the ordination of a few fossil samples outside the environmental envelope defined by modern PDFs suggests the occurrence of non-analogue vegetation during the early Holocene (Fig. 5.4).

*Detrital input: Ti/Sr*

Fe, Rb, Ti, and Zr resulted positively correlated in the record of lake Ocotitalito (Appendix 6.2). These elements are hardly movable and derive from land materials, being typically associated with erosional processes (Rothwell & Croudace 2015). In the Lacandon forest, the main erosive factor is the runoff produced by rainfall, suggesting these elements are a good proxy for rainfall. Specifically, the Ti record can be inferred as changes in total annual precipitation and/or seasonality (Vazquez-Molina et al. 2016), although it could also be associated with erosive processes triggered by vegetation changes caused by human activities. On the other hand, Sr is a mobile element fixed by calcifying organisms at the same time as Ca, being commonly used as a marker of strictly biogenic origin (Zaragosi et al. 2006). Indeed high Sr concentrations in the sediments of Lake Ocotitalito are associated with high abundances of ostracod and gastropod shells, in turn associated with low lake levels (Díaz et al. 2017). The negative correlation between terrigenous elements and Sr (Apéndice 5.2) suggest that carbonates likely have a diluting effect on the detrital mineral abundances. Thus, we used the Ti/Sr ratio to properly characterize detrital inputs to the lake,

removing such dilution effect and revealing otherwise undetectable variability patterns (Lowemark et al. 2011).

#### *5.4.2. Vegetation history at the Lacandon forest during the last 9,500 years*

The sedimentary sequence from lake Ocotulito provides a continuous record of vegetation dynamics at the Lacandon forest from ca. 9,500 BP to modern times. The most important changes that took place through this time period were: i) a replacement of LMRF by MRF at ca. 7,800 BP; ii) dominance of POF and open vegetation from ca. 6,200 to 4,000 BP; iii) a sharp reduction of forest cover from 4,000 to 1,600 BP, leading to the dominance of grasses and trees of secondary forest succession; and iv) forest recovery, increasing taxa of POF and MRF from 1,600 to present.

#### *Infilling of the lake and the expansion of tropical forest (from 9,500 to 8,200 BP)*

High percentages of *Alchornea*, *Brosimum*, and Moraceae in the bottom of the record (9,500 – 8,200 BP, Fig. 5.3) evidenced the establishment of a tropical forest, reported for ~10,500 BP for the regional lowlands (Correa-Metrio et al. 2012a). From ca. 9,500 to 9,000 BP, the abundances of these elements anti-phased high percentages of Amaranthaceae, Asteraceae, *Pinus*, and Cyperaceae. Given low pollen concentrations, these alternations were probably the result of substantial fluctuations of lake level causing poor pollen preservation in an incipient lake. The inception of regional humid warm conditions at ca. 10,500 BP (Leyden 1984; Correa-Metrio et al. 2012a) represented novel conditions after the aridity that characterized the deglaciation (Leyden et al. 1993; Correa-Metrio et al. 2012a). Higher precipitation was likely associated with the infilling lake, which stabilized

around 9,000 BP. Subsequently, and up to ca. 8,200 BP, pollen spectra showed high pollen concentration and were dominated by LMRF taxa with a dense canopy mostly composed of Moraceae, *Brosimum*, *Protium*, and *Ulmus*. High abundances of tropical taxa and high pollen concentrations suggest high ecosystem productivity favored by warm conditions with high precipitation well distributed throughout the year. The NMDS patterns indicate that tropical vegetation prevailed through the early Holocene, indicating warm and wet conditions (Fig. 5.5). The development of vigorous vegetation has also been recorded in other regions of the Maya lands commonly associated with the “Holocene thermal maximum”, a period dominated by warmer and wetter conditions (Ford & Nigh 2009; Wahl et al. 2016a). Low charcoal concentrations during this period indicate very low fire activity (Fig. 5.5) probably caused by low probability of ignition in LMRF characterized by large-diameter and moisture-laden fuels (Schüpbach et al. 2015). Predominance of clays and highest values of Tr/Sr during this period provided additional evidence of larger water supply and lacustrine sedimentary environments (Fig. 5.5). Humid conditions were also recorded in different places in the Maya lands (Islebe et al. 1996; Leyden 2002; Wahl et al. 2006), and it was consistent with the ITCZ reaching its northernmost position during the Holocene “thermal maximum” resulted from high summer-spring insolation (Fig. 5.5).

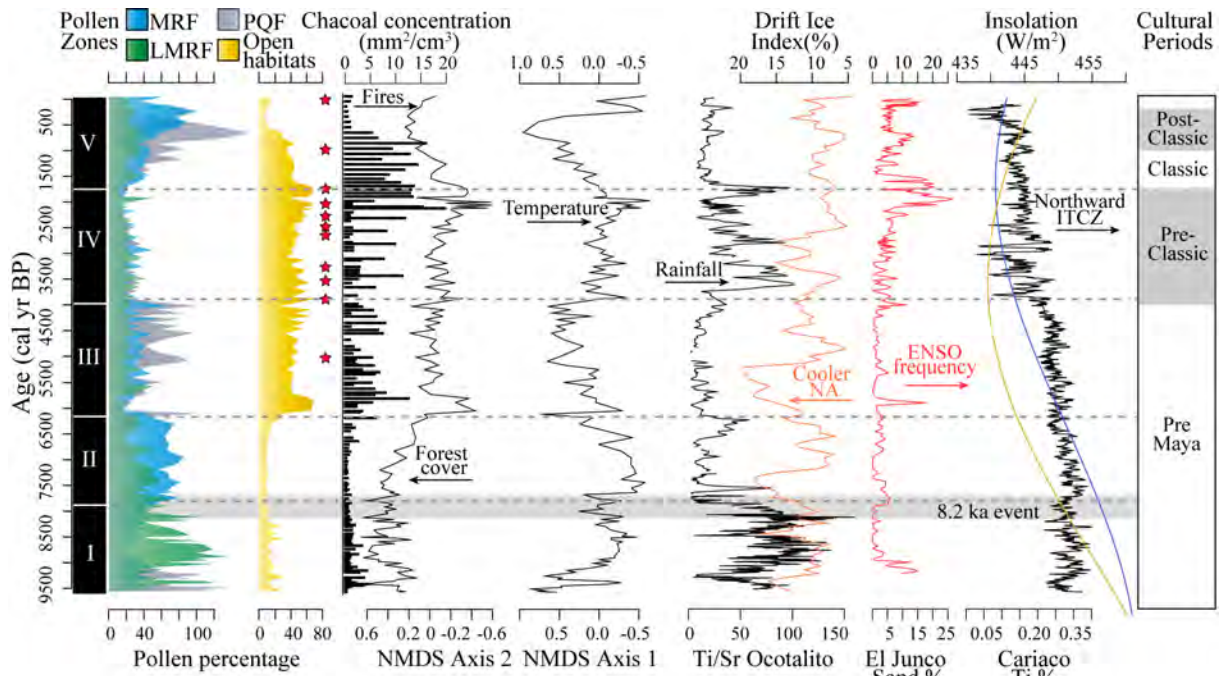


**Figure 5.5.** Environmental history of the Lacandon forest. From left to right, pollen percentages of montane rain forest (MRF, blue area), lower montane rain forest (LMRF, green area), *Pinus-Quercus* forest (PQF, gray area), and followed by open vegetation (yellow area) and presence of *Zea mays* (red stars). Charcoal concentration (black bars) and NMDS Axis 2 sample scores (black line). NMDS Axis 1 sample scores interpreted as temperature gradient (black line). Ti/Sr ratio along Ocotalito record associated with changes in precipitation. Percentage of lithic grains in the sediments of the North Atlantic as an index of drift ice (Bond et al. 2001). Sand percentages in the sediments of Lake El Junco, Galapagos islands (Conroy et al. 2008). Summer (blue line) and spring (yellow line) insolation, data from Analyseries 2.0 (Paillard et al. 1996) overlain on titanium weight percentages, in the sediments of Cariaco basin, northern Venezuela (Haug et al. 2001). A simplified Maya chronostratigraphy is shown in the last panel.

#### *From 8,200 to 7,800 BP: The 8.2 ka Event*

Ca. 8,200 BP, the pollen record of Lake Ocotalito showed a decrease of LMRF elements by ~40%, and replacement by elements of PQF (mainly *Alnus*, *Ilex*, and *Ulmus*) together with *Pinus* and *Quercus*. Although the vegetation turnover was substantial, it did not imply a reduction of the forest cover, but rather a replacement of LMRF thermophile taxa by more temperate elements such as *Pinus* and *Quercus* (Fig. 5.3). Therefore, pollen assemblages

indicate a progressive change from warm to relatively cold condition, as was also inferred in low scores of NMDS Axis 1. Ti/Sr ratios decreased abruptly during this period suggesting a substantial precipitation reduction (Fig. 5.5). Despite the strong change towards drought and relatively cold condition, fire activities remained suppressed according to low charcoal concentrations. There is likely that cold conditions and soils moisture-laden inhibited fire during this event. Therefore, vegetation change was associated with the transition of the climatic system towards slightly colder and dry seasonal conditions. Differently, vegetation from northern lowlands Neotropics not showed important changes during this period, despite evidence of substantial decrease in precipitation (Hillesheim et al. 2005). At ca. 8,200 BP a worldwide climatic event, known as the “8.2 ka” event, which was a short-lived cooling event triggered by freshwater inputs from proglacial lakes to the North Atlantic with effects experienced at a global scale (Alley et al. 1997). This event was most strongly expressed in the high to middle latitudes around the North Atlantic, where colder, drier, and partially more windy conditions were registered (Wiersma & Renssen 2006)(Wiersma & Renssen 2006). It seems that coolings in the North Atlantic only were reflected in substantial decrease of precipitation in low latitudes (Lachniet et al. 2004; Hillesheim et al. 2005). However, in the mountains of the Lacandon forest both temperature and precipitation declined, likely by their altitudinal/latitudinal position.

*The mid Holocene (from 7,800 to 4,000 BP): climatic disturbance*

Pollen assemblage dominated by Clusiaceae, Melastomataceae, *Myrica*, *Quercus*, *Spondias* and *Zanthoxylum* replaced the PQF of the 8.2 ka Event (Fig. 5.3). According to modern ecological affinities, these elements are typical of MRF and seasonal climatic regimes (Marchant et al. 2002; Rzedowski 2006). A strong reduction of regional moisture

availability is inferred from the abrupt decrease of Ti/Sr ratios, which however does not seem to have altered the forest structure during the mid Holocene. High percentages of Clusiaceae, Melastomataceae, *Myrica*, and *Zanthoxylum* from ca. 7,800 to 6,000 BP (Fig. 5.3) were likely associated with riparian communities that suggest the presence of low soil moisture deficit, also identified in low-lying depressions of Petén (Wahl et al. 2016a). These types of forests have been identified as characteristic of microrefugia for tropical taxa during periods of Pleistocene aridity (Meave & Kellman 1994) and are usually associated with the high capacity of the soil to store large amounts of water during dry years (Rzedowski 2006). This result suggests an important forest resilience to climatic perturbations in the Lacandon forest, which in turn have been recognized for tropical montane forest from other regions (Bush 2002; Figueroa-Rangel et al. 2010). Additionally, the dominance of these taxa and high scores of NMDS Axis 2 indicate prevalence of dense forest, whereas high scores of NMDS Axis 1 suggest a slight decrease in temperature in the Lacandon forest (Fig. 5.5). Therefore, the turnover from LMRF to MRF was probably associated with the end of the influence of the 8.2 ka event over regional climates.

Between ca. 6,000 and 4,000 BP, pollen assemblages showed an important decline in forest cover whereas PQF elements increased substantially (Fig. 5.5). However, PQF were broadly dominated by *Pinus*, suggesting a sparse forest because its preference for areas with open vegetation (González-Espinosa et al. 1991; Martínez-Icó et al. 2015). Nevertheless, the anemophilous pollination of *Pinus* could lead to its dominance of the pollen assemblages decoupled from the actual dominance of the vegetation by the parental taxa (Lozano-García & Xelhuantzi-López 1997; Correa-Metrio et al. 2011). In this palynological record, we found a high abundance of *Pinus* in association with some elements of PQF (Fig. 5.3), reinforcing the idea of *Pinus* as important arboreal element in

the actual vegetation. Additionally, NMDS Axis 2 scores decreased abruptly whereas increased *Ambrosia*, Asteraceae, and Poaceae point to the significant expansion of open vegetation in the region despite the establishment of the PQF (Fig. 5.5).

NMDS Axis 1 and Ti/Sr ratios seem synchronous with spring insolation from 6,200 BP to top of record (Fig. 5.5), suggesting a probably linking mechanism. Decreasing spring insolation could be associated with a southern displacement of the ITCZ, amplifying the dry season in the Northern Hemisphere. Also, drought episodes occurred during the last 6,200 years has been associated with North Atlantic coolings (Fig. 5.5), implying the incidence of multiple climatic forcings in the region. Therefore, the forest cover declined in response to low moisture availability in the region. Additionally, high fire disturbances were in antiphased with Ti/Sr, suggesting the preponderance of fire during a period dominated by dry conditions (Fig. 5.5). Although we found the first appearance of *Z. mays* at ca. 5,100 BP, its discontinuity through this period suggests sparse agricultural activities in the area. Therefore, other mechanisms of disturbance such as climate changes could play an important role in increases of fires and species turnover in the Lacandon forest. Particularly, the onset of El Niño activity at ca. 6,000 BP might have brought more seasonal conditions to the area. Indeed, our charcoal record shows a behavior in phase with the El Junco record of El Niño (Conroy et al. 2008) from the Galapagos Islands in Ecuador (Fig. 5.5). Therefore, it is possible that expression of a high frequency of El Niño in the Lacandon forest is an increase of droughts and fires, which can be causing substantial changes in the ecosystems given its potential as disturbance factor (e.g. Bush et al. 2016).

*Climatic and anthropogenic disturbances on vegetation structure (from 4,000 to 1,600 BP)*

This period was characterized by a high loss of forest cover in the area, evidenced by the abrupt decline of PQF and MRF, and a further expansion of open vegetation (Figs. 5.3 and 5.5). A substantial reduction of forests between 4,000 and 3,500 BP has been reported in paleoenvironmental studies of the south Maya lowlands (Islebe et al. 1996; Wahl et al. 2006) and northern Yucatan Peninsula (Carrillo-Bastos et al. 2010). Our record points to an important imprint of human activities on the landscape through this period of time, coinciding with a period when the ancient Maya communities expanded throughout the region (Sharer & Traxler 2006). Presence and persistence of *Z. mays* accompanied by important peaks of *Ambrosia* and charcoal suggest intensive human activities (Figs. 5.3 and 5.5), as it has been reported for other areas in the Maya lands (Goman & Byrne 1998; Leyden 2002; Nations 2010). The abrupt decrease of *Pinus* and arboreal elements from PQF and MRF accompanied by increases of *Acacia*, *Alnus*, and *Byrsonima* (Fig. 5.3) suggests the development of agricultural activities accompanied by some elements of the seasonal deciduous forest, typical of simplified environments from Lagos de Colón and perturbed sites from Lagunas de Montebello. NMDS Axis 1 apparently indicates an increase in the temperature, but the dominance of human-induced vegetation over forests suggests a blurring effect on the climate context based in pollen (Caballero-Rodríguez et al. 2017). NMDS Axis 2 indicates a substantial decrease of forest cover in an environment dominated by relatively warm conditions (Fig. 5.5). Highest and variable charcoal concentrations suggest the dominance of fire disturbances in the region. High variability in the charcoal concentrations likely indicate an emergent property of human-induced fires, different to the previous period where droughts lead to high and stable fires.

High values of Ti/Sr through this time period (Fig. 5.5) were likely a result of more intense erosion caused by anthropogenic vegetation clearance. Evidence of forest losses, agricultural activities, and monumental constructions through this time period has been consistently reported for other areas of the Maya region (Curtis et al. 1998; Goman & Byrne 1998; Lentz & Hockaday 2009; Franco-Gaviria et al. 2018b). Our results indicate regional expansion of agricultural practices and intensive landscape manipulation mostly in the Lacandon forest from ca. 4,000 to 1,600 BP. This also has been recorded in Montebello region (Franco-Gaviria et al. 2018b), indicating similar human occupation patterns in the Maya highlands. Although Northern Neotropics has been characterized by gradual decrease of moisture availability (Haug et al. 2001), this period was characterized by wet and variable conditions. These conditions were probably associated with the reported decreased of El Niño frequency between 4,000 and 2,000 BP (Fig. 5.5, Conroy et al. 2008). The lack of recurrent el Niño events, probably favored the establishment of regular seasonality, which in turn promoted human settlements and the persistence of the human-modified landscape.

*Forest recovery in the Lacandon forest (from 1600 to modern times)*

The beginning of this period ca. 1600 BP was characterized by a brief decreases of open vegetation and absence of *Z. mays* in the record (Figs. 5.3 and 5.5), suggesting an agricultural abandonment of the region. This event coincided with the cultural Preclassic abandonment or “Maya Hiatus”, defined as a break of the Maya population mostly recognized in the highlands of Mesoamerica (Dull 2004; Velez et al. 2011; Franco-Gaviria et al. 2018b). The reduction of open vegetation and human disturbances were accompanied by the establishment of forests dominated mostly by elements of POF and to a lesser extent,

elements of MRF and LMRF (Fig. 5.5). A substantial increase of NMDS Axis 2 scores points to high forest cover and the early forest regrowth in the mountains of the Lacandon forest (Fig. 5.5). Increasing of POF elements, mostly *Pinus*, suggest early stages of forest ecological succession because they have many heliophilous species that grow after disturbed areas and forest gaps (González-Espinosa et al. 1991). Consequently, dominance of POF from ca. 1,200 to 700 BP probably represents the initial stage of the ecological succession post-disturbance, which led subsequently to the establishment of dense montane forests, as it has occurred in the Lagunas of Montebello (Franco-Gaviria et al. 2018b). This initial phase of forest recovery (From 1,600 to 700 BP) occurred during the Classic period when human activities were relatively important in the region. However, very low abundances of *Ambrosia* and *Z. mays* indicate relatively low human impact in the Lacandon forest (Domínguez-Vásquez & Islebe 2008). Persistent fires were associated with high disturbance in the region, which could be explained by a high frequency of ENSO (Fig. 5.5). The sharp decline of NMDS Axis 1 scores and Ti/Sr ratio indicate the dominance of cold and dry conditions, which in turn could be derived from a re-invigorated El Niño and the Holocene long-term trend toward drought (Fig. 5.5).

The last 700 years are also part of the gradual forest recovery in the mountains from the Lacandon forest, the decline of POF elements and the expansion of LMRF and MRF characterized this sub period. Particularly, this was evidenced by the strong decline of *Pinus*, which is ecological opportunistic taxa and under milder environments is outcompeted by other taxa (González-Espinosa et al. 1991). Declines of POF elements together low fire activity marked the reduction of natural and anthropogenic disturbances in the region. Thus, increased temperate (e.g. *Ulmus*, Melastomataceae, and *Myrica*) and tropical (e.g. Moraceae and *Alchornea*) taxa commonly associated with tropical montane

forests (Fig. 5.5). Montane rain forests from Montebello (Franco-Gaviria et al. 2018b) and west-central Mexico (Figueroa-Rangel et al. 2010) were also reported as having expanded within the same time interval, point to a regional pattern of wetter conditions and low human influence on the vegetation. Dominance of MRF mixing with LMRF elements was probably a consequence of high moisture availability and relatively cold conditions (Fig. 5.5). Cold and wet conditions have been documented in other middle and high elevation records from Chiapas and Central America (Dull 2004; Vazquez-Molina et al. 2016; Franco-Gaviria et al. 2018b), indicating regional processes were operating. High humidity could be associated with local processes that include the geographic position of our study area in the mountains of Chiapas, which probably favored higher orographic precipitation (Vazquez-Molina et al. 2016; Franco-Gaviria et al. 2018b) and lower evaporation (Correa-Metrio et al. 2016). Additionally, a slight increase in spring insolation probably advanced the rainy season; this together low ENSO activity and low incidence of North Atlantic cooling favored the higher moisture availability in the region (Fig. 5.5). Therefore, we suggest that reduced human activities, combined with high moisture availability, promoted the progressive forest regeneration around Lake Ocotlito, beginning during the transition Preclassic-Classic (ca. 1,600-1,500 BP) and consolidating after ca. 700 BP. This differs from the vegetation dynamic in the Maya lowlands (e.g. Wahl et al. 2006; Mueller et al. 2010), where forest regrowth began ca. 800 BP after Terminal Classic abandonment without taking into account previous phases of forest successions.

## 5.5. Conclusions

Vegetation changes in the mountains of the Lacandon forest responded significantly to climate variability events and human activities throughout the Holocene. The increase of regional moisture favored the formation of the lake Ocotolito, allowing, together with warmer temperatures, the establishment and expansion of LMRF during early Holocene. However, between 8,200 and 6,000 BP, the abrupt transition toward dry conditions mostly affected the composition of these forests. Dense forests preserved their structure and responded to climate instability by recruiting key species during this period of time. This evidence suggests the presence of microrefugia for populations in the middle elevations that allowed the persistence of forest species even during times of high environmental stress. From 6,000 to 4,000 BP, an abrupt change towards drier conditions took place, reflected on intense fires and significant losses of forest cover. From 4,000 to 1,600 BP, vegetation changes were largely the product of strong anthropogenic impact on the region, whereas climate conditions were highly variable. The last 1,600 years were characterized by the forest recovery, beginning by the early occupation of opportunistic species such as *Pinus* and the subsequent establishment of modern vegetation composed by MRF and LMRF elements at ca. 800-700 BP, when environmental conditions were relatively milder.

The vegetation response to the Holocene climatic variability suggests that the Lacandon forest suffered different periods of change in their climate drivers (Fig. 5.5). The results suggest that in the early to middle Holocene, the regional trend towards dry conditions by a southward gradual migration of the ITCZ affect substantially the humidity regime in the Lacandon forest. Additionally, cooling in the North Atlantic influenced negatively the moisture availability in the region by recurrent droughts. At shorter time

scales (middle-late Holocene), it is likely that increased frequency of El Niño activity has introduced a climatic system highly unstable associated with losses in the forest cover.

### **Acknowledgments**

We thank Juan Beltrán, Esmeralda Cruz-Silva, Julián Hernández, and Melbi Ramos-Fabiel for their help in coring of Lake Ocotlito. The Lacandon community of Nahá, especially Miguel Garcia, for their generous fieldwork assistance and their valuable insights on the Lacandon forest. Financial support from PAPIIT-UNAM Grants IN107716 and IA100714.

## CAPÍTULO 6

### SÍNTESIS: VARIABILIDAD AMBIENTAL EN LAS MONTAÑAS DE CHIAPAS DURANTE EL HOLOCENO: ESTIMACIÓN CUANTITATIVA BASADA EN EL POLEN

#### 6.1. Introducción

El conocimiento del clima y el impacto humano en el pasado es importante para entender una amplia variedad de procesos ambientales modernos y para estimar las causas y los efectos de cambios ambientales futuros. Diferentes registros paleoambientales de las tierras Maya sugieren un incremento de la variabilidad ambiental durante el Holoceno medio y tardío con respecto al Holoceno temprano (Hodell et al. 2001; Leyden 2002). El Holoceno medio y tardío en las tierras Maya se caracterizó por presentar una tendencia hacia condiciones más secas que culminaron en fuertes sequías entre 1100 y 900 AP (Medina-Elizalde et al. 2010). La disminución sustancial de la humedad durante el Holoceno medio y tardío ha sido asociada con una posición más al sur de la ITCZ y la intensificación del fenómeno de EL Niño (Haug et al. 2001; Hodell et al. 2001). Condiciones más secas llevaron al reemplazamiento de elementos de bosque tropical por una mezcla de elementos de bosque estacional y vegetación abierta (Islebe et al. 1996; Curtis et al. 1998; Rosenmeier et al. 2002). Posteriormente, la predominancia de condiciones más secas y variables durante el Holoceno tardío, estuvo acompañada por el aumento de disturbios antrópicos en la región (Curtis et al. 1998; Leyden 2002; Wahl et al. 2006).

En términos generales, la región Maya ha sido ampliamente estudiada en términos de los efectos de la variabilidad climática y el impacto humano sobre las comunidades vegetales durante los últimos milenios. Sin embargo, el desconocimiento de la magnitud de los cambios causados por las actividades antrópicas debilita la interpretación paleoambiental regional, debido a la falta de sistematicidad que impide el reconocimiento de patrones y tendencias generales. La cuantificación de cada uno de los principales factores que estructuran las comunidades vegetales permitiría estimar la importancia relativa de cada atributo ambiental sobre la vegetación (Reitalu et al. 2013). La cuantificación de diferentes atributos del ambiente se podría basar en nuestra capacidad para comprender las relaciones numéricas entre el polen moderno, parámetros clave del clima y la influencia humana (Birks 2003). Por ejemplo, las relaciones sistemáticas encontradas entre el polen moderno y los gradientes ambientales (Capítulo 3) permitiría la reconstrucción cuantitativa de las condiciones climáticas y el impacto humano en las elevaciones medias y altas de la región Maya.

El objetivo de este capítulo es sintetizar la información proveniente del estudio de polen moderno, los atributos del ambiente y el registro fósil de las montañas de Chiapas, ofreciendo una estimación cuantitativa de los principales elementos de cambio en la vegetación. Así, se aplicaron modelos de regresión ponderada local (LOESS, por sus siglas en inglés) sobre una ordenación basada en las bases de datos modernas y fósiles presentadas en la tesis para cuantificar los registros paleoambientales de las Lagunas de Montebello y la Selva Lacandona, y así aproximar una respuesta a las siguientes preguntas:

- 1) ¿Cuáles son los principales gradientes ambientales expresados en los ensambles de polen moderno y fósil?;
- 2) ¿Cuál fue la magnitud de los cambios en el clima y el impacto durante periodos de estrés ambiental en las montañas de Chiapas?

## 6.2. Métodos

Las muestras de polen moderno (Capítulo 3) y fósiles (Capítulos 4 y 5) fueron analizadas en conjunto usando un Análisis de Correspondencia sin Tendencia (DCA, por sus siglas en inglés). Esta técnica resume la variabilidad reflejada por los diferentes taxa polínicos y ordena tanto registros modernos como fósiles en un espacio común dimensionalmente reducido (Hill & Gauch 1980). Entre diferentes técnicas de ordenación, el DCA fue elegido porque permite resumir atributos de la vegetación en ejes ortogonales además de extraer la señal ambiental de los ensambles de polen a través de gradientes ecológicos y ambientales amplios (Correa-Metrio et al. 2014).

La interpretación de la estructura ambiental que subyace a la ordenación palinológica se basó en regresiones de los atributos ambientales de cada localidad moderna muestreada como una función de los puntajes obtenidos por la muestra de polen de la localidad correspondiente. Así, la longitud, la latitud, la elevación, la temperatura media anual (MAT), la precipitación anual (APP), la estacionalidad de la precipitación (PSE, coeficiente de variación) y el Índice de Impacto Humano (HII) (Sanderson et al. 2002; Hijmans et al. 2005) fueron modelados como función de los puntajes de DCA. Las relaciones entre pares de variables tanto ambientales y de la vegetación (Eje 1 y Eje 2 del DCA) fueron estimadas mediante correlaciones de Pearson. Al encontrarse una alta redundancia entre la elevación y la temperatura se prefirió usar solo la elevación debido a que es una medida directa en campo, mientras que los valores de temperatura se basan en estimaciones mediante interpolaciones espaciales. Se realizó un análisis multivariado de la varianza (MANOVA, por sus siglas en inglés) para analizar la relación entre los dos

primeros ejes de la ordenación expresados como variables respuesta y el conjunto de las variables ambientales.

Una vez seleccionadas las variables que se expresaron en la ordenación bidimensional, se produjeron curvas de regresión LOESS (Cleveland & Devlin 1988) para cada variable ambiental como una función de los puntajes de los ejes de la ordenación. En el mismo espacio de la ordenación, las muestras fósiles se compararon con las estimaciones ambientales producidas por las regresiones LOESS, prediciendo para cada muestra fósil un valor de determinado atributo ambiental. Posteriormente, las muestras fósiles y sus respectivos valores ambientales se organizaron en orden estratigráfico, con lo cual se obtuvo una secuencia continua de los cambios ambientales reconstruidos.

Todo el procesamiento estadístico fue realizado usando R (R Core Team 2017), especialmente los paquetes MASS (Venables & Ripley 2002) y vegan (Oksanen et al. 2017).

## **¿Cuáles son los principales gradientes ambientales expresados en los ensambles polen moderno y fósil?**

La reconstrucción cuantitativa de los atributos ambientales basada en polen se caracteriza por entender inicialmente cuáles son los principales gradientes ambientales expresados en los ensambles polínicos (Hicks & Birks 1996). En tal sentido, la matriz de correlaciones mostró relaciones significativas entre la expresión del polen en los dos puntajes del DCA y atributos ambientales (Fig. 6.1). Especialmente la alta correlación de los puntajes del Eje 1 con la elevación ( $r = -0.73$ ) y el Eje 2 con la latitud ( $r = 0.30$ ). Esto sugiere que gradientes biogeográficos expresados en cambios en la elevación y latitud fueron captados por los ensambles de polen moderno y fósil. En las montañas de Chiapas se localiza en una zona de transición donde confluye tanto vegetación de origen Neártico como Neotropical (Rzedowski 2006), de manera que la proveniencia de los taxa en el tiempo puede variar notablemente.

Se encontró una alta correlación entre PSE y el HII ( $r = 0.45$ ), lo cual podría estar ligado a la predominancia de zonas agrícolas en la región Maya. La productividad de los cultivos incrementa bajo condiciones estacionales (Ray et al. 2015), así las actividades humanas relacionadas con la estacionalidad podrían corresponder en mayor medida a la agricultura. De hecho, más de la mitad de la producción agrícola temporal de México se concentra en el Sureste, especialmente en los estados de Chiapas, Campeche y Tabasco (SIAP, 2013). Una de las principales críticas al HII como herramienta para reconstruir el impacto humano, es el sesgo ocasionado por patrones que difícilmente son replicados en el pasado como los centros urbanos e infraestructura contemporánea. Sin embargo, la relación encontrada entre el HII y la estacionalidad sugiere que el HII en mayor medida representa

usos del suelo muy probablemente asociados a la agricultura, los cuales podrían replicarse en el pasado.

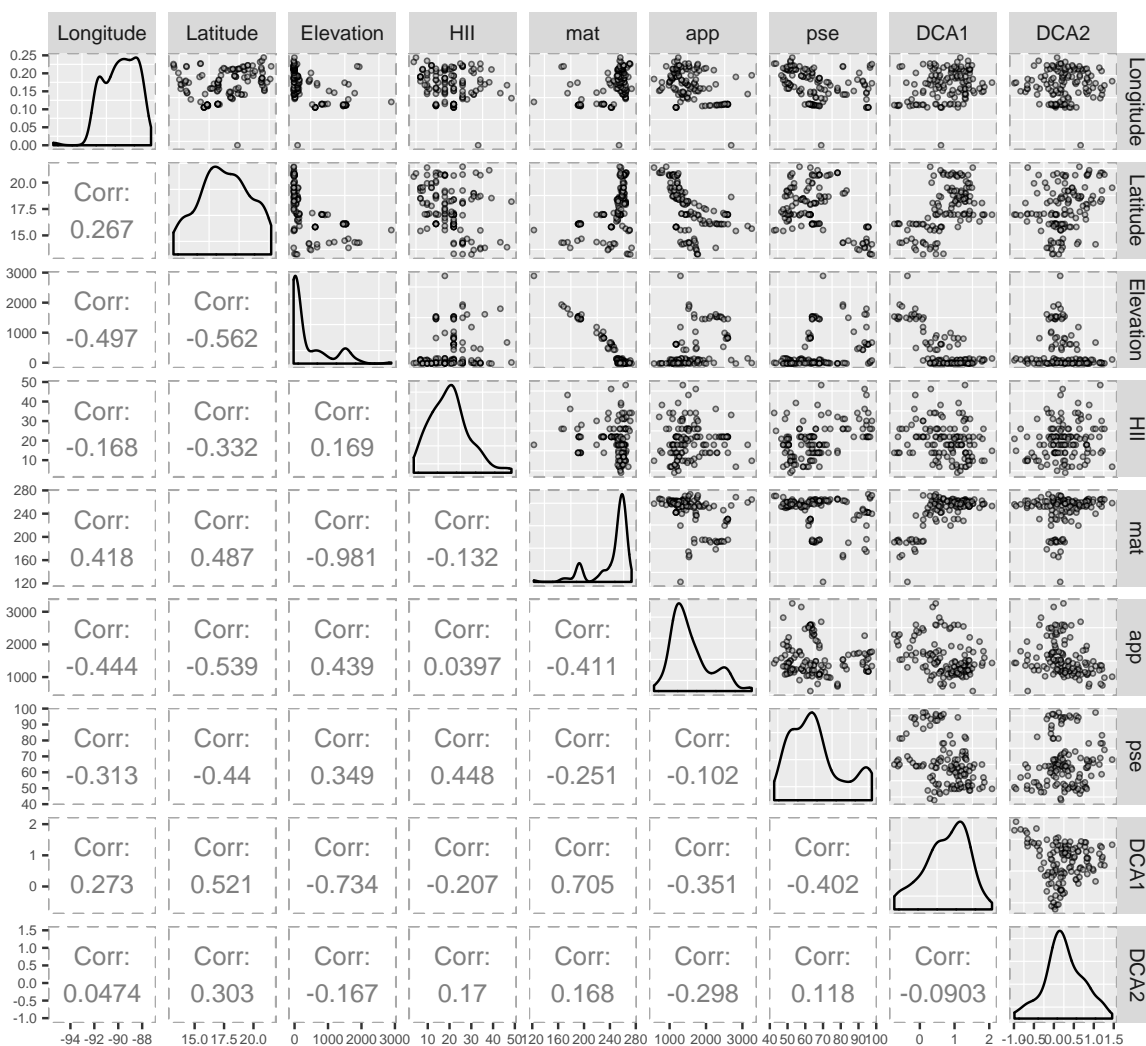


**Figure 6.1.** Matriz de correlación de atributos del ambiente y la vegetación. Histogramas modelados por funciones de densidad de probabilidad (diagonal principal), diagramas de dispersión (triángulo superior) y coeficientes de correlación de Pearson (triángulo inferior).

De acuerdo con los resultados del MANOVA, todas las variables ambientales excepto la precipitación se expresaron en los dos primeros ejes del DCA (Tabla 6.1). Es probable que la precipitación no guarde una relación con ambos ejes del DCA por el ruido generado en la inclusión de taxa asociados al disturbio antrópico (Correa-Metrio et al.

2011). De hecho, algunos estudios de polen moderno sugieren que el impacto humano y la precipitación anual son igualmente reflejadas en los espectros de polen (Li et al. 2014; Caballero-Rodríguez et al. 2017). Dado que en las tierras de la región Maya modernas difícilmente se encuentran sitios sin intervención humana, las reconstrucciones climáticas basadas en polen deberían considerar los sesgos al incluir la vegetación alterada por el hombre. Por lo tanto, se recomienda realizar previamente filtros basados en las relaciones funcionales entre cada taxón y las variables ambientales de interés. Por ejemplo, en el Capítulo 3 se encontraron 21 taxa asociados al impacto humano, esta clasificación sería de gran utilidad para reducir los posibles sesgos de las actividades humanas en las reconstrucciones climáticas de la región.

**Tabla 6.1.** Análisis multivariado de la varianza, con los puntajes de los ejes 1 y 2 del DCA como variables respuesta y los atributos del ambiente como variables explicativas.

| <b>Atributo ambiental</b>                | <b>Estadístico</b> | <b>F</b> | <b>GL (den)</b> | <b>Valor-p</b> |
|--|--------------------|----------|-----------------|----------------|
| Longitud                                 | 0.07714            | 5.099    | 122             | 0.007469       |
| Latitud                                  | 0.09461            | 6.374    | 122             | 0.002328       |
| Elevación                                | 0.43075            | 46.159   | 122             | 1.18E-15       |
| Índice de Influencia humana – HII        | 0.05202            | 3.347    | 122             | 0.038437       |
| Precipitación anual - APP                | 0.04524            | 2.891    | 122             | 0.059356       |
| Estacionalidad de la precipitación - PSE | 0.07512            | 4.954    | 122             | 0.008535       |

Las variables ambientales mejor expresadas en la ordenación, se modelaron en el espacio bidimensional (Fig. 6.2), obteniendo superficies de tendencia en el que se distinguieron diferentes patrones. Por ejemplo, es posible distinguir patrones espaciales en la distribución de la elevación, la influencia humana y la estacionalidad a lo largo de los dos ejes del DCA. La elevación se expresó a lo largo del Eje 1 del DCA con valores mas altos hacia el extremo negativo que disminuyeron progresivamente hacia el extremo positivo de la ordenación. De forma opuesta, la influencia humana y la estacionalidad se

expresaron a lo largo del Eje 2 del DCA con valores altos en el extremo positivo y bajos hacia el extremo negativo ordenación. Por lo tanto, la ordenación de los espectros de polen modernos y fósiles de las montañas de Chiapas mostró un gradiente de elevación a través de su Eje 1, mientras que en términos del Eje 2 se reflejaron gradientes de influencia humana y estacionalidad. Sin embargo, permanece la necesidad de un método multi-respuesta que distinga la contribución relativa de cada variable ambiental para explicar la ordenación.

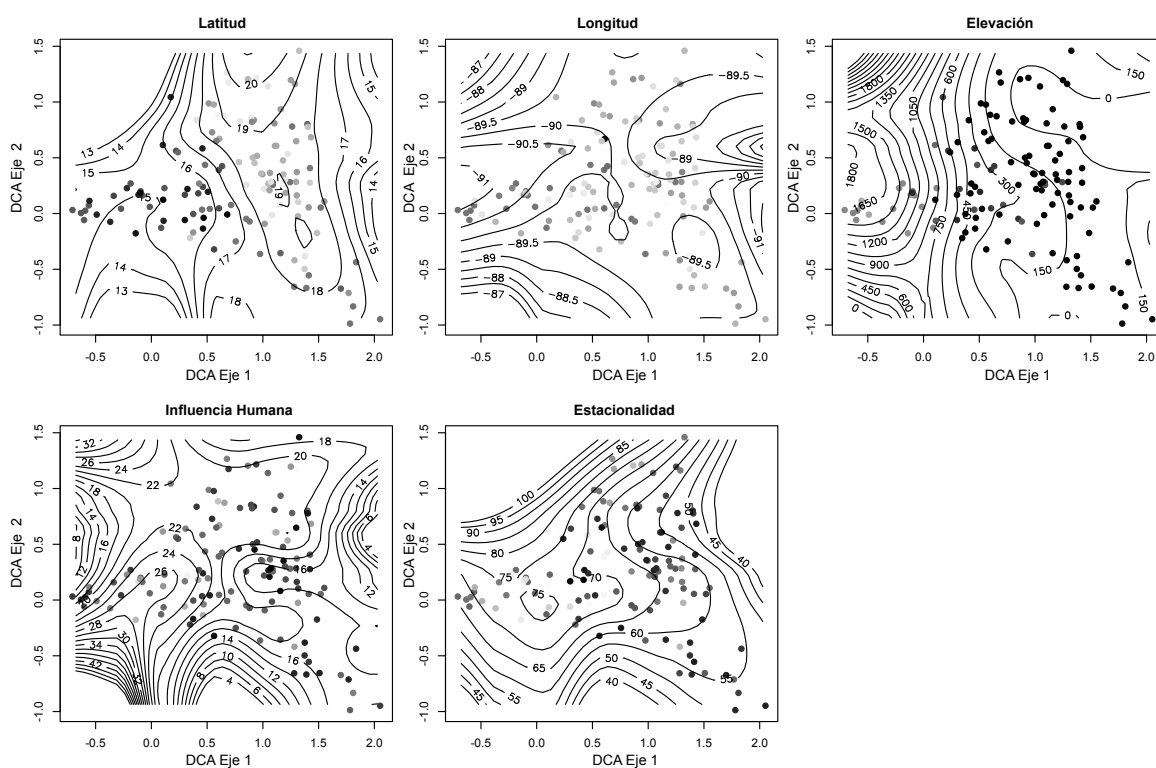


**Figure 6.2.** Variables ambientales estimadas como modelos de regresión ponderada local (LOESS) en el plano de dos dimensiones definido en el análisis de correspondencia sin tendencia (DCA). Muestras fósiles representadas por los puntos.

## **¿Cuál fue la magnitud de los cambios en el clima y el impacto humano durante el Holoceno, en las montañas de Chiapas?**

Durante el Holoceno temprano, los patrones biogeográficos inferidos de los cambios en latitud y longitud mostraron una dominancia de coordenadas asociadas a las tierras bajas de Petén (~ 17.5°N y 89.5°W) donde los taxa tropicales son ampliamente dominantes (Fig. 6.3). También, durante este periodo la elevación reconstruida sugiere la dominancia de condiciones relativamente cálidas, las cuales fueron acompañadas por condiciones húmedas y poco estacionales (CV=50% en promedio). Condiciones climáticas relativamente estables fueron congruentes con los diferentes registros paleoclimáticos de la región (Curtis et al. 1998; Haug et al. 2001; Hillesheim et al. 2005), en los cuales la migración hacia el norte de la ITCZ fue un factor fundamental en el establecimiento de condiciones climáticas favorables para la vegetación. En tal sentido, condiciones climáticas cálidas, húmedas y poco estacionales favorecieron el establecimiento de bosques tropicales en las montañas de Chiapas (Capítulo 5). De acuerdo con el impacto humano en la región, sus efectos fueron bajos (HII= 14 en promedio), muy probablemente porque las antiguas comunidades que habitaban las tierras Maya representaban a grupos nómadas dedicados a la caza y recolección de alimentos con bajo impacto en el territorio (Sharer & Traxler 2006).

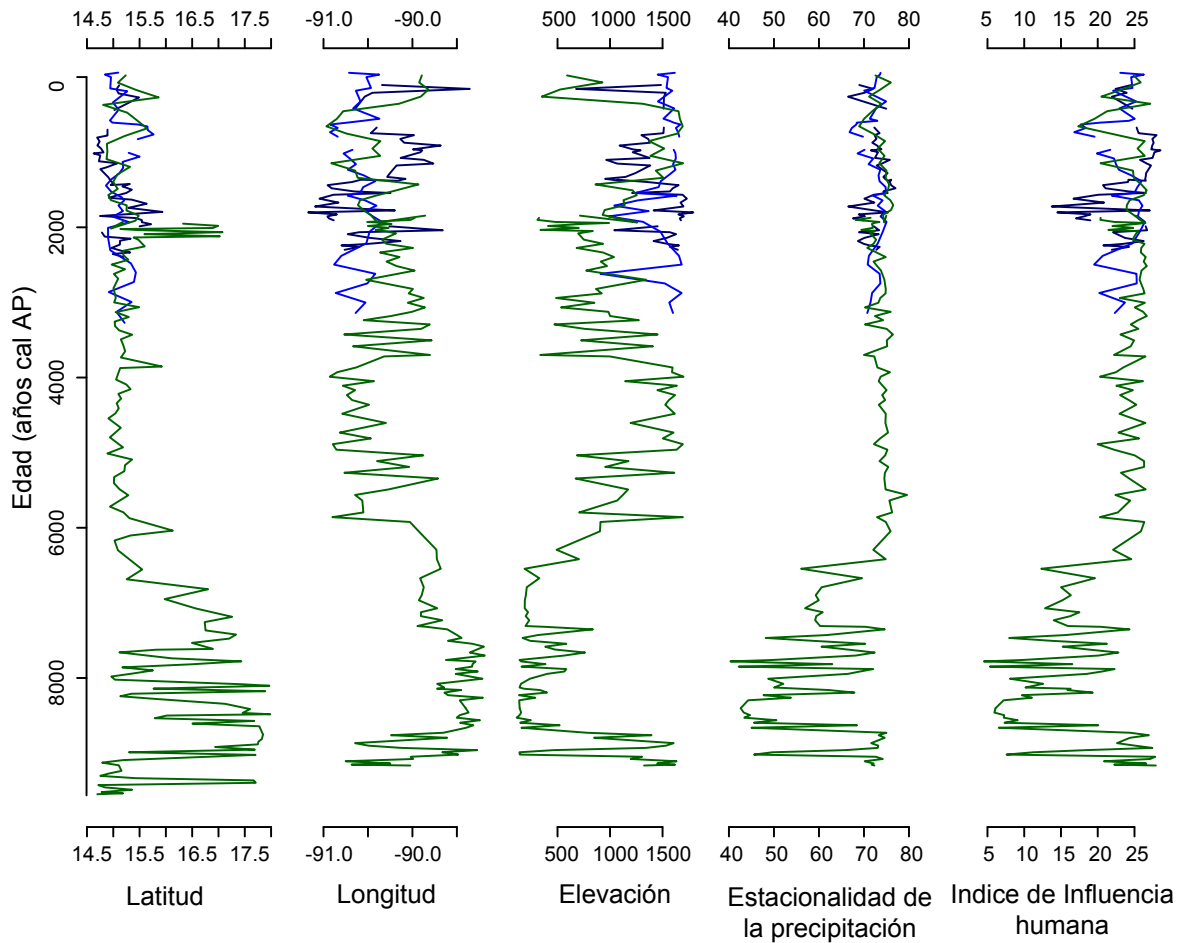


**Fig. 6.3.** Reconstrucción cuantitativa de los atributos ambientales de los registros paleoambientales de la Selva Lacandona (línea verde) y las Lagunas de Montebello (líneas azules).

El Holoceno medio se caracterizó por presentar un cambio abrupto en todos los atributos del ambiente reconstruidos (Fig. 6.3). La latitud y longitud mostraron una disminución debido a un efecto importante de las muestras provenientes de las tierras altas del norte de Guatemala (~15°N y 91°W), dónde los espectros de polen son dominados por taxa de origen Neártico como *Pinus* y *Quercus*. Las reconstrucciones climáticas mostraron una disminución de la temperatura inferida por un incremento sustancial de la elevación y

la estacionalidad de la precipitación (de 55 a 78 %). Condiciones relativamente secas y estacionales también han sido reportadas en las tierras bajas y atribuidas a la migración de la ITZC hacia el Sur y una mayor frecuencia de ocurrencias del fenómeno de El Niño (Haug et al. 2003; Hodell et al. 2007; Wahl et al. 2014). Durante este periodo, los incendios incrementaron y se convirtieron en importantes elementos de disturbio en la región, lo cual coincidió con una mayor variabilidad climática ocasionada por El Niño (Capítulo 5). Como consecuencia de estos cambios ambientales, los bosques tropicales fueron reemplazados por bosques de *Pinus* y *Quercus*. Cabe agregar, que especies de los géneros *Pinus* y *Quercus* se caracterizan por su resistencia a los incendios debido a mecanismos de adaptación como cortezas más densas y un alto potencial de rebrote (González-Espinosa et al. 1991). Es probable que el impacto humano haya jugado un papel importante como mecanismo de disturbio, de acuerdo con el incremento sustancial del HII reconstruido (10-25). Sin embargo, la ausencia de evidencia palinológica asociada a un alto impacto humano sugiere que los disturbios fueron muy probablemente ocasionados por una mayor variabilidad climática. Una posible confusión entre la señal climática y antropogénica podría considerarse por las altas abundancias de herbáceas como *Ambrosia* y *Asteraceae* en el registro (Capítulo 5). Estos elementos podrían alterar la señal polínica debido a su asociación tanto a ambientes secos como de alta actividad humana (Marchant et al. 2002). No obstante, la poca presencia de *Zea mays* en el registro, indicador por excelencia de agricultura y del impacto humano en la zona Maya (Piperno & Flannery 2001), sugiere que las actividades humanas fueron reducidas durante el Holoceno medio.

Durante los últimos 4,000 años, las estimaciones cuantitativas de condiciones climáticas y el impacto humano fueron congruentes con los registros de la Selva Lacandona y las Lagunas de Montebello (Fig. 6.3). La coincidencia de ambos registros en cuanto a

periodos de alta influencia humana (entre 4,000 y 1,500 AP), interrupción temprana de las actividades humanas (~1,500 AP) y similares procesos de recuperación del bosque (entre 800 AP al presente) señala la correspondencia regional de los registros (Capítulos 4 y 5). Por lo tanto, la historia ambiental del Holoceno temprano y medio interpretada del registro fósil de la Selva Lacandona podría representar las condiciones ambientales de las lagunas de Montebello y en un sentido mas amplio las montañas de Chiapas.

El Holoceno tardío en las montañas de Chiapas se caracterizó por presentar dos periodos contrastantes. El primero corresponde al periodo entre 4,000 y 1,500 AP, donde las variables reconstruidas como la longitud y elevación presentaron una alta variación, mientras la latitud y la estacionalidad permanecieron constantes (Fig. 6.3). Sin embargo, la variabilidad en algunos elementos ambientales reconstruidos, así como la reducción sustancial de los bosques (Capítulos 4 y 5) sugiere que otros mecanismos diferentes al clima operaron en la región. De acuerdo con los altos valores del HII (25) se presentó una intensificación de las actividades humanas en la región que pudo ser un factor fundamental de la alta variabilidad ambiental. Una mayor presencia de *Zea mays* y *Ambrosia* en los registros palinológicos indican una incidencia importante de la agricultura en lo patrones de ocupación de las montañas de Chiapas (Capítulos 4 y 5). Esto no es sorprendente, porque evidencia temprana de actividades agrícolas en las tierras Maya data alrededor de 7,000 AP (Pope et al. 2001). También, resultó interesante la relación entre la estacionalidad y el incremento de la influencia humana, particularmente durante el Holoceno tardío (Fig. 6.3). Esto podría explicarse por la habilidad de las antiguas comunidades en usar efectivamente los meses de lluvia para generar reservorios de agua que les permitiera subsistir durante varios meses secos (Dunning & Kowalski 1994). Estos procesos también se vieron

reflejados en una agricultura altamente adaptada a los ritmos estacionales de la precipitación regional (Piperno 2006; Sharer & Traxler 2006).

El segundo periodo del Holoceno tardío (los últimos 1500 años) se caracterizó por una marcada reducción de la precipitación inferida principalmente por los registros geoquímicos de los lagos estudiados. En tal caso, las adaptaciones de la agricultura a las sequías tempranas del Holoceno tardío fallaron durante las sequías mas severas ocurridas entre 1,100 y 800 AP. Estas sequías coincidieron con el Clásico Terminal Maya, periodo caracterizado por el colapso de la antigua Civilización Maya y en cual diferentes estudios paleoclimáticos han cuantificado una reducción de la precipitación hasta un 70 % (Evans et al. 2018). En cuanto a las variables reconstruidas, solo el HII mostro una reducción de la influencia humana a valores 15, mientras las demás no mostraron cambios importantes durante este periodo. La vegetación mostró una reducción sustancial de los taxa de disturbio mientras incrementaron los elementos arbóreos asociados principalmente a bosques de *Pinus* y *Quercus* y bosques montanos (Capítulos 4 y 5). Los últimos 800 años mostraron un leve incremento de la temperatura así como una mayor incidencia de taxa Neotropicales según los aumentos en latitud y longitud (Fig. 6.3). De tal modo, la mezcla entre vegetación tropical y templada dan origen a los bosques de montaña que hoy en día se reconocen en las montañas de Chiapas. La sincronía en la recuperación de los bosques después de estos episodios de sequía e influencia humana implica la existencia de áreas en las montañas de Chiapas que favorecieron la persistencia de pequeñas poblaciones, permitiendo la subsecuente colonización del área. La dominancia de un relieve accidentado en las Montaña de Chiapas caracterizado por pendientes muy inclinadas y cañadas pudo albergar y proteger especies durante periodos de alto estrés ambiental.

## CONCLUSIONES Y PERSPECTIVAS

El análisis de polen moderno en las tierras Maya elucidó los principales patrones de la relación entre el polen y la vegetación, ayudando a mejorar las reconstrucciones paleoecológicas. En términos generales, se resalta la habilidad del polen en reflejar diferentes gradientes ecológicos y ambientales, confirmando su uso potencial en las reconstrucciones paleoambientales. Sin embargo, las reconstrucciones se hacen más robustas con la incorporación de otros indicadores como fue el caso de este trabajo. Para refinar nuestro conocimiento del polen moderno en las tierras Maya, será necesario un esfuerzo adicional para correlacionar los patrones en la deposición del polen con la vegetación moderna. Para esto, se deberían realizar muestreos de vegetación junto con los muestreos de polen, idealmente a lo largo de transectos que cubran amplios gradientes ecológicos y ambientales. Con este tipo de información se podría estimar cuantitativamente parámetros estructurales de la vegetación como la densidad, área basal, diámetro medio o la altura del dosel.

Los resultados de los registros paleoecológicos sugieren que durante los últimos 10,000 años, condiciones ambientales altamente variables han prevalecido en las montañas de Chiapas. Esta variabilidad se ha manifestado principalmente en cambios en patrones biogeográficos, climáticos y de uso del suelo. Los registros paleoecológicos estudiados mostraron una dominancia sistemática de taxa de origen Neártico durante periodos de condiciones ambientales estresantes para la vegetación (e.g. *Pinus*, *Quercus* y *Alnus*, Gentry, 1982). Sin embargo, bajo condiciones climáticas estables y poca influencia humana, la vegetación fue dominada por taxa Neotropicales (e.g. *Hedyosmum*, *Alchornea*, *Moraceae* y *Melastomataceae*, Gentry, 1982). Estos patrones fueron probablemente el resultado de

una respuesta diferencial de los taxa según su proveniencia, pues elementos Neárticos respondieron de forma oportunista a perturbaciones naturales y antrópicas, mientras los elementos Neotropicales en mayor medida fueron el resultado de sucesiones ecológicas mediadas por la expresión de sus nichos ambientales (sensu González-Espinosa et al. 1991).

El análisis de los ensambles de polen modernos y fósiles mostró que la vegetación de las montañas de Chiapas no ha salido del envoltorio representado por el mosaico de vegetación regional moderno (Capítulos 4 y 5). Esto no implica que la vegetación regional haya sido estable, mas bien implica que los patrones de diversidad expresados en el área a través del tiempo también están representados hoy. De hecho, los bosques de montaña que ocupan el área hoy, en términos de la composición de los diferentes taxa y sus abundancias relativas, no tienen mas de 800 años. Condiciones climáticas relativamente estables y una reducción sustancial del impacto humano han favorecido la sucesión y el establecimiento de estos ensambles de vegetación, aparentemente novedosos para el Holoceno. Por lo tanto, es muy probable que los diferentes tipos de vegetación que actualmente existen en las montañas de Chiapas sean el producto de procesos ecológicos que han actuado bajo un legado de siglos de disturbios naturales y antrópicos. No obstante, la ocupación humana de la región durante los últimos 50 años amenaza la supervivencia de estos bosques.

A través de los últimos 10,000 años, los incendios han sido un elemento constante en las dinámicas ecosistémicas. Los periodos de mayor frecuencia de incendios coincidieron con periodos de alta estacionalidad de la precipitación y fuerte ocupación humana. No obstante el fuego ha sido un mecanismo catalizador del recambio de la vegetación, los mecanismos que promovieron la expansión de incendios permanecen en el campo de la especulación. En el registro de material carbonizado de la Selva Lacandona se

encontró una relación entre la variabilidad de los incendios y su fuente de disturbio (Capítulo 5). Los incendios altamente variables estuvieron asociados con disturbios antropogénicos, mientras que incendios de baja variabilidad reflejaron disturbios asociados a sequías. Sin embargo, se requieren análisis numéricos más robustos que permitan abordar dichas relaciones. También se podría estudiar la sensibilidad de los diferentes tipos de vegetación a los incendios, identificando diferentes morfotipos de material carbonizado en los sedimentos (e.g. Jensen et al. 2007).

Aún queda bastante por hacer antes de poder obtener una comprensión más profunda de la estabilidad, la resiliencia y la recuperación de los ecosistemas montañosos del trópico mexicano. Sin embargo, con los resultados aquí presentados se ha encontrado en la paleoecología una herramienta poderosa para entender el funcionamiento moderno y pasado de los ecosistemas forestales. Así mismo, este tipo de trabajos reduce la distancia en un camino que busca desentrañar los procesos y factores que llevaron a los ecosistemas de montaña a ser como son hoy en día.

## REFERENCIAS

- Adams, R.E.W. 1973. The collapse of maya civilization: a review of previous theories. In: Culbert, T.P. (ed.) *The Classic Maya Collapse*, pp. 21-34. University of New Mexico Press, Albuquerque.
- Adams, R.M. 1961. Changing Patterns of Territorial Organization in the Central Highlands of Chiapas, Mexico. *American Antiquity* 26: 341-360.
- Alcocer, J., Oseguera, L.A., Sánchez, G., González, C.G., Martínez, J.R. & González, R. 2016. Bathymetric and morphometric surveys of the Montebello Lakes, Chiapas. *Journal of Limnology*.
- Alley, R.B., Mayewski, P.A., Sowers, T., Stuiver, M., Taylor, K.C. & Clark, P.U. 1997. Holocene climatic instability: A prominent, widespread event 8200 yr ago.
- Anderson, L. & Wahl, D. 2016. Two Holocene paleofire records from Peten, Guatemala: Implications for natural fire regime and prehispanic Maya land use. *Global and Planetary Change* 138: 82-92.
- Anselmetti, F.S., Ariztegui, D., Hodell, D.A., Hillesheim, M.B., Brenner, M., Gilli, A., McKenzie, J.A. & Mueller, A.D. 2006. Late Quaternary climate-induced lake level variations in Lake Petén Itzá, Guatemala, inferred from seismic stratigraphic analysis. *Palaeogeography, Palaeoclimatology, Palaeoecology* 230: 52-69.
- Anselmetti, F.S., Hodell, D.A., Ariztegui, D., Brenner, M. & Rosenmeier, M.F. 2007. Quantification of soil erosion rates related to ancient Maya deforestation. *Geology* 35: 915-918.
- Arriaga, L., Espinoza, J.M., Aguilar, C., Martínez, E., Gómez, L. & Loa, E. 2000. *Regiones terrestres prioritarias de México*. Comisión Nacional para el Conocimiento y uso de la Biodiversidad, México.
- Baker, M.E. & King, R.S. 2010. A new method for detecting and interpreting biodiversity and ecological community thresholds. *Methods in Ecology and Evolution* 1: 25-37.
- Baker, M.E. & King, R.S. 2013. Of TITAN and straw men: an appeal for greater understanding of community data. *Freshwater Science* 32: 489-506.
- Baker, M.E., King, R.S. & Kahle, D. 2015. TITAN2: Threshold Indicator Taxa Analysis. In: The R Project for Statistical Computing <https://CRAN.R-project.org/package=TITAN2>.
- Battistel, D., Roman, M., Marchetti, A., Kehrwald, N.M., Radaelli, M., Balliana, E., Toscano, G. & Barbante, C. 2018. Anthropogenic impact in the Maya Lowlands of Petén, Guatemala, during the last 5500 years. *Journal of Quaternary Science* 33: 166-176.
- Beach, T., Dunning, N., Luzzadder-Beach, S., Cook, D.E. & Lohse, J. 2006. Impacts of the ancient Maya on soils and soil erosion in the central Maya Lowlands. *CATENA* 65: 166-178.
- Bernal, J.P., Lachniet, M.S., McCulloch, M.T., Mortimer, G., Morales, P. & Cienfuegos, E. 2011. A speleothem record of Holocene climate variability from southwestern Mexico. *Quaternary Research* 75: 104-113.
- Bhattacharya, T., Beach, T. & Wahl, D. 2011. An analysis of modern pollen rain from the Maya lowlands of northern Belize. *Review of Palaeobotany & Palynology* 164: 109-120.

- Bhattacharya, T., Byrne, R., Böhnell, H., Wogau, K., Kienel, U., Ingram, B.L. & Zimmerman, S. 2015. Cultural implications of late Holocene climate change in the Cuenca Oriental, Mexico. *Proceedings of the National Academy of Sciences* 112: 1693-1698.
- Bhattacharya, T. & Chiang, J.C.H. 2014. Spatial variability and mechanisms underlying El Niño-induced droughts in Mexico. *Climate Dynamics* 43: 3309-3326.
- Birks, H.J.B. 2003. Quantitative palaeoenvironmental reconstructions from Holocene biological data. In: Mackay, A., Battarbee, R., Birks, J. & Oldfield, F. (eds.) *Global change in the Holocene*, pp. 107-123. Arnold, London.
- Birks, H.J.B. & Gordon, A.D. 1985. *Numerical Methods in Quaternary Pollen Analysis*. Academic Press, London.
- Blaauw, M. & Christen, J.A. 2011. Flexible paleoclimate age-depth models using an autoregressive gamma process. *Bayesian Anal.* 457-474.
- Bolker, B.M. 2008. *Ecological models and data in R*. Princeton University Press, Princeton, NJ.
- Bond, G., Kromer, B., Beer, J., Muscheler, R., Evans, M.N., Showers, W., Hoffmann, S., Lotti-Bond, R., Hajdas, I. & Bonani, G. 2001. Persistent solar influence on North Atlantic climate during the Holocene. *Science* 294: 2130-2136.
- Bond, G., Showers, W., Cheseby, M., Lotti, R., Almasi, P., Demenocal, P., Priore, P., Cullen, H., Hajdas, I. & Bonani, G. 1997. A pervasive millennial-scale cycle in North Atlantic Holocene and glacial climates. *Science* 278: 1257-1266.
- Bradley, R.S. 2015. *Paleoclimatology: reconstructing climates of the Quaternary*. Elsevier Inc., Oxford, UK.
- Braje, T.J., Dillehay, T.D., Erlandson, J.M., Klein, R.G. & Rick, T.C. 2017. Finding the first Americans. *Science* 358: 592-594.
- Bray, D.B. & Klepeis, P. 2005. Deforestation, Forest Transitions, and Institutions for Sustainability in Southeastern Mexico, 1900-2000. *Environment and History* 11: 195-223.
- Breedlove, D.E. 1981. *Flora of Chiapas, part I: Introduction to the Flora of Chiapas*. The California Academy of Sciences, San Francisco.
- Brenner, M., Rosenmeier, M.F., Hodell, D.A. & Curtis, J.H. 2002. Paleolimnology of the Maya lowlands: long-term perspectives on interactions among, climate, environment and humans. *Ancient Mesoamerica* 13: 141-157.
- Bruijnzeel, L.A., Scatena, F.N. & Hamilton, L.S. 2011. *Tropical Montane Cloud Forests: Science for Conservation and Management*. Cambridge University Press.
- Brun, C. 2011. Anthropogenic indicators in pollen diagrams in eastern France: a critical review. *Vegetation History and Archaeobotany* 20: 135-142.
- Bryant, D. & Clark, J.E. 1983. Los Primeros Mayas Precolombinos de la Cuenca Superior del Río Grijalva. En *Antropología e Historia de los Mixe-Zoques y Mayas: Homenaje a Frans Blom*. In: Ochoa, L. & Lee, T. (eds.), pp. 223-239. Universidad Nacional Autónoma de México and Brigham Young University.
- Bryant, D.D., Clark, J.E. & Cheetham, D. 2005. *Ceramic Sequence of the Upper Grijalva Region, Chiapas, Mexico*. New World Archaeological Foundation, Brigham Young University.
- Bush, M.B. 2002a. Distributional change and conservation on the Andean flank: A palaeoecological perspective. *Global Ecology and Biogeography* 11: 463-467.

- Bush, M.B. 2002b. On the interpretation of fossil Poaceae pollen in the lowland humid neotropics. *Palaeogeography, Palaeoclimatology, Palaeoecology* 177: 5-17.
- Bush, M.B. & Colinvaux, P.A. 1990. A pollen record of a complete glacial cycle from lowland Panama. *Journal of Vegetation Science* 1: 105-119.
- Bush, M.B., Correa-Metrio, A., McMichael, C.H., Sully, S., Shadik, C.R., Valencia, B.G., Guilderson, T., Steinitz-Kannan, M. & Overpeck, J.T. 2016. A 6900-year history of landscape modification by humans in lowland Amazonia. *Quaternary Science Reviews* 141: 52-64.
- Bush, M.B., Moreno, E., De Oliveira, P.E., Asanza, E. & Colinvaux, P.A. 2001. The influence of biogeographic and ecological heterogeneity on Amazonian pollen spectra. *Journal of Tropical Ecology* 17: 729-743.
- Bush, M.B. & Weng, C. 2007. Introducing a new (freeware) tool for palynology. *Journal of Biogeography* 34: 377-380.
- Caballero-Rodríguez, D., Lozano-García, S. & Correa-Metrio, A. 2017. Vegetation assemblages of central Mexico through the late Quaternary: modern analogs and compositional turnover. *Journal of Vegetation Science* 28: 504-514.
- Cardoso, P., Rigal, F., Fattorini, S., Terzopoulou, S. & Borges, P.A.V. 2013. Integrating Landscape Disturbance and Indicator Species in Conservation Studies. *PLoS ONE* 8: e63294.
- Carlson, M.C. 1954. Floral elements of the pine-oak-liquidambar forest of Montebello, Chiapas, Mexico. *Bulletin of the Torrey Botanical Club*: 387-399.
- Carrillo-Bastos, A., Islebe, G.A., Torrescano-Valle, N. & González, N.E. 2010. Holocene vegetation and climate history of central Quintana Roo, Yucatan Peninsula, Mexico. *Review of Palaeobotany & Palynology* 160: 189-196.
- Cayuela, L., Golicher, J., Rey Benayas, J.M., González-Espinosa, M. & Ramírez-Marcial, N. 2006. Fragmentation, disturbance and tree diversity conservation in tropical montane forests. *Journal of Applied Ecology* 43: 1172-1181.
- Cheng, H., Fleitmann, D., Edwards, R.L., Wang, X., Cruz, F.W., Auler, A.S., Mangini, A., Wang, Y., Kong, X., Burns, S.J. & Matter, A. 2009. Timing and structure of the 8.2 kyr B.P. event inferred from  $\delta^{18}\text{O}$  records of stalagmites from China, Oman, and Brazil. *Geology* 37: 1007-1010.
- Clark, J.S. 1988. Particle motion and the theory of charcoal analysis: source area, transport, deposition, and sampling. *Quaternary Research* 30: 67-80.
- Cleveland, W.S. & Devlin, S.J. 1988. Locally weighted regression: An approach to regression analysis by local fitting. *Journal of the American Statistical Association* 83: 596-610.
- Colinvaux, P., de Olivera, P.E. & Moreno, P.J.E. 1999a. *Amazon Pollen Manual and Atlas*. Harwood Academic Publishers, Amsterdam.
- Colinvaux, P.A., De Oliveira, P.E. & Moreno, J.E. 1999b. *Amazon pollen manual and atlas*. Harwood Academic Press., New York.
- CONABIO 2013. *La biodiversidad en Chiapas: Estudio de Estado*, Mexico.
- Conroy, J.L., Overpeck, J.T., Cole, J.E., Shanahan, T.M. & Steinitz-Kannan, M. 2008. Holocene changes in eastern tropical Pacific climate inferred from a Galápagos lake sediment record. *Quaternary Science Reviews* 27: 1166-1180.
- Correa-Metrio, A. & Bush, M.B. 2012. *The late Quaternary in the Central American lowlands. An 86,000-year-long history of regional environmental response to global*

- climate change*. LAP LAMBERT Academic Publishing GmbH & Co. KG, Saarbrücken, Deutschland.
- Correa-Metrio, A., Bush, M.B., Cabrera, K.R., Sully, S., Brenner, M., Hodell, D.A., Escobar, J. & Guilderson, T. 2012a. Rapid climate change and no-analog vegetation in lowland Central America during the last 86,000 years. *Quaternary Science Reviews* 38: 63-75.
- Correa-Metrio, A., Bush, M.B., Hodell, D.A., Brenner, M., Escobar, J. & Guilderson, T. 2012b. The influence of abrupt climate change on the ice-age vegetation of the Central American lowlands. *Journal of Biogeography* 39: 497-509.
- Correa-Metrio, A., Bush, M.B., Lozano-García, M.S. & Sosa-Nájera, S. 2013. Millennial-scale temperature change velocity in the continental northern Neotropics. *PLoS ONE* 8: e81958.
- Correa-Metrio, A., Bush, M.B., Pérez, L., Schwalb, A. & Cabrera, K.R. 2011. Pollen distribution along climatic and biogeographic gradients in northern Central America. *The Holocene* 21: 681-692.
- Correa-Metrio, A., Cabrera, K.R. & Bush, M.B. 2010. Quantifying ecological change through Discriminant Analysis: a paleoecological example from the Peruvian Amazon. *Journal of Vegetation Science* 21: 695-704.
- Correa-Metrio, A., Dechnik, Y., Lozano-García, M.S. & Caballero, M. 2014. Detrended correspondence analysis: A useful tool to quantify ecological change from fossil data sets. *Boletín de la Sociedad Geológica Mexicana* 66: 135-143.
- Correa-Metrio, A., Lozano-García, M.S., Xeltzuantzi, S. & Sosa-Nájera, M.S. 2012c. Vegetation in western central Mexico during the last 50 000 years: modern analogs and climate in Zacapu Basin. *Journal of Quaternary Science* 27: 509-518.
- Correa - Metrio, A., Vélez, M., Escobar, J., St - Jacques, J.M., López - Pérez, M., Curtis, J. & Cosford, J. 2016. Mid - elevation ecosystems of Panama: future uncertainties in light of past global climatic variability. *Journal of Quaternary Science* 31: 731-740.
- Curtis, J.H., Brenner, M., Hodell, D.A., Balsler, R.A., Islebe, G.A. & Hooghiemstra, H. 1998. A multi-proxy study of Holocene environmental change in the Maya lowlands of Peten, Guatemala. *Journal of Paleolimnology* 19: 139-159.
- Curtis, J.H. & Hodell, D.A. 1996. Climate variability on the Yucatan Peninsula (Mexico) during the past 3500 years, and implications for Maya cultural evolution. *Quaternary Research* 46: 37-47.
- Dearing, J.A. 2006. Climate-human-environment interactions: resolving our past. *Clim. Past* 2: 187-203.
- Deevey, E.S., Rice, D.S., Rice, P.M., Vaughan, H.H., Brenner, M. & Flannery, M.S. 1979. Mayan urbanism: impact on a tropical karst environment. *Science*: 298-306.
- Deevey, K.A., Brenner, M., Flannery, M.S. & Yezdani, G.H. 1980. Lakes Yaxha and Scanab, Peten, Guatemala: limnology and hydrology. *Archives of Hydrobiology* 57: 419-460.
- Delcourt, H.R. & Delcourt, P.A. 1991. *Quaternary Ecology: A paleoecological perspective*. Chapman & Hall, Cornwall, UK.
- Demarest, A. 2004. *Ancient Maya: The Rise and Fall of a Rainforest Civilization*. Cambridge University Press.
- deMenocal, P.B. 2001. Cultural Responses to Climate Change During the Late Holocene. *Science* 292: 667-673.

- Díaz, K.A., Pérez, L., Correa-Metrio, A., Franco-Gaviria, J.F., Echeverría, P., Curtis, J. & Brenner, M. 2017. Holocene environmental history of tropical, mid-altitude Lake Ocotitalito, México, inferred from ostracodes and non-biological indicators. *The Holocene* 27: 1308-1317.
- Domínguez-Vásquez, G. & Islebe, G.A. 2008. Protracted drought during the late Holocene in the Lacandon rain forest, Mexico. *Vegetation History and Archaeobotany* 17: 327-333.
- Domínguez-Vásquez, G., Islebe, G.A. & Villanueva-Gutiérrez, R. 2004. Modern pollen deposition in Lacandon forest, Chiapas, Mexico. *Review of Palaeobotany & Palynology* 131: 105-116.
- Douglas, P.M.J., Pagani, M., Canuto, M.A., Brenner, M., Hodell, D.A., Eglinton, T.I. & Curtis, J.H. 2015. Drought, agricultural adaptation, and sociopolitical collapse in the Maya Lowlands. *Proceedings of the National Academy of Sciences* 112: 5607-5612.
- Dufrene, M. & Legendre, P. 1997. Species assemblages and indicator species: the need for a flexible asymmetrical approach. *Ecological monographs* 67: 345-366.
- Dufrêne, M. & Legendre, P. 1997. SPECIES ASSEMBLAGES AND INDICATOR SPECIES: THE NEED FOR A FLEXIBLE ASYMMETRICAL APPROACH. *Ecological Monographs* 67: 345-366.
- Dull, R.A. 2004a. An 8000-yr record of vegetation, climate, and human disturbance from the Sierra de Apaneca, El Salvador. *Quaternary Research* 61: 159-167.
- Dull, R.A. 2004b. A Holocene record of Neotropical savanna dynamics from El Salvador. *Journal of Paleolimnology* 32: 219-231.
- Dunning, N.P. & Kowalski, J.K. 1994. LORDS OF THE HILLS: Classic Maya settlement patterns and political iconography in the Puuc region, Mexico. *Ancient Mesoamerica* 5: 63-95.
- Ellis, E.C., Kaplan, J.O., Fuller, D.Q., Vavrus, S., Klein Goldewijk, K. & Verburg, P.H. 2013. Used planet: A global history. *Proceedings of the National Academy of Sciences* 110: 7978-7985.
- Espadas-Manrique, C., Durán, R. & Argáez, J. 2003. Phytogeographic analysis of taxa endemic to the Yucatan Peninsula using geographic information systems, the domain heuristic methods and parsimony analysis of endemism. *Diversity and Distributions* 9: 313-330.
- Estrada-Loera, E. 1991. Phytogeographic relationships of the Yucatan Peninsula. *Journal of Biogeography* 18: 687-697.
- Eugster, H.P. & Hardie, L.A. 1978. Lakes, Chemistry, Geology, Physics. In: Lerman, A. (ed.) *Saline lakes*. Springer, Berlin.
- Evans, N.P., Bauska, T.K., Gázquez-Sánchez, F., Brenner, M., Curtis, J.H. & Hodell, D.A. 2018. Quantification of drought during the collapse of the classic Maya civilization. *Science* 361: 498-501.
- Faegri, K. & Iversen, J. 1989. *Textbook of pollen analysis*. 4th ed. Wiley, Chichester.
- Faith, D.P., Minchin, P.R. & Belbin, L. 1987. Compositional dissimilarity as a robust measure of ecological distance. In: Prentice, I.C. & van der Maarel, E. (eds.) *Theory and models in vegetation science: Proceedings of Symposium, Uppsala, July 8-13, 1985*, pp. 57-68. Springer Netherlands, Dordrecht.
- Farjon, A. & Styles, B.T. 1997. Pinus (Pinaceae). *Flora Neotropica* 75: 1-291.

- Felde, V.A., Peglar, S.M., Bjune, A.E., Grytnes, J.-A. & Birks, H.J.B. 2014. The relationship between vegetation composition, vegetation zones and modern pollen assemblages in Setesdal, southern Norway. *The Holocene* 24: 985-1001.
- Ferguson, W.M. & Adams, R.E.W. 2001. *Mesoamerica's Ancient Cities: Aerial Views of Pre-Columbian Ruins in Mexico, Guatemala, Belize, and Honduras*. University of New Mexico Press.
- Figueroa-Rangel, B.L., Willis, K.J. & Olvera-Vargas, M. 2010. Cloud forest dynamics in the Mexican Neotropics during the last 1300 years. *Global Change Biology* 16: 1689-1704.
- Ford, A. & Nigh, R. 2009. Origins of the Maya Forest Garden: Maya resource management. *Journal of Ethnobiology* 29: 213-236.
- Franco-Gaviria, F., Caballero-Rodríguez, D., Correa-Metrio, A., Pérez, L., Schwalb, A., Cohuo, S. & Macario-González, L. 2018a. The human impact imprint on the modern pollen spectra of the Maya lands. *Boletín de la Sociedad Geológica Mexicana* 70: 61-78.
- Franco-Gaviria, F., Correa-Metrio, A., Cordero-Oviedo, C., López-Pérez, M., Cárdenes-Sandí, G.M. & Romero, F.M. 2018b. Effects of late Holocene climate variability and anthropogenic stressors on the vegetation of the Maya highlands. *Quaternary Science Reviews* 189: 76-90.
- Gaillard, M.-J., Kleinen, T., Samuelsson, P., Nielsen, A., Bergh, J., Kaplan, J., Poska, A., Sandström, C., Strandberg, G., Trondman, A.-K. & Wramneby, A. 2015. Causes of Regional Change—Land Cover. In: The, B.I.I.A.T. (ed.) *Second Assessment of Climate Change for the Baltic Sea Basin*, pp. 453-477. Springer International Publishing.
- García, E. 1998. Climas (Clasificación de Köppen, modificado por García). In: Comisión Nacional para el Conocimiento y Uso de la Biodiversidad (CONABIO), México.
- Gauch, H.G., Jr. 1982. *Multivariate analysis in community ecology*. Cambridge University Press, Cambridge.
- Gentry, A.H. 1982. Neotropical floristic diversity: Phytogeographical connections between Central and South America, Pleistocene climatic fluctuations, or an accident of the Andean orogeny? *Annals of the Missouri Botanical Garden* 69: 557-593.
- Goman, M. & Byrne, R. 1998. A 5000-year record of agriculture and tropical forest clearance in the Tuxtlas, Veracruz, Mexico. *The Holocene* 8: 83-89.
- González-Espinosa, M., Quintana-Ascencio, P., Ramírez-Marcial, N. & Gaytán-Guzmán, P. 1991. Secondary Succession in Disturbed Pinus-Quercus Forests in the Highlands of Chiapas, Mexico. *Journal of Vegetation Science* 2: 351-360.
- Gornitz, V. 2009. *Encyclopedia of Paleoclimatology and Ancient Environments*. Springer.
- Graham, A. 2010. *A natural history of the New World: the ecology and evolution of plants in the Americas*. University of Chicago Press, Chicago.
- Hall, S.A. 1981. Deteriorated pollen grains and the interpretation of quaternary pollen diagrams. *Review of Palaeobotany and Palynology* 32: 193-206.
- Hamilton, L.S., Juvik, J.O. & Scatena, F.N. 1995. *Tropical montane cloud forests*. Springer-Verlag.
- Hansen, E.F., Rodríguez-Navarro, C. & Hansen, R.D. 2011. Incipient Maya Burnt-Lime Technology: Characterization and Chronological Variations in Preclassic Plaster, Stucco and Mortar at Nakbe, Guatemala. *MRS Proceedings* 462.

- Haug, G.H., Gunther, D., Peterson, L.C., Sigman, D.M., Hughen, K.A. & Aeschlimann, B. 2003. Climate and the collapse of Maya civilization. *Science* 299: 1731-1734.
- Haug, G.H., Hughen, K.A., Sigman, D.M., Peterson, L.C. & Rohl, U. 2001. Southward migration of the Intertropical Convergence Zone through the Holocene. *Science* 293: 1304-1308.
- Hernández-Nava, J. 2003. Áreas de protección de flora y fauna de Nahá y Metzabok. Chiapas, México: Ficha informativa de los humedales de Ramsar. In.
- Hicks, S. & Birks, H.J.B. 1996. Numerical analysis of modern and fossil pollen spectra as a tool for elucidating the nature of fine-scale human activities in boreal areas. *Vegetation History and Archeobotany* 5: 257-272.
- Hijmans, R.J., Cameron, S.E., Parra, J.L., Jones, P.G. & Jarvis, A. 2005. Very high resolution interpolated climate surfaces for global land areas. *International Journal of Climatology* 25: 1965-1978.
- Hill, M.O. & Gauch, H.G. 1980. Detrended correspondence analysis: an improved ordination technique. *Vegetatio* 42: 41-58.
- Hillesheim, M.B., Hodell, D.A., Leyden, B.W., Brenner, M., Curtis, J.H., Anselmetti, F.S., Ariztegui, D., Buck, D.G., Guilderson, T.P., Rosenmeier, M.F. & Schnurrenberger, D.W. 2005. Climate change in lowland Central America during the late deglacial and early Holocene. *Journal of Quaternary Science* 20: 363-376.
- Hodell, D.A., Anselmetti, F.S., Ariztegui, D., Brenner, M., Curtis, J.H., Gilli, A., Grzesik, A., Guilderson, T.J., Müller, A.D., Bush, M.B., Correa-Metrio, A., Escobar, J. & Kutterolf, S. 2008. An 85-ka record of climate change in lowland Central America. *Quaternary Science Reviews* 27: 1152-1165.
- Hodell, D.A., Brenner, M. & Curtis, J.H. 2007. Climate and cultural history of the Northeastern Yucatan Peninsula, Quintana Roo, Mexico. *Climatic Change* 83: 215-240.
- Hodell, D.A., Brenner, M. & Curtis, J.H. 2005a. Terminal Classic drought in the northern Maya lowlands inferred from multiple sediment cores in Lake Chichancanab (Mexico). *Quaternary Science Reviews* 24: 1413-1427.
- Hodell, D.A., Brenner, M., Curtis, J.H. & Guilderson, T. 2001. Solar forcing of drought frequency in the Maya lowlands. *Science* 292: 1367-1370.
- Hodell, D.A., Brenner, M., Curtis, J.H., Medina-González, R., Ildefonso-Chan Can, E., Albornaz-Pat, A. & Guilderson, T.P. 2005b. Climate change on the Yucatan Peninsula during the Little Ice Age. *Quaternary Research* 63: 109-121.
- Hodell, D.A., Curtis, J.H. & Brenner, M. 1995. Possible role of climate in the collapse of ancient Maya civilization. *Nature* 357: 391-394.
- Hodell, D.A., Turchyn, A.V., Wiseman, C.J., Escobar, J., Curtis, J.H., Brenner, M., Gilli, A., Mueller, A.D., Anselmetti, F., Ariztegui, D. & Brown, E.T. 2012. Late Glacial temperature and precipitation changes in the lowland Neotropics by tandem measurement of  $\delta^{18}\text{O}$  in biogenic carbonate and gypsum hydration water. *Geochimica et Cosmochimica Acta* 77: 352-368.
- Ibarra-Manríquez, G. & Oyama, K. 1992. Ecological correlates of reproductive traits of Mexican rain forest trees. *American Journal of Botany* 79: 383-394.
- Ibarra-Manríquez, G., Villaseñor, J.L., Durán, R. & Meave, J. 2002. Biogeographical analysis of the tree flora of the Yucatan Peninsula. *Journal of Biogeography* 29: 17-29.

- Islebe, G.A., Calmé, S., León-Cortés, J.L. & Schmook, B. 2015. *Biodiversity and Conservation of the Yucatán Peninsula*. Springer International Publishing.
- Islebe, G.A. & Hooghiemstra, H. 1997. Vegetation and climate history of montane Costa Rica since the last glacial. *Quaternary Science Reviews* 16: 589-604.
- Islebe, G.A., Hooghiemstra, H., Brenner, M., Curtis, J.H. & Hodell, D.A. 1996. A Holocene vegetation history from lowland Guatemala. *The Holocene* 6: 265-271.
- Islebe, G.A., Villanueva-Gutiérrez, R. & Sánchez-Sánchez, O. 2001. Relación lluvia de pollen-vegetación en Selvas de Quinatan Roo. *Boletín de la Sociedad Botánica de México* 69: 29-36.
- Jensen, K., Lynch, E.A., Calcote, R. & Hotchkiss, S.C. 2007. Interpretation of charcoal morphotypes in sediments from Ferry Lake, Wisconsin, USA: do different plant fuel sources produce distinctive charcoal morphotypes? *The Holocene* 17: 907-915.
- Johnsen, S.J., Dahl-Jensen, D., Gundestrup, N., Steffensen, J.P., Clausen, H.B., Miller, H., Masson-Delmotte, V., Sveinbjörnsdóttir, A.E. & White, J. 2001. Oxygen isotope and palaeotemperature records from six Greenland ice-core stations: Camp Century, Dye-3, GRIP, GISP2, Renland and NorthGRIP. *Journal of Quaternary Science* 16: 299-307.
- Juggins, S. 2007. C2. In, pp. Software for ecological and palaeoecological data analysis and visualisation, Newcastle, England.
- Konfirst, M.A., Kuhn, G., Monien, D. & Scherer, R.P. 2011. Correlation of Early Pliocene diatomite to low amplitude Milankovitch cycles in the ANDRILL AND-1B drill core. *Marine Micropaleontology* 80: 114-124.
- Kovalenko, K.E., Brady, V.J., Brown, T.N., Ciborowski, J.J.H., Danz, N.P., Gathman, J.P., Host, G.E., Howe, R.W., Johnson, L.B., Niemi, G.J. & Reavie, E.D. 2014. Congruence of community thresholds in response to anthropogenic stress in Great Lakes coastal wetlands. *Freshwater Science* 33: 958-971.
- Krukowski, S.T. 1988. Sodium metatungstate; a new heavy-mineral separation medium for the extraction of conodonts from insoluble residues. *Journal of Paleontology* 62: 314-316.
- Kylander, M.E., Ampel, L., Wohlfarth, B. & Veres, D. 2011. High - resolution X - ray fluorescence core scanning analysis of Les Echets (France) sedimentary sequence: new insights from chemical proxies. *Journal of Quaternary Science* 26: 109-117.
- Lachniet, M.S., Burns, S.J., Piperno, D.R., Asmerom, Y., Polyak, V.J., Moy, C.M. & Christenson, K. 2004. A 1500-year El Niño/Southern Oscillation and rainfall history for the Isthmus of Panama from speleothem calcite. *Journal of Geophysical Research: Atmospheres* 109: n/a-n/a.
- Legendre, P. & Legendre, L. 1998. *Numerical Ecology*. Elsevier Scientific, Oxford.
- Lentz, D.L. & Hockaday, B. 2009. Tikal timbers and temples: ancient Maya agroforestry and the end of time. *Journal of Archaeological Science* 36: 1342-1353.
- Leyden, B.W. 1984. Guatemalan forest synthesis after Pleistocene aridity. *Proceedings of the National Academy of Sciences USA* 81: 4856-4859.
- Leyden, B.W. 1987. Man and climate in the Maya lowlands. *Quaternary Research* 28: 407-414.
- Leyden, B.W. 2002. Pollen evidence for climatic variability and cultural disturbance in the Maya lowlands. *Ancient Mesoamerica* 13: 85-101.

- Leyden, B.W., Brenner, M., Hodell, D.A. & Curtis, J.A. 1993. Late Pleistocene climate in the Central American lowlands. *Geophysical Monograph* 78: 165-178.
- Li, J., Zhao, Y., Xu, Q., Zheng, Z., Lu, H., Luo, Y., Li, Y., Li, C. & Seppä, H. 2014. Human influence as a potential source of bias in pollen-based quantitative climate reconstructions. *Quaternary Science Reviews* 99: 112-121.
- Loveland, T.R., Reed, B.C., Brown, J.F., Ohlen, D.O., Zhu, Z., Yang, L. & Merchant, J.W. 2000. Development of a global land cover characteristics database and IGBP DISCover from 1 km AVHRR data. *International Journal of Remote Sensing* 21: 1303-1330.
- Lowemark, L., Chen, H.F., Yang, T.N., Kylander, M., Yu, E.F., Hsu, Y.W., Lee, T.Q., Song, S.R. & Jarvis, S.W. 2011. Normalizing XRF-scanner data: A cautionary note on the interpretation of high-resolution records from organic-rich lakes. *Journal of Asian Earth Sciences* 40: 1250-1256.
- Lozano-Garcia, M.S., Caballero-Miranda, M., Ortega-Guerrero, B., Rodríguez, A. & Sosa-Najera, M.S. 2007. Tracing the effects of the Little Ice Age in the tropical lowlands of eastern Mesoamerica. *PNAS* 104: 16200-16203.
- Lozano-Garcia, M.S. & Xelhuantzi-López, M.S. 1997. Some problems with the late Quaternary pollen records of Central Mexico: Basins of Mexico and Zacapu. *Quaternary International* 43/44: 117-123.
- Magaña, V., Amador, J.A. & Medina, S. 1999. The midsummer drought over Mexico and Central America. *Journal of Climate* 12: 1577-1588.
- Magaña, V.O., Vázquez, J.L., Pérez, J.L. & Pérez, J.B. 2003. Impact of El Niño on precipitation in Mexico. *Geofísica Internacional* 42: 313-330.
- Marchant, R., Almeida, L., Behling, H., Berrio, J.C., Bush, M., Cleef, A., Duivenvoorden, J., Kappelle, M., de Oliveira, P., de Oliveira-Filho, A.T., Lozano-Garcia, S., Hooghiemstra, H., Ledru, M.-P., Ludlow-Wiechers, B., Markgraf, V., Mancini, V., Paez, M., Preto, A., Rangel, O. & Salgado-Labouriau, M.L. 2002. Distribution and ecology of parent taxa of pollen lodged within the Latin American Pollen Database. *Review of Palaeobotany and Palynology* 121: 1-75.
- Martínez-Icó, M., Cetzal-Ix, W., Noguera-Savelli, E. & Hernández-Juárez, R. 2015. Flora vascular de la comunidad de Bazom, Los Altos de Chiapas, México. *Botanical Sciences* 93: 53-72.
- Mayewski, P.A., Rohling, E.E., Stager, J.C., Karlén, W., Maasch, K.A., Meeker, L.D., Meyerson, E.A., Gasse, F., van Kreveland, S., Holmgren, K., Lee-Thorp, J., Rosqvist, G., Rack, F. & Staubwasser, M. 2004. Holocene climate variability. *Quaternary Research* 62: 243-255.
- Mazier, F., Galop, D., Brun, C. & Buttler, A. 2006. Modern pollen assemblages from grazed vegetation in the western Pyrenees, France: a numerical tool for more precise reconstruction of past cultural landscapes. *The Holocene* 16: 91-103.
- McCune, B., Grace, J.B. & Urban, D.L. 2002. *Analysis of ecological communities*. MjM software design Gleneden Beach, OR.
- McNeil, C.L. 2012. Deforestation, agroforestry, and sustainable land management practices among the Classic period Maya. *Quaternary International* 249: 19-30.
- McNeil, C.L., Burney, D.A. & Burney, L.P. 2010. Evidence disputing deforestation as the cause for the collapse of the ancient Maya polity of Copan, Honduras. *Proceedings of the National Academy of Sciences* 107: 1017-1022.

- Meave, J. & Kellman, M. 1994. Maintenance of rain forest diversity in riparian forests of tropical savannas: implications for species conservation during Pleistocene drought. *Journal of Biogeography* 21: 121-135.
- Medina-Elizalde, M., Burns, S.J., Lea, D.W., Asmerom, Y., von Gunten, L., Polyak, V., Vuille, M. & Karmalkar, A. 2010. High resolution stalagmite climate record from the Yucatan Peninsula spanning the Maya terminal classic period. *Earth and Planetary Science Letters* 298: 255-262.
- Meltzer, D.J. 1997. Monte Verde and the Pleistocene Peopling of the Americas. *Science* 276: 754-755.
- Méndez, M. & Magaña, V. 2010. Regional Aspects of Prolonged Meteorological Droughts over Mexico and Central America. *Journal of Climate* 23: 1175-1188.
- Mestas-Núñez, A.M., Enfield, D.B. & Zhang, C. 2007. Water vapor fluxes over the Intra-Americas Sea: Seasonal and interannual variability and associations with rainfall. *Journal of Climate* 20: 1910-1922.
- Metcalfe, S., Breen, A., Murray, M., Furley, P., Fallick, A. & McKenzie, A. 2009. Environmental change in northern Belize since the latest Pleistocene. *Journal of Quaternary Science* 24: 627-641.
- Miranda, F. & Hernández, E. 1963. Los tipos de vegetación de México y su clasificación. *Boletín de la Sociedad Botánica de México* 28: 29-179.
- Moreno-Mayar, J.V., Potter, B.A., Vinner, L., Steinrücken, M., Rasmussen, S., Terhorst, J., Kamm, J.A., Albrechtsen, A., Malaspina, A.-S., Sikora, M., Reuther, J.D., Irish, J.D., Malhi, R.S., Orlando, L., Song, Y.S., Nielsen, R., Meltzer, D.J. & Willerslev, E. 2018. Terminal Pleistocene Alaskan genome reveals first founding population of Native Americans. *Nature* 553: 203.
- Moy, C.M., Seltzer, G.O., Rodbell, D.T. & Anderson, D.M. 2002. Variability of El Niño/Southern Oscillation activity at millennial timescales during the Holocene epoch. *Nature* 420: 162-165.
- Mueller, A.D., Islebe, G.A., Anselmetti, F., Aristegui, D., Brenner, M., Hodell, D.A., Hajdas, I., Hamann, Y., Haug, G.H. & Kennett, D.J. 2010. Recovery of the forest ecosystem in the tropical lowlands of northern Guatemala after disintegration of classic Maya polities. *Geology* 38: 523-526.
- Mueller, A.D., Islebe, G.A., Hillesheim, M.B., Grzesik, D.A., Anselmetti, F.S., Ariztegui, D., Brenner, M., Curtis, J.H., Hodell, D.A. & Venz, K.A. 2009. Climate drying and associated forest decline in the lowlands of northern Guatemala during the Holocene. *Quaternary Research* 71: 133-141.
- Müllerried, F. 1957. *La geología de Chiapas, Gobierno Constitucional del estado de Chiapas*.
- Nations, J.D. 2010. *The Maya Tropical Forest: People, Parks, and Ancient Cities*. University of Texas Press.
- Navarrete, C. 2006. El complejo escénico de Chinkuntic, Chiapas.in. In: *XX Simposio de Investigaciones Arqueológicas en Guatemala*, Museo Nacional de Arqueología y Etnología, Guatemala City.
- Nigh, R. & Diemont, S.A.W. 2013. The Maya Milpa: fire and the legacy of living soil. *Frontiers in Ecology and the Environment* 11: 45-54.
- Nixon, K.C. 2006. Global and neotropical distribution and diversity of oak (genus *Quercus*) and oak forests. In: Kappelle, M. (ed.) *Ecology and conservation of neotropical montane oak forests*, pp. 4-13. Springer, Berlin Heidelberg.

- Oksanen, J., Blanchet, G., Kindt, R., Legendre, P., O'Hara, B., Simpson, G.L., Solymos, P., Stevens, M.H.H. & Wagner, H. 2017. vegan: Community Ecology Package. In. The R Project for Statistical Computing. <http://CRAN.R-project.org/package=vegan>.
- Ortega-Gutiérrez, F., Mitre-Salazar, L.M., J., R.-Q., Aranda-Gómez, J.J., Morán-Zenteno, D., Alaniz-Álvarez, S.A. & Nieto-Samaniego, A.F. 1992. Texto explicativo de la quinta edición de la carta geológica de la República Mexicana escala 1:2'000,000: Universidad Nacional Autónoma de México, Instituto de Geología y SEMIP Consejo de Recursos Minerales. . In.
- Overpeck, J.T., Webb, T.I. & Prentice, I.C. 1985. Quantitative interpretation of fossil pollen spectra: Dissimilarity coefficients and the method of modern analogs. *Quaternary Research* 23: 87-708.
- Padilla-Sánchez, R.J. 2007. Evolución geológica del sureste mexicano desde el Mesozoico al presente en el contexto regional del Golfo de México. *Boletín de la Sociedad Geológica Mexicana*.
- Paillard, D., Labeyrie, L. & Yiou, P. 1996. Macintosh program performs time-series analysis. *Eos Trans. AGU* 77: 379.
- Palacios-Chávez, R., Ludlow-Wiechers, B. & G, V.G.V. 1991. *Flora palinológica de la Reserva de la Biosfera de Sian Ka'an, Quintana Roo, México*. Centro de Investigaciones de Quintana Roo.
- Palka, J.W. 2009. Historical Archaeology of Indigenous Culture Change in Mesoamerica. *J Archaeol Res* 17: 297-346.
- Palka, J.W. 2014. *Maya Pilgrimage to Ritual Landscapes: Insights from Archaeology, History, and Ethnography*. University of New Mexico Press.
- Pennington, T.D. & Sarukhán, J. 2005. *Árboles tropicales de México : manual para la identificación de las principales especies*. UNAM.
- Piperno, D.R. 2006. Quaternary environmental history and agricultural impact on vegetation in Central America. *Annals of the Missouri Botanical Garden* 93: 274-296.
- Piperno, D.R. & Flannery, K.V. 2001. The earliest archaeological maize (*Zea mays* L.) from highland Mexico: new accelerator mass spectrometry dates and their implications. *Proceedings of the National Academy of Sciences* 98: 2101-2103.
- Pohl, M.D., Pope, K.O., Jones, J.G., Jacob, J.S., Piperno, D.R., deFrance, S.D., Lentz, D.L., Gifford, J.A., Danforth, M.E. & Josserand, J.K. 1996. Early Agriculture in the Maya Lowlands. *Latin American Antiquity* 7: 355-372.
- Pope, K.O., Pohl, M.E.D., Jones, J.G., Lentz, D.L., von Nagy, C., Vega, F.J. & Quitmyer, I.R. 2001. Origin and environmental setting of ancient agriculture in the lowlands of mesoamerica. *Science* 292: 1370-1373.
- Quintana-Ascencio, P.F., Gonzalez-Espinosa, M., Ramirez-Marcial, N., Dominguez-Vazquez, G. & Martinez-Ico, M. 1996. Soil Seed Banks and Regeneration of Tropical Rain Forest from Milpa Fields at the Selva Lacandona, Chiapas, Mexico. *Biotropica* 28: 192-209.
- R Core Team 2017. R: A Language and Environment for Statistical Computing. In. R Foundation for Statistical Computing, Vienna, Austria. <http://www.R-project.org/>.
- Ramírez-Marcial, N. 2003. Survival and growth of tree seedlings in anthropogenically disturbed Mexican montane rain forests. *Journal of Vegetation Science* 14: 881-890.

- Ramirez-Marcial, N., González-Espinosa, M., Camacho-Cruz, A. & Ortiz-Aguilar, D. 2010. Forest Restoration in Lagunas de Montebello National Park, Chiapas, Mexico. *Ecological Restoration* 28: 354-360.
- Ramirez-Marcial, N., González-Espinosa, M. & Williams-Linera, G. 2001. Anthropogenic disturbance and tree diversity in Montane Rain Forests in Chiapas, Mexico. *Forest Ecology and Management* 154: 311-326.
- Rasband, W.S. 2005. ImageJ version 1.32j. In: National Institute of Health, USA, Bethesda.
- Ray, D.K., Gerber, J.S., MacDonald, G.K. & West, P.C. 2015. Climate variation explains a third of global crop yield variability. *Nature Communications* 6: 5989.
- Reimer, P.J., Bard, E., Bayliss, A., Beck, J.W., Blackwell, P.G., Bronk Ramsey, C., Buck, C.E., Cheng, H., Edwards, R.L., Friedrich, M., Grootes, P.M., Guilderson, T.P., Hafliadason, H., Hajdas, I., Hatté, C., Heaton, T.J., Hoffmann, D.L., Hogg, A.G., Hughen, K.A., Kaiser, K.F., Kromer, B., Manning, S.W., Niu, M., Reimer, R.W., Richards, D.A., Scott, E.M., Southon, J.R., Staff, R.A., Turney, C.S.M. & van der Plicht, J. 2013. IntCal13 and Marine13 radiocarbon age calibration curves 0-50,000 years cal BP. *Radiocarbon* 55: 1869-1887.
- Reitalu, T., Seppä, H., Sugita, S., Kangur, M., Koff, T., Avel, E., Kihno, K., Vassiljev, J., Renssen, H., Hammarlund, D., Heikkilä, M., Saarse, L., Poska, A. & Veski, S. 2013. Long-term drivers of forest composition in a boreonemoral region: the relative importance of climate and human impact. *Journal of Biogeography* 40: 1524-1534.
- Roberts, N. 1998. *The Holocene: An Environmental History*. Wiley.
- Rodgers, J.C. & Horn, S.P. 1996. Modern pollen spectra from Costa Rica. *Palaeogeography, Palaeoclimatology, Palaeoecology* 124: 53-71.
- Rodrigues, M.E., de Oliveira Roque, F., Quintero, J.M.O., de Castro Pena, J.C., de Sousa, D.C. & De Marco Junior, P. 2016. Nonlinear responses in damselfly community along a gradient of habitat loss in a savanna landscape. *Biological Conservation* 194: 113-120.
- Romero-Centeno, R., Zavala-Hidalgo, J., Gallegos, A. & O'Brien, J.J. 2003. Isthmus of Tehuantepec Wind Climatology and ENSO Signal. *Journal of Climate* 16: 2628-2639.
- Rosenmeier, M.F., Hodell, D.A., Brenner, M., Curtis, J.H. & Guilderson, T.P. 2002. A 4000-Year Lacustrine Record of Environmental Change in the Southern Maya Lowlands, Petén, Guatemala. *Quaternary Research* 57: 183-190.
- Rothwell, R.G. & Croudace, I.W. 2015. Twenty Years of XRF Core Scanning Marine Sediments: What Do Geochemical Proxies Tell Us? In: Croudace, I.W. & Rothwell, R.G. (eds.) *Micro-XRF Studies of Sediment Cores: Applications of a non-destructive tool for the environmental sciences*, pp. 25-102. Springer Netherlands, Dordrecht.
- Roubik, D.W. & Moreno, P.J.E. 1991. *Pollen and Spores of Barro Colorado Island*. Monographs in Systematic Botany 36, Missouri Botanical Garden.
- Rzedowski, J. 2006. *Vegetación de México*. 1ra. Edición digital ed. Comisión Nacional para el Conocimiento y Uso de la Biodiversidad, México D.F.
- Sanderson, E.W., Jaiteh, M., Levy, M.A., Redford, K.H., Wannebo, A.V. & Woolmer, G. 2002. The Human Footprint and the Last of the Wild: The human footprint is a global map of human influence on the land surface, which suggests that human beings are stewards of nature, whether we like it or not. *BioScience* 52: 891-904.

- Schüpbach, S., Kirchgeorg, T., Colombaroli, D., Beffa, G., Radaelli, M., Kehrwald, N.M. & Barbante, C. 2015. Combining charcoal sediment and molecular markers to infer a Holocene fire history in the Maya Lowlands of Petén, Guatemala. *Quaternary Science Reviews* 115: 123-131.
- Sharer, R.J. & Traxler, L.P. 2006. *The Ancient Maya*. Stanford University Press.
- Silverman, B.W. 1986. *Density estimation for statistics and data analysis*. Chapman and Hall, London.
- Tejada-Cruz, C., Naranjo, E.J., Cuarón, A.D., Perales, H. & Cruz-Burguete, J.L. 2009. Habitat use of wild ungulates in fragmented landscapes of the Lacandon Forest, Southern Mexico. *Mammalia* 73: 211-219.
- Trenberth, K.E. 1997. The definition of El Niño. *Bulletin of the American Meteorological Society* 78: 2771-2777.
- Udvardy, M. 1975. A classification of the biogeographical provinces of the world. Morges (Switzerland): International Union of Conservation of Nature and Natural Resources. *IUCN Occasional Paper*.
- UNHCR 2001. La integración de refugiados Guatemaltecos en Chiapas. In.
- van't Veer, R. & Hooghiemstra, H. 2000. Montane forest evolution during the last 650 000 yr in Colombia: a multivariate approach based on pollen record Funza-I. *Journal of Quaternary Science* 15: 329-346.
- Vazquez-Molina, Y., Correa-Metrio, A., Zawisza, E., Franco-Gaviria, F., Pérez, L., Romero, F., Prado, B., Charqueño-Celis, F. & Esperón-Rodríguez, M. 2016. Decoupled lake history and regional moisture availability in the middle elevations of tropical Mexico. *Revista Mexicana de Ciencias Geológicas*. 355-364.
- Velez, M.I., Curtis, J.H., Brenner, M., Escobar, J., Leyden, B.W. & Popeone de Hatch, M. 2011. Environmental and cultural changes in highland Guatemala inferred from Lake Amatitlan sediments. *Geoarchaeology* 26: 346-364.
- Venables, W.N. & Ripley, B.D. 2002. *Modern applied statistics with S*. 4th ed. Springer, New York.
- Wahl, D., Byrne, R. & Anderson, L. 2014. An 8700 year paleoclimate reconstruction from the southern Maya lowlands. *Quaternary Science Reviews* 103: 19-25.
- Wahl, D., Byrne, R., Schreiner, T. & Hansen, R. 2006. Holocene vegetation change in the northern Peten and its implications for Maya prehistory. *Quaternary Research* 65: 380-389.
- Wahl, D., Hansen, R.D., Byrne, R., Anderson, L. & Schreiner, T. 2016. Holocene climate variability and anthropogenic impacts from Lago Paixban, a perennial wetland in Peten, Guatemala. *Global and Planetary Change*.
- Walker, M.J.C., Berkelhammer, M., Björck, S., Cwynar, L.C., Fisher, D.A., Long, A.J., Lowe, J.J., Newnham, R.M., Rasmussen, S.O. & Weiss, H. 2012. Formal subdivision of the Holocene Series/Epoch: a Discussion Paper by a Working Group of INTIMATE (Integration of ice-core, marine and terrestrial records) and the Subcommission on Quaternary Stratigraphy (International Commission on Stratigraphy). *Journal of Quaternary Science* 27: 649-659.
- Wang, C., Enfield, D.B., Lee, S.K. & Landsea, C.W. 2006. Influences of the Atlantic Warm pool on Western Hemisphere summer rainfall and Atlantic hurricanes. *Journal of Climate* 19: 3011-3028.
- Webster, J.W., Brook, G.A., Railsback, L.B., Cheng, H., Edwards, R.L., Alexander, C. & Reeder, P.P. 2007. Stalagmite evidence from Belize indicating significant droughts

- at the time of Preclassic Abandonment, the Maya Hiatus, and the Classic Maya collapse. *Palaeogeography, Palaeoclimatology, Palaeoecology* 250: 1-17.
- Weidie, A.E. 1985. Geology of the Yucatán platform. In: Weidie, A.E., Ward, W.C. & Back, W. (eds.) *Geology and hydrogeology of the Yucatán and Quaternary geology of northeastern Yucatán Peninsula*. New Orleans Geological Society., New Orleans.
- Weng, C., Bush, M.B. & Silman, M.R. 2004. An analysis of modern pollen rain on an elevational gradient in southern Peru. *Journal of Tropical Ecology* 20: 113-124.
- Wiersma, A.P. & Renssen, H. 2006. Model–data comparison for the 8.2kaBP event: confirmation of a forcing mechanism by catastrophic drainage of Laurentide Lakes. *Quaternary Science Reviews* 25: 63-88.
- Wilson, E.M. 1980. Physical geography of the Yucatan Peninsula. In: Moseley, E.H. & Terry, E.D. (eds.) *Yucatan: a world apart*, pp. 5-40. The University of Alabama Press, Tuscaloosa.
- Zaragosi, S., Bourillet, J.-F., Eynaud, F., Toucanne, S., Denhard, B., Van Toer, A. & Lanfumeu, V. 2006. The impact of the last European deglaciation on the deep-sea turbidite systems of the Celtic-Armorican margin (Bay of Biscay). *Geo-Marine Letters* 26: 317-329.
- Zheng, Z., Wei, J., Huang, K., Xu, Q., Lu, H., Tarasov, P., Luo, C., Beaudouin, C., Deng, Y., Pan, A., Zheng, Y., Luo, Y., Nakagawa, T., Li, C., Yang, S., Peng, H. & Cheddadi, R. 2014. East Asian pollen database: modern pollen distribution and its quantitative relationship with vegetation and climate. *Journal of Biogeography* 41: 1819-1832.

## APÉNDICES

**Apéndice 3.1.** Lista de lagos muestreados en la interface agua-sedimento (Correa-Metrio et al., 2011). Localización geográfica, altitud (m s.n.m.) e impacto humano (HII, Sanderson et al., 2012) por muestra.

| Número de lago | Lago             | Longitud     | Latitud     | Altitud | HII  |
|----------------|------------------|--------------|-------------|---------|------|
| 1              | Almond Hill      | -88.31       | 17.46       | 0       | 18   |
| 2              | Amatitlán        | -90.55       | 14.43       | 1191    | 32.5 |
| 3              | Apastepeque *    | -88.74483611 | 13.69245556 | 509     | 31   |
| 4              | Atescatempa      | -89.69       | 14.22       | 686     | 22   |
| 5              | Atitlán *        | -91.16       | 14.73       | 1602    | 23   |
| 6              | Azul             | -90.643306   | 18.645639   | 18      | 14   |
| 7              | Bacab            | -88.36       | 17.56       | 15      | 20   |
| 8              | Bacalar          | -88.39       | 18.67       | 23      | 36.5 |
| 9              | Bacalar 2 *      | -88.381944   | 18.700775   | 4       | 31   |
| 10             | Belize 1         | -88.97       | 17.24       | 80      | 21   |
| 11             | Belize 2         | -88.49       | 17.31       | 23      | 14   |
| 12             | Calderas *       | -90.59133611 | 14.41171389 | 1790    | 43   |
| 13             | Camp *           | -90.988675   | 18.037019   | 43      | 26   |
| 14             | Candelaria *     | -91.05       | 18.18       | 37      | 48   |
| 15             | Caobas           | -89.10075    | 19.444389   | 126     | 7    |
| 16             | Cayucón          | -90.98       | 18.04       | 42      | 26   |
| 17             | Celestún         | -90.38       | 20.86       | 1       | 33   |
| 18             | Cenote 14        | -88.38       | 18.23       | 10      | 17   |
| 19             | Cenote Timul     | -89.36       | 20.59       | 15      | 16   |
| 20             | Cenote Yokdzonot | -88.73       | 20.71       | 28      | 14   |
| 21             | Chacan-Bata      | -89.17       | 19.19       | 95      | 7    |
| 22             | Chacan-Lara      | -89.09       | 18.48       | 132     | 9    |
| 23             | Chacanbacab *    | -89.086889   | 18.477667   | 109     | 9    |
| 24             | Chacchoben *     | -88.181056   | 19.037186   | 6       | 18   |
| 25             | Chanmico *       | -89.35412222 | 13.77857222 | 477     | 36   |
| 26             | Chantzip *       | -91.5701652  | 16.9701469  | 1000    | 12   |
| 27             | Chencha          | -89.88       | 20.69       | 10      | 26   |
| 28             | Chichancanab *   | -88.77       | 19.88       | 3       | 11   |
| 29             | Chihuol *        | -89.612      | 20.63502    | 23      | 26   |
| 30             | Chiligatoro *    | -88.18298056 | 14.3756     | 1925    | 26   |
| 31             | Chuina *         | -90.712728   | 18.961433   | 17      | 31   |
| 32             | 5 Lakes small    | -91.69       | 16.15       | 1534    | 22   |
| 33             | 5 Lakes Big      | -91.68       | 16.11       | 1534    | 16   |
| 34             | Cobá             | -87.74       | 20.5        | 12      | 4    |

Apéndice 3.1. Continuación

| Número del lago | Lago              | Longitud     | Latitud     | Altitud | HII  |
|-----------------|-------------------|--------------|-------------|---------|------|
| 35              | Colón 1           | -91.89       | 15.83       | 634     | 26   |
| 36              | Colón 2           | -91.89       | 15.83       | 634     | 26   |
| 37              | Colón 3           | -91.9        | 15.83       | 630     | 33   |
| 38              | Colón 4           | -91.9        | 15.83       | 630     | 33   |
| 39              | Colón 5           | -91.89       | 15.83       | 630     | 26   |
| 40              | Crooked Tree      | -88.53       | 17.78       | 2       | 12   |
| 41              | El Espino         | -89.86521389 | 13.95296667 | 689     | 48   |
| 42              | El Muchacho *     | -90.19177222 | 13.88918056 | 3       | 30   |
| 43              | El Pino *         | -90.39413611 | 14.34471389 | 1038    | 21   |
| 44              | Emiliano Zapata * | -88.469056   | 19.196672   | 23      | 11   |
| 45              | Escondido *       | -91.68       | 16.11       | 1515    | 16   |
| 46              | Esmeralda *       | -91.728607   | 16.118065   | 1473    | 16   |
| 47              | Gemelas           | -91.64       | 16.09       | 1458    | 22   |
| 48              | Gloria 1          | -90.37       | 16.95       | 131     | 18   |
| 49              | Guija             | -89.55       | 14.25       | 452     | 24   |
| 50              | Honey Camp 13 *   | -88.44       | 18.05       | 0       | 8    |
| 51              | Ipala             | -89.63944722 | 14.55705556 | 1495    | 26   |
| 52              | Ixlu              | -89.69       | 16.97       | 129     | 16.5 |
| 53              | Jamolun           | -89.5        | 19.47       | 133     | 7    |
| 54              | Jobal             | -90.11       | 18.7        | 116     | 14   |
| 55              | Jocotal *         | -88.25185833 | 13.33713333 | 26      | 26   |
| 56              | Juarez *          | -87.34       | 20.8        | 23      | 7    |
| 57              | Jucutuma *        | -87.90278611 | 15.51226944 | 27      | 37   |
| 58              | Kana *            | -88.39543    | 19.5008     | 5       | 8    |
| 59              | Kichayil *        | -91.66       | 16.1        | 1530    | 18   |
| 60              | La perdida 2 *    | -90.575683   | 18.0338     | 49      | 14   |
| 61              | Lacandón *        | -91.58979722 | 17.01544444 | 812     | 22   |
| 62              | Lachuá *          | -90.67319722 | 15.91837778 | 170     | 18   |
| 63              | Lago Amarillo     | -91.59666667 | 16.98411667 | 859     | 20   |
| 64              | Laguna Chan *     | -90.210917   | 18.479639   | 67      | 14   |
| 65              | Laguna Perdida    | -90.21       | 17.07       | 76      | 11   |
| 66              | Las Pozas *       | -90.17       | 16.34       | 154     | 22   |
| 67              | Los negritos      | -87.936975   | 13.28305    | 102     | 32   |
| 68              | Macanche *        | -89.63       | 16.97       | 166     | 15   |
| 69              | Madre vieja *     | -88.13762222 | 14.35692222 | 1866    | 24   |
| 70              | Magdalena *       | -91.39561944 | 15.54258056 | 2863    | 18   |
| 71              | Metapán *         | -89.46553333 | 14.30943611 | 450     | 33   |
| 72              | Metzabok *        | -91.627778   | 17.120833   | 546     | 16   |
| 73              | Miguel Hidalgo *  | -88.367389   | 18.785639   | 31      | 14   |

|    |          |        |       |   |       |
|----|----------|--------|-------|---|-------|
| 74 | Milagros | -88.43 | 18.51 | 0 | 32.75 |
|----|----------|--------|-------|---|-------|

Apéndice 3.1. Continuación

| Número del lago | Lago                    | Longitud     | Latitud     | Altitud | HII   |
|-----------------|-------------------------|--------------|-------------|---------|-------|
| 75              | Misteriosa              | -90.48       | 18.05       | 70      | 10    |
| 76              | Montebello              | -91.71       | 16.11       | 1539    | 14    |
| 77              | Nahá 1                  | -91.6        | 16.97621667 | 829     | 22    |
| 78              | Nahá 2                  | -91.59656389 | 16.97902778 | 832     | 16    |
| 79              | Nahá 3                  | -91.58911944 | 16.98333333 | 835     | 20    |
| 80              | Nohbec                  | -88.18       | 19.15       | 0       | 22.5  |
| 81              | Ocotalito               | -91.60172778 | 16.94420833 | 920     | 24    |
| 82              | Olomega*                | -88.055075   | 13.30723333 | 66      | 25    |
| 83              | Ocom                    | -88.05       | 19.47       | 13      | 12    |
| 84              | Oquevix                 | -89.74       | 16.66       | 157     | 16    |
| 85              | Oxola                   | -89.24165    | 20.67823    | 18      | 17    |
| 86              | Peñasquito*             | -91.75222    | 16.1322     | 1454    | 14    |
| 87              | Petén de Monos          | -90.32       | 20.85       | 7       | 16.25 |
| 88              | Petén Itzá 5            | -89.85       | 17.01       | 111     | 9.5   |
| 89              | Petén Itzá M            | -89.86       | 17.01       | 111     | 9.5   |
| 90              | Petexbatun              | -90.18       | 16.42       | 110     | 18    |
| 91              | Pojoj                   | -91.67       | 16.1        | 1537    | 16    |
| 92              | Progreso                | -88.42       | 18.22       | 14      | 20    |
| 93              | Punta Laguna            | -87.64       | 20.65       | 2       | 10    |
| 94              | Río Cuba                | -90.48       | 17.95       | 79      | 18    |
| 95              | Río Guerrero            | -90.73       | 19.21       | 4       | 26    |
| 96              | Rosario                 | -90.16       | 16.53       | 115     | 22    |
| 97              | Sabak-há*               | -89.5881     | 20.57997    | 18      | 18    |
| 98              | Sabanita*               | -88.57       | 18.4        | 30      | 28    |
| 99              | Sacalaca*               | -88.599703   | 20.066669   | 28      | 14    |
| 100             | Sacnab*                 | -89.37246667 | 17.05826111 | 170     | 18    |
| 101             | Sacpuy                  | -90.02       | 16.98       | 122     | 12    |
| 102             | Salpetén                | -89.68       | 16.98       | 106     | 21    |
| 103             | Salto grande*           | -91.120217   | 18.196956   | 30      | 24    |
| 104             | San Diego               | -90.42       | 16.92       | 135     | 26    |
| 105             | San Francisco Kana      | -90.12       | 20.86       | 6       | 14    |
| 106             | San Francisco Mateos    | -90.66       | 17.9        | 53      | 14    |
| 107             | San José de la Montaña* | -89.012028   | 18.368694   | 118     | 16    |
| 108             | San José Aguilar*       | -89.01       | 18.37       | 125     | 16    |
| 109             | San Miguel 2*           | -88.99831    | 19.93465    | 32      | 14    |
| 110             | Señor*                  | -88.07748    | 19.87646    | 3       | 12    |
| 111             | Sijil Noh ha*           | -88.05543    | 19.4731     | 0       | 12    |

|     |          |        |       |    |    |
|-----|----------|--------|-------|----|----|
| 112 | Silvituc | -90.29 | 18.64 | 47 | 14 |
| 113 | Tekom    | -88.27 | 20.6  | 26 | 22 |

Apéndice 3.1. Continuación

| Número del lago | Lago             | Longitud     | Latitud     | Altitud | HII   |
|-----------------|------------------|--------------|-------------|---------|-------|
| 114             | Ticamaya *       | -87.88972778 | 15.55060556 | 17      | 32.5  |
| 115             | Vallehermoso *   | -88.5216     | 19.17812    | 18      | 18    |
| 116             | Verde *          | -89.787175   | 13.89146667 | 1609    | 27    |
| 117             | Vuelta el agua * | -91.77       | 16.147222   | 1454    | 20    |
| 118             | Xbacab *         | -90.720156   | 18.939875   | 18      | 26    |
| 119             | Xlakah           | -89.6        | 21.09       | 9       | 37    |
| 120             | Yaa'x ek         | -88.42       | 20.62       | 29      | 20.25 |
| 121             | Yalahau          | -89.22       | 20.66       | 11      | 18    |
| 122             | Yalahau 2 *      | -89.217008   | 20.657072   | 2       | 18    |
| 123             | Yalaluch         | -91.66       | 16.09       | 1503    | 22    |
| 124             | Yalaluch 2 *     | -91.646403   | 16.092628   | 1448    | 22    |
| 125             | Yaxhá            | -89.41       | 17.07       | 164     | 14    |

\* Muestras nuevas

**Apéndice 3.2.** Threshold Indicator Taxa Analysis at taxon level in response to human influence gradient in Maya lands.

| <b>Taxon</b>        | <b>Obs</b> | <b>P</b> | <b>Z score</b> | <b>5%</b> | <b>50%</b> | <b>95%</b> | <b>Purity</b> | <b>Reliability</b> | <b>Response</b> |
|---------------------|------------|----------|----------------|-----------|------------|------------|---------------|--------------------|-----------------|
| <i>Acacia</i>       | 18         | 0.008    | 3.53           | 7.5       | 18         | 36.5       | 0.718         | 0.992              | Z-              |
| <i>Acalypha</i>     | 9.25       | 0.128    | 1.12           | 9.25      | 18         | 34.5       | 0.71          | 0.606              | 0               |
| <i>Alchornea</i>    | 12         | 0.02     | 2.9            | 11.5      | 16         | 22.1       | 0.95          | 0.904              | 0               |
| <i>Alnus</i>        | 24         | 0.024    | 2.64           | 14        | 23.5       | 40         | 0.72          | 0.928              | 0               |
| Alternanthera       | 14         | 0.096    | 1.31           | 12        | 17.5       | 31         | 0.542         | 0.702              | 0               |
| Amaranthaceae       | 22.25      | 0.004    | 3.82           | 14        | 22.5       | 33.075     | 0.976         | 0.952              | Z+              |
| Amaryllidaceae      | 14         | 0.08     | 1.66           | 14        | 18.5       | 36.7625    | 0.504         | 0.68               | 0               |
| <i>Ambrosia</i>     | 20         | 0.04     | 1.94           | 14        | 21         | 32.875     | 0.824         | 0.788              | 0               |
| Anacardiaceae       | 14         | 0.012    | 2.83           | 12        | 14.25      | 36.75      | 0.6           | 0.594              | 0               |
| Apocynaceae         | 36.75      | 0.064    | 1.89           | 12        | 22         | 37.05      | 0.81          | 0.746              | 0               |
| Arecaceae           | 16         | 0.064    | 1.81           | 10        | 20         | 32.625     | 0.834         | 0.734              | 0               |
| Asteraceae          | 7.5        | 0.036    | 2.06           | 7         | 13         | 32.625     | 0.8           | 0.75               | 0               |
| <i>Begonia</i>      | 11         | 0.048    | 1.95           | 9.7125    | 17.5       | 34.5       | 0.832         | 0.764              | 0               |
| Bignoniaceae        | 36.75      | 0.16     | 1.07           | 9.5       | 16         | 36.75      | 0.546         | 0.706              | 0               |
| Bombacaceae         | 11         | 0.22     | 0.79           | 11.5      | 16         | 33         | 0.432         | 0.394              | 0               |
| <i>Borreria</i>     | 16         | 0.108    | 1.29           | 11        | 20.5       | 36.5125    | 0.798         | 0.658              | 0               |
| <i>Brassicaceae</i> | 22         | 0.244    | 0.46           | 7.5       | 18         | 36.75      | 0.488         | 0.604              | 0               |
| <i>Brosimum</i>     | 15.5       | 0.004    | 4.24           | 12        | 16         | 26.5       | 0.996         | 0.994              | Z-              |
| <i>Bursera</i>      | 14         | 0.004    | 4.02           | 12        | 14         | 26         | 0.846         | 0.968              | Z-              |
| <i>Byrsonima</i>    | 18         | 0.004    | 4.98           | 14        | 17.5       | 28.025     | 0.996         | 0.994              | Z+              |
| <i>Caesalpinia</i>  | 24         | 0.184    | 0.84           | 14        | 26         | 37         | 0.718         | 0.538              | 0               |
| <i>Casuarina</i>    | 26         | 0.124    | 1.12           | 10.5      | 20.375     | 32.5       | 0.558         | 0.51               | 0               |
| <i>Cecropia</i>     | 22         | 0.004    | 5.44           | 11.475    | 22         | 26         | 1             | 1                  | Z-              |
| <i>Celtis</i>       | 33         | 0.008    | 2.88           | 9.25      | 32.25      | 36.5       | 0.804         | 0.942              | 0               |
| <i>Clethra</i>      | 27.5       | 0.196    | 1.12           | 12        | 22         | 29         | 0.694         | 0.49               | 0               |
| Clusiaceae          | 24         | 0.004    | 4.55           | 16.71875  | 24         | 34.5       | 0.984         | 0.952              | Z+              |
| Convolvulaceae      | 11.5       | 0.028    | 2.07           | 8         | 11.5       | 30.5       | 0.786         | 0.692              | 0               |
| <i>Cordia</i>       | 31         | 0.008    | 3.62           | 12        | 27         | 33         | 0.906         | 0.9                | 0               |
| Cucurbitaceae       | 26         | 0.044    | 2.23           | 13        | 26         | 33         | 0.906         | 0.804              | 0               |
| <i>Eugenia</i>      | 9.75       | 0.004    | 3.98           | 7.5       | 10.5       | 32.625     | 0.894         | 0.994              | Z-              |
| Euphorbiaceae       | 24         | 0.004    | 4.22           | 12        | 24.5       | 34.7625    | 0.97          | 0.958              | Z+              |
| Fabaceae            | 32.875     | 0.06     | 2.08           | 10.5      | 24         | 36.75      | 0.966         | 0.876              | 0               |
| <i>Ficus</i>        | 14         | 0.008    | 4.51           | 10.5      | 14         | 16         | 0.988         | 0.988              | Z-              |
| <i>Guettarda</i>    | 24         | 0.008    | 3.24           | 7.475     | 23.5       | 26         | 0.974         | 0.944              | 0               |
| <i>Gustavia</i>     | 17.5       | 0.128    | 1.4            | 7.5       | 18         | 33         | 0.794         | 0.748              | 0               |

Apéndice 3.2. Continuación

| <b>Taxon</b>       | <b>Obs</b> | <b>P</b> | <b>Z score</b> | <b>5%</b> | <b>50%</b> | <b>95%</b> | <b>Purity</b> | <b>Reliability</b> | <b>Response</b> |
|--------------------|------------|----------|----------------|-----------|------------|------------|---------------|--------------------|-----------------|
| <i>Hedyosmum</i>   | 14         | 0.116    | 1.29           | 14        | 18         | 25         | 0.614         | 0.49               | 0               |
| <i>Hymenaea</i>    | 18         | 0.028    | 2.53           | 9.5       | 16.375     | 36.25      | 0.836         | 0.882              | 0               |
| <i>Ilex</i>        | 18         | 0.04     | 2.26           | 11.5      | 18         | 26         | 0.868         | 0.822              | 0               |
| <i>Inga</i>        | 14         | 0.064    | 2.02           | 12        | 16.125     | 39.7625    | 0.73          | 0.622              | 0               |
| <i>Iresine</i>     | 10.5       | 0.148    | 1.01           | 8.5       | 20         | 37         | 0.518         | 0.81               | 0               |
| <i>Liquidambar</i> | 14         | 0.02     | 3.19           | 13        | 16         | 33         | 0.99          | 0.932              | 0               |
| <i>Machaerium</i>  | 18         | 0.028    | 2.69           | 14        | 18         | 36.0125    | 0.802         | 0.87               | 0               |
| Malpighiaceae      | 24.5       | 0.02     | 2.86           | 12        | 24.75      | 36.75      | 0.944         | 0.906              | 0               |
| Malvaceae          | 36.25      | 0.196    | 0.79           | 10.5      | 20         | 31.55      | 0.38          | 0.53               | 0               |
| Mecardonia         | 14         | 0.004    | 4.35           | 10        | 15         | 37         | 0.622         | 0.95               | Z-              |
| Melastomataceae    | 7.5        | 0.372    | 0.32           | 7.5       | 20.5625    | 36.75      | 0.502         | 0.666              | 0               |
| Meliaceae          | 23.5       | 0.02     | 2.64           | 7         | 23         | 40         | 0.86          | 0.884              | 0               |
| <i>Mimosa</i>      | 7.5        | 0.008    | 4.3            | 7.475     | 12         | 22         | 0.964         | 0.954              | Z-              |
| Moraceae           | 26         | 0.08     | 1.69           | 12        | 22         | 36.75      | 0.846         | 0.752              | 0               |
| <i>Myrica</i>      | 14         | 0.004    | 4.16           | 14        | 16         | 25         | 0.952         | 0.972              | Z+              |
| <i>Myrsine</i>     | 23.5       | 0.056    | 1.73           | 9.75      | 16.375     | 24         | 0.9           | 0.72               | 0               |
| Myrtaceae          | 18         | 0.004    | 4.24           | 11        | 18         | 20         | 0.962         | 0.942              | 0               |
| <i>Nymphaea</i>    | 26         | 0.212    | 0.77           | 7         | 16         | 26         | 0.546         | 0.582              | 0               |
| <i>Paullinia</i>   | 7.5        | 0.028    | 2.27           | 7         | 16.125     | 26         | 0.928         | 0.872              | 0               |
| <i>Pinus</i>       | 14         | 0.004    | 4.43           | 12        | 14         | 18         | 1             | 1                  | Z+              |
| Piperaceae         | 24         | 0.012    | 3.43           | 24        | 26         | 37         | 0.982         | 0.914              | 0               |
| Poaceae            | 14         | 0.012    | 3.17           | 12        | 16         | 24         | 0.962         | 0.898              | 0               |
| <i>Polygonum</i>   | 26.5       | 0.024    | 2.37           | 7.5       | 26         | 31.5       | 0.738         | 0.866              | 0               |
| <i>Protium</i>     | 14         | 0.032    | 2.28           | 10        | 20.8125    | 34.5       | 0.648         | 0.624              | 0               |
| <i>Psychotria</i>  | 22.25      | 0.004    | 3.81           | 16        | 23.5       | 32.25      | 0.942         | 0.922              | 0               |
| <i>Quercus</i>     | 14         | 0.004    | 3.22           | 8         | 16         | 26         | 0.938         | 0.966              | Z+              |
| Rubiaceae          | 24         | 0.052    | 2.1            | 14        | 24         | 34.5       | 0.738         | 0.782              | 0               |
| Rutaceae           | 14         | 0.32     | 0.34           | 7         | 16.25      | 27.025     | 0.52          | 0.516              | 0               |
| Sapindaceae        | 18         | 0.108    | 1.49           | 8         | 18         | 37         | 0.77          | 0.672              | 0               |
| <i>Sapium</i>      | 16         | 0.076    | 1.96           | 10        | 18         | 27.05      | 0.646         | 0.798              | 0               |
| Sapotaceae         | 14         | 0.004    | 3.41           | 13        | 14         | 29         | 0.728         | 0.97               | Z-              |
| <i>Serjania</i>    | 18         | 0.176    | 0.95           | 11        | 18         | 34.5125    | 0.696         | 0.538              | 0               |
| Solanaceae         | 24         | 0.008    | 3.18           | 10.5      | 24.5       | 29.5       | 0.97          | 0.96               | Z+              |
| <i>Spondias</i>    | 14         | 0.012    | 3.39           | 8         | 14         | 23         | 0.896         | 0.896              | 0               |
| <i>Trema</i>       | 18         | 0.004    | 4.18           | 14        | 18         | 25.5       | 1             | 0.998              | Z-              |
| <i>Trichilia</i>   | 14         | 0.12     | 1.34           | 11.5      | 18         | 34.5       | 0.452         | 0.758              | 0               |
| <i>Typha</i>       | 7.5        | 0.092    | 1.3            | 7         | 14.5       | 26         | 0.844         | 0.672              | 0               |
| <i>Ulmus</i>       | 18         | 0.016    | 2.78           | 17        | 21.5       | 37         | 0.962         | 0.868              | 0               |
| <i>Vitex</i>       | 7.5        | 0.008    | 5.32           | 7         | 9.25       | 23.525     | 0.964         | 0.982              | Z-              |
| <i>Zanthoxylum</i> | 26         | 0.076    | 1.87           | 11.975    | 22         | 31         | 0.602         | 0.794              | 0               |
| <i>Zea</i>         | 31         | 0.004    | 5.84           | 24        | 30.5       | 32         | 0.984         | 0.988              | Z+              |

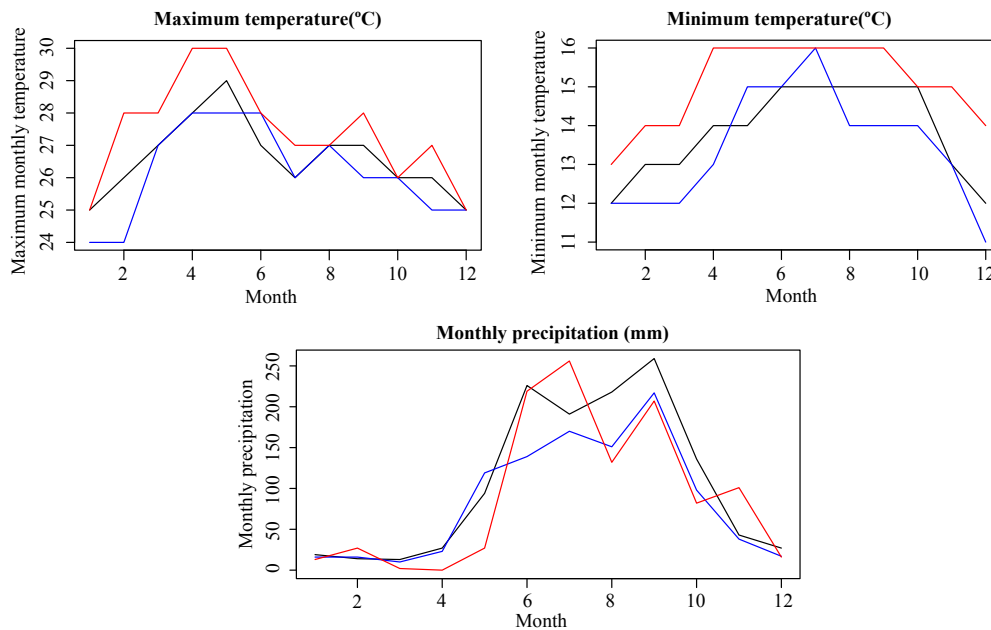
**Apéndice 4.1.** Pearson correlation for the analyzed elements. Highly significant correlations (p-value <0.005) shaded in grey.

| <b>Core</b>  |           | <b>Sr</b> | <b>Fe</b> | <b>Zr</b> | <b>Mn</b> | <b>Pb</b> | <b>Rb</b> | <b>Ti</b> |
|--------------|-----------|-----------|-----------|-----------|-----------|-----------|-----------|-----------|
| <b>LIQ13</b> | <b>Ca</b> | 0.97      | -0.82     | -0.78     | 0.23      | -0.24     | -0.7      | -0.94     |
|              | <b>Sr</b> |           | -0.78     | -0.73     | 0.35      | -0.14     | -0.59     | -0.94     |
|              | <b>Fe</b> |           |           | 0.8       | -0.1      | 0.45      | 0.71      | 0.77      |
|              | <b>Zr</b> |           |           |           | -0.08     | 0.54      | 0.6       | 0.79      |
|              | <b>Mn</b> |           |           |           |           | 0.16      | -0.06     | -0.3      |
|              | <b>Pb</b> |           |           |           |           |           | 0.49      | 0.25      |
|              | <b>Rb</b> |           |           |           |           |           |           | 0.61      |
| <b>ESM12</b> | <b>Ca</b> | 0.64      | -0.45     | -0.43     |           |           |           |           |
|              | <b>Sr</b> |           | -0.51     | -0.43     |           |           |           |           |
|              | <b>Fe</b> |           |           | 0.95      |           |           |           |           |

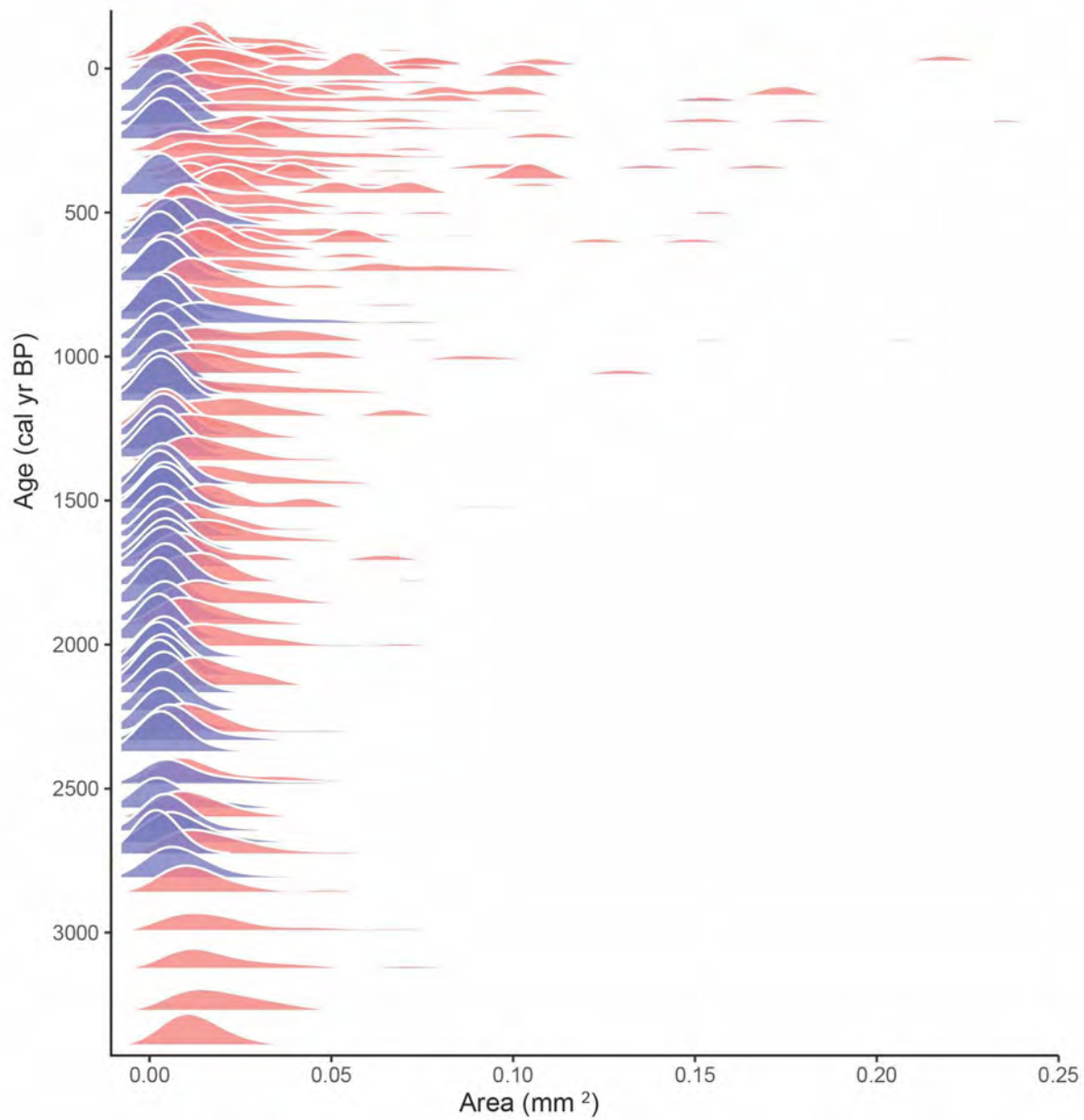
**Apéndice 4.2.** Detailed of the step-wise backward environmental variable selection. Significant  $\beta$  estimated ( $p$ -value  $< 0.001$ ) in shade grey.

| Response Variables | Explanatory Variables | Step 1<br>$\beta$ | Step 2<br>$\beta$ | Step 3<br>$\beta$ | Step 4<br>$\beta$ | Step 5<br>$\beta$ | Step 6<br>$\beta$ |
|--------------------|-----------------------|-------------------|-------------------|-------------------|-------------------|-------------------|-------------------|
| <b>NMDS1</b>       | Constant              | 5.68E-01          | –                 | 5.29E-01          | 2.68E+00          | 2.84              |                   |
|                    | Longitude             | 6.41E-02          | 6.26E-02          | 6.15E-02          | 7.75E-02          | 7.74E-02          |                   |
|                    | Latitude              | 2.76E-01          | 2.72E-01          | 2.58E-01          | 2.75E-01          | 2.72E-01          |                   |
|                    | HII                   | 1.78E-02          | 1.76E-02          | 1.81E-02          | 2.05E-02          | 2.04E-02          |                   |
|                    | APP                   | -1.46E-04         | -1.37E-04         | -1.17E-04         | -1.99E-04         | -2.00E-04         |                   |
|                    | IST                   | 1.95E-02          | 1.93E-02          | 1.48E-02          | 1.59E-03          |                   |                   |
|                    | Zone A                | -5.31E-01         | -5.36E-01         | -5.09E-01         |                   |                   |                   |
|                    | Zone B                | 1.95E-01          | 2.34E-01          | 2.61E-01          |                   |                   |                   |
|                    | MDR                   | -2.05E-03         | -1.91E-03         |                   |                   |                   |                   |
|                    | Altitude              | -4.83E-05         |                   |                   |                   |                   |                   |
|                    | <b>NMDS2</b>          | Constant          | -5.25E-01         | -6.26E-01         | -4.84E-01         | -7.97E-01         | -1.43             |
| Latitude           |                       | 2.14E-01          | 2.08E-01          | 2.03E-01          | 1.99E-01          | 2.19E-01          | 1.53E-01          |
| Zone A             |                       | 8.69E-01          | 8.55E-01          | 8.83E-01          | 8.95E-01          | 8.33E-01          | 8.50E-01          |
| Zone B             |                       | 1.21E+00          | 1.21E+00          | 1.24E+00          | 1.35E+00          | 1.30E+00          | 1.35E+00          |
| HII                |                       | 9.40E-03          | 9.55E-03          | 9.77E-03          | 9.08E-03          | 9.46E-03          |                   |
| Longitude          |                       | 3.21E-02          | 3.06E-02          | 3.07E-02          | 2.84E-02          | 3.38E-02          |                   |
| IST                |                       | -8.08E-03         | -8.71E-03         | -1.14E-02         | -1.17E-02         |                   |                   |
| ALT                |                       | -1.31E-04         | -1.19E-04         | -1.22E-04         |                   |                   |                   |
| MDR                |                       | -1.45E-03         | -9.61E-04         |                   |                   |                   |                   |
| APP                |                       | -1.97E-05         |                   |                   |                   |                   |                   |
| <b>NMDS3</b>       |                       | Constant          | -1.88E+00         | -1.85E+00         | -1.80E+00         | -1.78E+00         | -1.73E+00         |
|                    | Latitude              | -4.61E-04         | 1.26E-01          | 1.24E-01          | 1.25E-01          | 1.37E-01          |                   |
|                    | Zone A                | 4.25E-01          | 4.23E-01          | 4.26E-01          | 4.30E-01          | 5.10E-01          |                   |
|                    | Zone B                | 4.96E-01          | 4.94E-01          | 4.97E-01          | 4.89E-01          | 5.55E-01          |                   |
|                    | HII                   | -8.60E-03         | -8.60E-03         | -8.59E-03         | -8.53E-03         | -9.20E-03         |                   |
|                    | MDR                   | -4.34E-03         | -4.35E-03         | -4.24E-03         | -4.27E-03         | -5.66E-03         |                   |
|                    | APP                   | 6.55E-05          | 6.52E-05          | 6.57E-05          | 6.36E-05          |                   |                   |
|                    | ALT                   | 1.33E-05          | 1.28E-05          | 1.29E-05          |                   |                   |                   |
|                    | IST                   | 6.15E-04          | 6.68E-04          |                   |                   |                   |                   |
|                    | Longitude             | -4.61E-04         |                   |                   |                   |                   |                   |

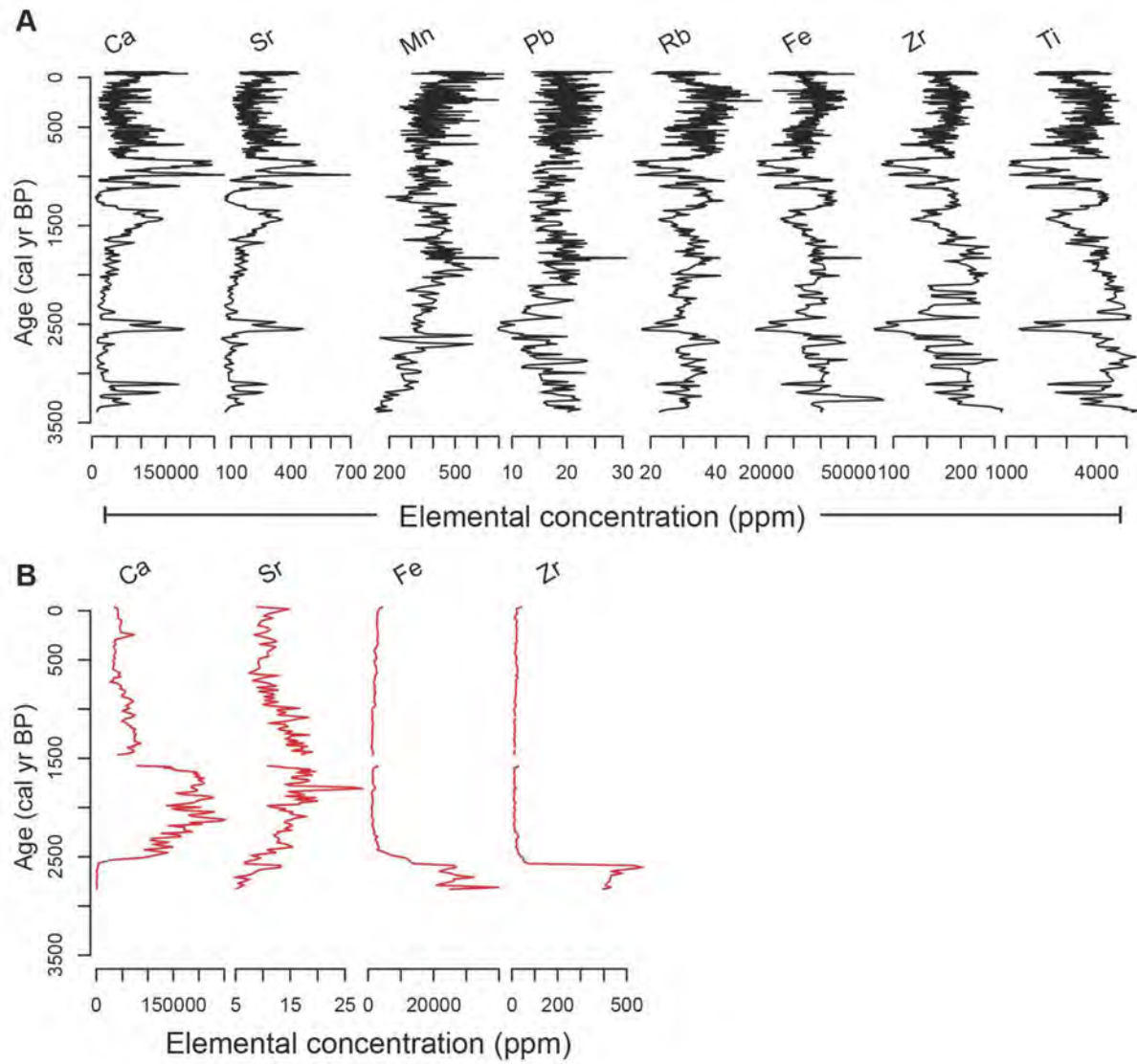
**Apéndice 4.3.** Monthly minimum and maximum temperature, and monthly precipitation of La Soledad meteorological station (~29 km north of Montebello National Park). Each month of information from the meteorological station was classified into El Niño (red lines), regular (black lines) and La Niña conditions (blue lines), according to the ENSO multivariate index (MEI, Wolter and Timlin, 2011), following Bush et al. (2017). Analyses were based on La Soledad meteorological station because it represents the longest and most complete instrumental record of the region, offering a higher number of observations per ENSO phase, and therefore more robust results. Whereas the record from Tzisco contains data from August 1977 to November 1996, and from October 1998 to February 2003, the record from La Soledad is continuous from February 1961 to May 2015.



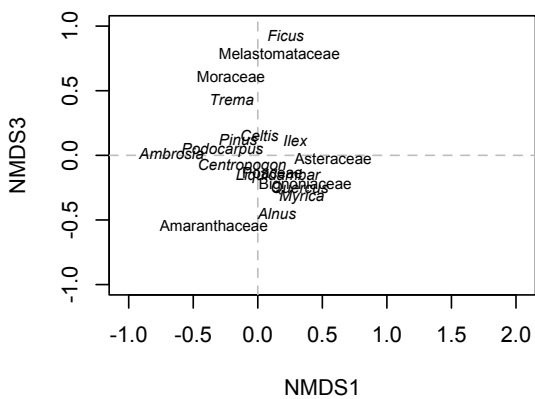
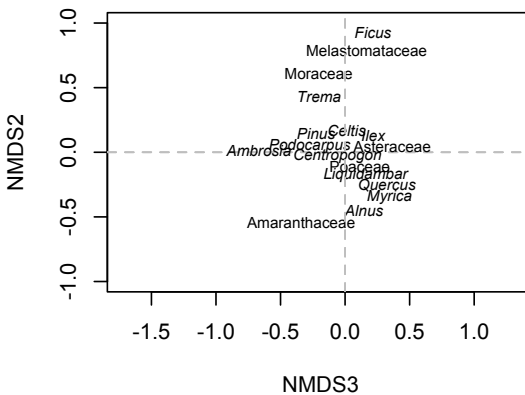
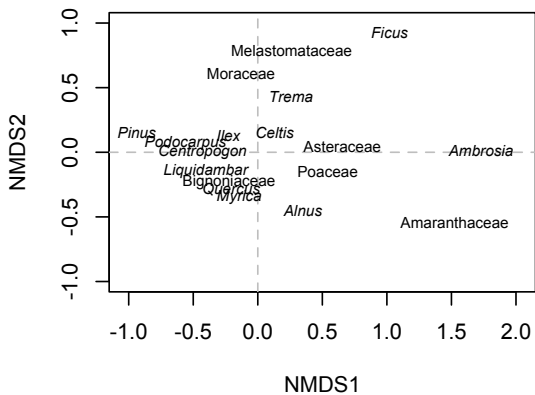
**Apéndice 4.4.** Probability density functions of charcoal size (mm<sup>2</sup>) distribution per sample for the sediment cores from Lakes San Lorenzo (LIQ13, red distributions) and Esmeralda (ESM12, blue distributions).



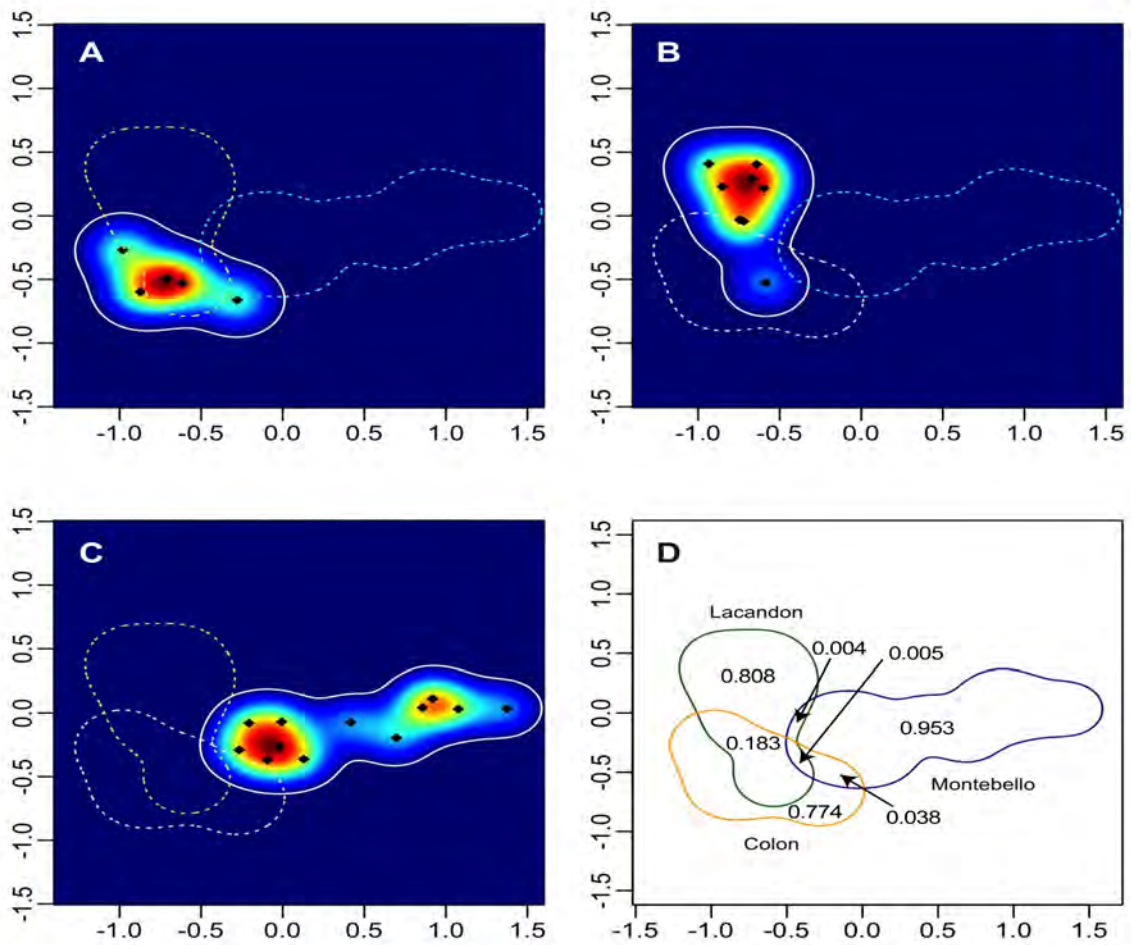
**Apéndice 4.5.** Elemental records for the sediment cores from Lakes San Lorenzo (A. LIQ13) and Esmeralda (B. ESM12).



**Apéndice 4.6.** Projection of taxa on the non-metric multidimensional scaling.



**Apéndice 5.1.** Bivariate probability density functions with a 95 % confidence region for the space occupied by modern samples separated by localities. **A.** Lagos de Colón. **B.** Lacandon forest. **C.** Lagunas de Montebello. **D.** Probability of each location and overlapping events.



**Apéndice 5.2. A.** Elemental records for OCO12-II (blue line) and OCO16G-I (green line).  
**B.** Correlation plane of Principal Component Analysis for the elemental composition of sediments from Lake Ocotitalito.

